

Application of selected control algorithms for nonlinear systems in unmanned bicycle robot stabilized by an inertial drive

Zastosowanie wybranych algorytmów sterowania systemów nieliniowych w bezzałogowym pojeździe jednośladowym stabilizowanym napędem inercyjnym



**by
Adam Owczarkowski**

DOCTORAL DISSERTATION

**Institute of Control and Information Engineering Faculty
of Electrical Engineering Poznań University of
Technology**

**Instytut Automatyki i Inżynierii Informatycznej Wydział Elektryczny Politechnika
Poznańska**

Advisor: Dariusz Horla, Ph.D.,D.Sc.

Poznań, Poland, April 4, 2017

Abstract

This thesis consists of two main parts: the first describing the reaction wheel principles and the other describing the bicycle with the reaction wheel. These two parts are complementing each other and form a complete dissertation.

The first main part describes the main principles of operation of the reaction wheel. It explains in detail how and where action and reaction forces are created in the mechanical device. There relationship between acting body and reacting body is well-explained therein. The full set of differential equations is formulated with many partial results obtained from examples of linear and rotary motions where the reaction forces are created. This namely allows to model a completely new object very important for this research: the reaction wheel pendulum. It is deeply analysed using control theory techniques. Controlling this object is difficult because it is underactuated (less control signals than actuators) and control signals are very limited. The reaction torque is used, which occurs only when the reaction wheel is accelerated or decelerated and there is a need to put a huge care to angular velocity never to exceed the limit value. The system is nonlinear and therefore control techniques are proposed to stabilize it. Finally, the linear quadratic controller is designed which is based on the algebraic Riccati equations. A fully-detailed description of all necessary mathematical equations is used to create the control law. The classical LQR control law and its modified version (LQI) based on the additional loop which integrates state signals is used. The linear quadratic algorithm allows to control the whole state of the object which is a great advantage of this algorithm. In addition, it is a tracking control technique which allows to move the system from one state to another during the operation. Object described mathematically with proposed control algorithms give the full description of this automatic control system. Eigenvalue and step response analysis confirms the stability in the considered point of operation. Furthermore, this stability is checked when several parameters change such us: the mass and radius of the reaction wheel, the height of the reaction wheel mounting and the coefficients of friction. A through analysis of the energy flow in the considered inverted pendulum is constructed. This analysis confirms the high energy efficiency of this type of actuator. The proposed control law is tested by numerous computer simulations, which perfectly illustrate the real behaviour of the machine. The real object is created and described and physical parameters are identified. Experimental tests confirm the suitability of control algorithms used. An important aspect is the description of hardware solutions related with

measuring system. There is a novel method of determining the angle from the vertical position using only gyroscope with its imperfections – the drift. Additionally, the explanation how to use it is given with the linear quadratic regulation to estimate the position.

The second part of this work is focused on the bicycle with and without the reaction wheel module. It starts from a deep analysis of the mathematical models available in the literature. The aim is to find as good differential equations as possible to describe the most important states of the real single-track vehicles. Finally, one model is selected which is at this moment the reference for the bicycle models. This system of mathematical equations is transformed into state-space form. Next, these equations are gathered together with the whole description of the reaction wheel pendulum. This gives the complete description of the new object that is difficult to find in the currently available literature. This is the vital base of this scientific work. It allows one to develop a complete control law for optimal stabilization based on the handlebar control and reaction wheel control. The LQR control algorithm is used to ensure minimization of quadratic performance indices and stabilization of all state variables using several control signals simultaneously. There is a series of stability analysis and computer simulations of the bicycle with and without additional reaction unit. The detailed comparison of these two objects is performed. It is proven that in a certain range of velocity the bicycle is self stable, thus it does not need any control to keep balance. There are many conclusions drawn when the handlebar control or the reaction wheel control gives better results. Thus, it proves that the reaction wheel in some conditions improves the stability of the bicycle and sometimes allows keeping stability (balance) of the bicycle.

Streszczenie

Niniejsza rozprawa składa się z dwóch głównych części: pierwszej opisującej zasady działania koła reakcyjnego oraz drugiej opisującej rower z kołem reakcyjnym. Obie te części się wzajemnie uzupełniają i tworzą jedną całość.

W pierwszej głównej części opisano zasadę działania koła reakcyjnego. Szczegółowo wyjaśniono jak i gdzie powstają siły akcji i reakcji w urządzeniu mechanicznym. Opisano matematycznie niezbędną relację między układem wykonawczym a układem reagującym. Dzięki zastosowaniu modelowych przykładów odnoszących się do ruchu liniowego a następnie ruchu obrotowego wyprowadzono kompletny zestaw równań różniczkowych opisujących ten proces. To z kolei umożliwiło zamodelować obiekt wysoce istotny w tej sprawie: wahadło odwrócone z kołem reakcyjnym. Wahadło poddano szczegółowej analizie wykorzystując techniki z teorii sterowania. Sterowanie wahadłem odwróconym z kołem reakcyjnym jest trudne, ponieważ jest to układ niedosterowany (o mniejszej liczbie sterowań niż stopni swobody) i o bardzo ograniczonym sterowaniu. Wykorzystywany jest reakcyjny moment siły, który powstaje tylko, gdy wirująca masa jest rozpoczęta bądź hamowana i należy bardzo dbać o to, aby prędkość obrotowa nigdy nie przekroczyła dopuszczalnej wartości. Układ jest nieliniowy i zaproponowano takie techniki sterowania, które są w stanie go ustabilizować. Wybrano optymalne sterowanie liniowo kwadratowe oparte na algebraicznym równaniu Riccatiego. Szczegółowo opisano wszystkie niezbędne równania matematyczne tej techniki sterowania. Wykorzystano klasyczne prawo sterowania LQR oraz wersję zmodyfikowaną w oparciu o dodatkową pętlą całkującą stan obiektu LQI. Regulacja liniowo kwadratowa pozwala na sterowanie całego wektora stanu obiektu co stanowi wielką zaletę tego algorytmu. Zaproponowano również różne sposoby regulacji nadążnej pozwalającej przechodzenie maszyny z jednego stanu do drugiego w trakcie działania systemu. Mając zaprojektowane prawo sterowania otrzymano kompletny układ regulacji automatycznej. Sprawdzono jego stabilność wykreślając linie pierwiastkowe dla układu bez ograniczeń oraz odpowiedzi skokowe. Wyznaczono wpływ najważniejszych parametrów układu na stabilność takich jak: masa i promień koła zamachowego, wysokość zamocowania koła zamachowego oraz współczynniki tarcia. Gruntownie przeanalizowano przemiany energii w rozważanym wahadle odwróconym. Analiza ta potwierdza wysoką efektywność energetyczną działania wymuszenia reakcyjnego. Zaproponowane prawo sterowania przetestowano na licznych symulacjach komputerowych, które doskonale dają obraz działania realnej maszyny. Oprac-

cowano realny obiekt oraz zidentyfikowano jego parametry fizyczne. Test eksperymentalne potwierdzają poprawność opracowanych algorytmów sterowania. Ważnym aspektem jest opis wykorzystanych rozwiązań sprzętowych związanych z sensoryką. Zaproponowano nowatorski sposób wyznaczania kąta odchylenia od pionu przy pomocy niedoskonałego żyroskopu obarczonego błędem pomiaru w postaci dryfu. Wykorzystując właściwości regulacji liniowo kwadratowej przedstawiono sposób estymacji położenia chwiejnego punktu równowagi.

W drugiej części rozprawy skupiono się na pojeździe rowerowym oraz jego modyfikacji o dodatkowy moduł stabilizacji opartej o koło reakcyjne. Na początek głęboko przeanalizowano model matematyczny roweru oraz przeszukano dostępną na ten temat literaturę. Celem jest odnalezienie takiego modelu roweru, aby odzwierciedlał najważniejsze stany dynamiczni realnych pojazdów jednośladowych. Wybrano jeden z nich, który w obecnej chwili stanowi referencje spośród dostępnych modeli rowerów. Zaproponowany układ równań dynamiczni ruchu przetworzono w formę równań zmiennych stanu. Następnie dokonano połączenia tak opisanego systemu z równaniami wahadła odwróconego z kołem reakcyjnym. W ten sposób otrzymano kompletny opis obiektu sterowania, który trudno odnaleźć w dostępnej obecnie literaturze oraz który stanowi najważniejszy fundament tej pracy naukowej. Następnie zostało opracowane rozbudowane prawo sterowania zapewniające optymalną stabilizację w oparciu o sterowanie kierownicą i kołem reakcyjnym. Wybrano algorytm sterowania LQR zapewniający minimalizację kwadratowego wskaźnika jakości stabilizując wszystkie zmienne stanu układu kontrolując wiele sygnałów sterujących równocześnie. Wykonano serię analiz stabilności oraz symulacji komputerowych roweru bez dodatkowego systemu oraz z systemem stabilizacji reakcyjnej. Dokonano szczegółowego porównania tych dwóch obiektów. Przy okazji udowodniono, że dla pewnego zakresu prędkości liniowych roweru wykazuje on właściwości samo stabilizacji, a zatem nie wymaga żadnego sterowania, aby utrzymać równowagę. Postawiono liczne wnioski kiedy sterowanie samą kierownicą jest lepsze od sterowania kołem reakcyjnym i na odwrót. Tym samym udowodniono, że koło reakcyjne dla pewnych zakresów prędkości roweru doskonale poprawia a czasem nawet umożliwia zachowanie stabilności (równowagi) roweru w rozumieniu utrzymania pozycji pionowej.

List of symbols

- \underline{x} – state vector
 \underline{x}_d – desired state vector
 \underline{x}_0 – initial state vector
 \underline{x}_m – measured state vector
 \underline{x}_i – integrated state vector
 \underline{x}_r – reference state vector
 \underline{u} – control vector
 μ – friction torque
 b – coefficient of friction
 g – gravity vector
 \mathbf{A} – state matrix
 \mathbf{B} – input matrix
 \mathbf{C} – output matrix
 \mathbf{D} – feedthrough matrix
 \mathbf{A}_z – state matrix of closed-loop system
 \underline{q} – vector of generalized variables
 λ – eigen vector
 E – energy
 P – power
 J – performance indices

vi

\mathcal{L}^{-1} – inverse Laplace transform operator

$G(s)$ – transfer function

Nomenclature

BIBO – Bounded Input Bounded Output
CARE – Continuous-time Algebraic Riccati Equation
CMG – Control Moment Gyroscope
COM – Center of Mass
DARE – Discrete time Algebraic Riccati Equation
FBL – Feedback Linearization
FIR – Finite Impulse Response filter
IMU – Inertial Measurement Unit
MBD – Multibody Dynamics
MEMS – Microelectromechanical System
MIMO – Multiple-Input Multiple-Output
LQI – Linear-Quadratic-Integral regulator
LQR – Linear-Quadratic Regulator
RW – Reaction Wheel
SISO – Single-Input Single-Output

Contents

1	Introduction	3
1.1	Problem statement	3
1.2	Overview of the dissertation	5
2	Background	7
3	Reaction wheel	11
3.1	Idea of the system with the reaction wheel	11
3.2	Mathematical modelling	13
3.3	Control algorithm design	18
3.3.1	Overview of stabilization techniques	18
3.3.2	Fundamentals of quadratic control	19
3.3.3	General control law	21
3.3.4	Tracking modification	22
3.3.5	State integration system LQI	23
3.4	Stability of the system with reaction wheel	26
3.5	Angle estimation with gyroscopic sensor	32
3.6	Computer simulations	38
3.7	Energy efficiency considerations	48
3.8	Tests on a real robot	53
3.8.1	Reaction wheel robot description	53
3.8.2	Results of experiments	56
4	Bicycle with reaction wheel	63
4.1	Overview of bicycle mathematical models	63
4.2	Detailed mathematical modeling and bicycle modification	65
4.2.1	Complete model of the bicycle	65
4.2.2	Full model of bicycle with reaction wheel	69
4.3	Appropriate control system design	74
4.4	Classical approach to stability analysis	83
4.5	Computer simulation and evaluation	95

5 Conclusions	109
5.1 Summary	109
5.2 Conclusions and contribution	111
5.3 Future work	113
A Physical parameters of the bicycle	115
B Physical parameters of the reaction wheel mounted on the bicycle	119

Chapter 1

Introduction

1.1 Problem statement

Bicycle is a well-known mechanical structure for over one hundred years. Officially, bicycle was invented on June 12, 1817 by Karl von Drais [25, 42, 47]. The proportions and materials of this structure were much different from its current construction but the main concept remains the same right now. It is obvious that bicycle has to transport people. It has various applications: sport, entertainment, getting to job and others.

Shortly after revealing this invention, it turned out that almost everyone could not determine conditions how to keep balance on the two-wheeled machine. This was a huge impulse for physicians and mathematicians to find the scientific explanation for this phenomenon. Luckily, there were many tools available to deal with this problem at that time. The fundamental approach of finding how the world works was by Newtonian physics. Every action and reaction, every force in mechanical machine could be described by differential equations based on Newton's laws.

There have been various kinds of full mathematical models of the bicycle. That differed from each other because of the numerous parameters. The first is the number of degrees of freedom. Some of the models had two degrees of freedom and others much more (above ten). There were linear and nonlinear models, precise and simplified. Some descriptions took the human body sitting on the bicycle saddle into account. A human is the additional mass which is generally the heaviest part of the structure. Furthermore, sitting person can also interact with the bicycle not only by handlebar. They can dynamically move the center of mass of the system which is extremely significant in the stabilization process. Some models omit the human body completely.

A solid and reliable mathematical model is usually insufficient. The question is how to use this model to predict dynamics in the real machine. Today it is possible to use computer simulations. The main idea is to integrate differential equations and to find the trajectories in the state space. In the far past this operation was not possible, because there were no computing machines capable to solve such mathematical problems. Today, this is a typical path in development process starting from the computer simulation and ending on the production phase.

Nowadays Multibody Dynamics (MBD) computer software is getting more and more popular, which is intended to solve a multibody dynamics problems and to find trajectories of all state-space variables. There is a variety iterative algorithms used which are able to deal with objects with hundreds of parts. This would not be possible to calculate by hand. The MBD software is an attractive way to verify these mathematical models.

The fundamental principle in robotics is to replace humans by machines. Robots should help people in their everyday life. Today almost every industry has some robots which perform actions automatically. This is a huge inspiration to make research for the scientists. The Author of this work has been always focused on bicycles. Through his whole life he was wondering if it was possible to control such a machine automatically without any help from human. Furthermore, he was wondering if automatic control system can manipulate a bicycle better than a human person does. Keeping balance is the biggest challenge when riding bicycle. If the velocity is too small it loses stability. That is why he decided to use additional actuator to keep balance even if the bicycle does not move forward. From many possible solutions (which are listed and briefly described in the following Chapters) the Author has chosen the reaction wheel system.

In this work, the bicycle is treated as a specified dynamic controllable object and it consists of: the rigid frame, two wheels and the handlebar. Generally, this object has two degrees of freedom: the angle from the vertical position of the frame and the angle of the handlebar. Additionally, it is also able to travel forward with specified velocity, which is treated only as a fixed parameter not as an additional degree of freedom. When each degree of freedom is near to zero for some period of time then the biycycle is defined as stable. It can be analysed as an open-loop system (without feedback control) and as a closed-loop system (with regulator). Finally, for both of them the stability can be determined which again is based on these two degrees of freedom.

The classic design of the bicycle is brilliant what strongly contributes to its such long-lasting popularity. It is interesting how to improve something already so perfect, and how to improve the bicycle construction idea. It is interesting whether the reaction wheel is able to put a permanent change to this solution. Currently, it is difficult to find meaningful use of controlled rotating mass especially in any areas with a clear gravitational interaction – the reaction wheel is mainly used in the stabilization systems of satellites. The combination of the bicycle and the reaction wheel is interesting, intriguing, promising and is a very good research material, which with appropriate assumptions can lead to interesting results.

Finally, the main thesis of the dissertation is stated as follows:

- **The use of the reaction wheel combined with selected control algorithms improves bicycle stability.**

There are important questions that can help to solve the main problem:

1. Is the reaction wheel able to stabilize the inverted pendulum? How to test it? Which control law should be used?
2. How to describe the bicycle mathematically with the reaction wheel to test the most important states when keeping balance is difficult?
3. Which algorithm should be used to control the whole state of the bicycle with the reaction wheel using available control signals (the handlebar torque and the reaction wheel torque)?

4. Are there any conditions, when the reaction wheel control is better than the handlebar control to stabilize the bicycle? How to evaluate it?

1.2 Overview of the dissertation

This dissertation is divided into several Chapters. At the beginning, the mathematical models are presented. The following objects are considered: two degrees of freedom reaction wheel pendulum, two degrees of freedom bicycle and three degrees of freedom bicycle with the reaction wheel unit. Each one is treated separately and many symbols are repeated (in order to increase the transparency of mathematical formulas). Considered objects are expressed by detailed kinematic schemes. There are various differential equations and many explanations why it is decided to take a scientific solution. The complete mathematical model is summarized and presented by differential state-space equations. Next, the control techniques are presented. At the beginning, there are some concepts of control laws with the most important formulas are introduced. After that, the detailed stability analysis is presented and each considered model is explored. The analysis gives a lot of beneficial information which is of a great value, when selecting the parameters of the model. It also informs what are the limits of the considered construction when it must reject external disturbances. After that the result of computer simulations is presented. The improvement of stability of the bicycle with reaction wheel unit attached is presented. After that the energy flow analysis is taken into account which is generally focused on the reaction wheel system. It is showed where the energy flows and where the energy is converted into another form in this case. In Chapter 3 the experimental results presented. The real reaction unit has been prepared, identified and tested. It shows the main principle of operation of the system and it also approves the possibilities offered by stabilization unit. Finally, the whole considerations are summarized and concluded.

The essential content of this work has been included in two Chapters: 3 and 4.

In Chapter 3 the reaction wheel is presented. It includes the theoretical description of action and reaction physical principle, the verification via series of computer simulations and, finally, result of experiments on the real robot. This Chapter contains a series of arguments why to use the reaction wheel in the real applications. Additionally, there are: control design procedure, stability analysis, energy calculations and state estimation techniques based on the real sensory system.

In Chapter 4 the bicycle with the reaction wheel is presented. The full mathematical models of the bicycle with and without the reaction wheel is described in detail and the control design is considered. Using the stability analysis and computer simulations it is proved that the reaction wheel improves bicycle stability in certain range of physical conditions.

In this dissertation the reaction wheel is described in detail by physical equations, tested by computer simulations and, finally, the model is verified by an experiment on the real machine. The same applies to the bicycle except of the experiments. For this object the dissertation is focused on theoretical approach.

The subject of this work includes term: inertial drive. Actually it means here the actuator

which uses inertia as a main principle. In the literature the most common term is the reaction wheel and finally decided to use it in this dissertation.

Chapter 2

Background

The nominal operating point of bicycles is the upright unstable equilibrium point. The same applies to moving a human body. In many animal species, the nature decided through evolution to use this analogy. The inverted pendulum-like objects are characterized by huge dynamics. They usually are underactuated which means they have less actuators than degrees of freedom. Thus all of this is natural. Probably, this is the reason why people enjoy riding a bicycle rather than three- or four-wheeled vehicles. Bicycles are also: underactuated and dynamic. The connection a human body with the bicycle makes a new object, which is easily controllable by a human.

Unfortunately, riding the bicycle at extremely low velocities is impossible [96]. In this dissertation, it was decided to deal with this problem. The main goal is to analyse the additional actuator which can help to stabilize the system. Generally, there are three possible ways to do that without using the surrounding environment: shifting the center of mass, using a gyro drive or a reaction wheel drive.

The first one requires the system which can translate some a in a distance exactly specified by a controller [51, 55]. The same effect is used by cyclists – moving the body to the left or right side moves also the position of center of mass of the system. Such system has some disadvantages: it is usually quite large and it needs a huge additional mass. Its advantage is that it needs a little energy to operate.

The second balancing method relies on the gyroscopic effect (this effect is described in detail in [93] and tests on the bicycle in [15, 22]). Such systems always have an electric motor which accelerates the rotating mass to very high angular velocities (usually above 50000 rpm). When the axis (x of Cartesian coordinate system) of rotation of the disc is rotated along the second axis (y) it creates a torque in the third axis (z). Unfortunately it cannot produce stabilizing torque through infinite time – turning around the axis of rotation of the disc produces the sinusoidal torque in the third axis. Additionally, keeping high angular velocity requires a lot of energy to operate. The advantage of this system is that it can be successfully miniaturised. Sometimes a good concept is to use two or more small gyro actuators instead of a single big disc. There are some additional advantages using multiple gyro actuators at once – it helps the system to return to the initial state of after a series of disturbances (for details see [63–65]). In spacecraft controlling by gyroscopes is called CMG – Control Moment Gyroscope (good description of it can be found in [54]).

The third solution is very promising – it requires small amount of energy to operate, which is one of the biggest advantage of this solution. Unfortunately, it needs a relatively large reaction wheel to operate that needs to be installed on the machine. The large term means big or heavy, or both. Anyway, the moment of inertia needs to be big enough to

absorb as much kinetic energy as the object needs to be stabilized. Furthermore, the torque is being produced only during the acceleration of the rotating mass, and when the electric motor reaches the maximum angular velocity it does not produce the accelerating torque anymore. If it happens, the system loses the ability to use feedback signals.

At this moment the leading solution in stabilising motorcycles is Lit Motors Inc. from San Francisco founded by Daniel K. Kim in 2010 [17]. They are conducting research on fully electric, gyroscopically stabilized vehicle. The company aims to create mass production of this device. The main goal of it is to create a vehicle moving on two wheels transporting a passenger in a sealed cabin the same way as in the car.

The best results in reaction wheel stabilisation have been achieved in Cubli project in Swiss Federal Institute of Technology in Zurich (ETH Zurich) [35, 77, 78]. They have created a small cubical dice having three reaction wheels (one in each of the three dimensions). Researchers presented the advanced control algorithms that allowed balance on its corner.

At this year the Honda Motor Co., Ltd. company exposed on Consumer Electronics Show (CES 2017) in Las Vegas the Honda Riding Assist [16]. It is autonomous system which fully takes control of the front fork (by changing its angle) what results in keeping balance of the motorcycle moving at velocity lower than 5 m/s. The company wanted to implement a system to help maneuver heavy motorcycles, and thus encourage a larger number of users to use is.

In this dissertation, the Author has chosen the reaction unit to help to stabilize the bicycle. Advantages and disadvantages of this unit are presented and analysed. A deep review of current trends proves that this approach is original and novel. Today, it is hard to find the mathematical analysis of the bicycle combined with the reaction wheel together.

Losing stability of the bicycle is not only caused by too low velocity. It can also fall down if the handlebar control fails. For example people with limited mobility or blind people are not able to control a bicycle and this is the reason why they stop doing sport at all. With the reaction stabilization unit they could still use the two wheeled bicycle instead of struggling with three wheels or more and could feel as normal, healthy person again.

Using the stabilizing unit can increase a comfort of riding a bicycle. It is possible to stop the bicycle and keep balance without any external help. The futuristic vision is to let the robots travel by bicycles. Any supporting system in stabilization increases the robustness.

Today, the most known application of the reaction wheel is in geostationary satellites (for example neural control of the reaction wheel [98] or fault-tolerant control of the reaction wheel [12]). Usually, there are three reaction wheels in three different axes which are used to rotate the whole system to any orientation. This is the solution to the problem how to actuate the satellite using electric power from solar panels in no gravity region. Alternatively, the jet propulsion can be used there, but it uses extremely precious fuel gases which can not be refueled in space.

A very good idea is to use specially-shaped batteries to be rotated instead of steel as a reaction inertia. A stabilizing unit must be supplied by electricity so it must include a battery. Usually, increase in battery weight is undesired so why not take advantage of it?

It is possible that the future of human transportation is connected with autonomous ve-

hicles. Scientists have already considered such an idea [24, 108]. Why should people need single-track vehicles? Clear philosophy about an anthropological perspectives can be found in [105]. Generally, there are more and more people on the Earth and living areas become more and more crowded. People need to be transported and bicycles or motorcycles are perfect solutions because of their small size. The bicycle still evolves and some directions of it can be found in [11]. The idea of this dissertation is to give yet another new possible configuration of well-known bicycle using automatic control theory.

Bicycle was invented in the 19th century and since then it has been improving [13, 20, 44, 101]. There is a literature which describes the current technology how bicycles are constructed (it appears regularly – some examples are [45, 56, 85, 95]). Today, the urban infrastructure takes bicycles into account [33, 40]. The technology is changing: materials, geometry, mechanical solutions and design develop significantly almost in every year. Improving the stability of the bicycle could be undoubtedly a huge development in this area.

This work describes the analytical approach to the automatic control of the new object. A good mathematical model is crucial in this case. A vital information about bicycle modeling can be found in [74, 102]. This literature gives a great view of typical issues connected with the bicycle dynamics like: breaking, accelerating, friction, velocity, power, aerodynamics and many others.

Chapter 3

Reaction wheel

3.1 Idea of the system with the reaction wheel

The reaction phenomenon can be found everywhere where the Newton's third law applies (a great literature about physics principles is [2, 79, 88, 103]). Almost in every part of nature when some body acts on the other body using force then the same force is created but in the opposite direction and is called the reaction force. The same applies to torques. This effect is almost ubiquitous in our environment and without it the world would not work properly at all. In the correct configuration it can be used as a driving force for the body.

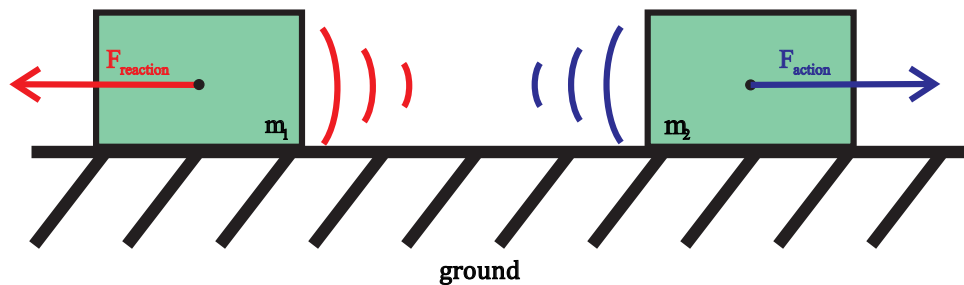


Figure 3.1: Linear reaction system

Figure 3.1 presents the linear reaction system. There are two bodies which slide on the surface without friction. The first body has a mass m_1 and the second has a mass m_2 . In this Figure, the repelling force is created – like between two magnets positioned to each other with the same poles. When the distance between them gets smaller, the magnetic force increases. The first body acts on the second body by acting force F_{action} which accelerates it. In response a second body acts the first body by reaction force $F_{reaction}$ which accelerates it but in the opposite direction this time. Usually, the direction of the reaction force can be reversed. When magnets are used in the appropriate position of different poles to one another, which must be ensured, since then first body attracts the second body and the second body attracts the first body. In other words, these two bodies accelerate with the same force value and with acceleration dependent on body mass on which this force acts. To sum up, the only parameter these body connects is the reaction force value. In the automatic control field, a good example of the linear reaction system is electromagnet with ferromagnetic material. The acting force is a controllable magnetic force of attraction. The reaction force has the same value, but the opposite direction. This leads to an important conclusion that reaction force can be controllable. This phenomenon can be used in many real applications. It is worth to

mention, that in this case it is difficult to control this force precisely, because the force of attraction of electromagnet is dependent on the current which flows in its coil and the distance between electromagnet and ferromagnetic part.

Fortunately, the rotating reaction system is much more convenient and suitable to control the reaction torque (Fig. 3.2). A great example is a DC electric motor with permanent magnets. Based on physical nature and the mathematical model of this machine [87] the torque is proportional to the current which flows in motor coils and almost completely independent from the motor shaft angle. Therefore, using the analogy it is possible and relatively easy achievable to control the reaction force in the electric motor. Such magnetic connection can be used in real applications. Thinking about real machines it is worth to imagine two bodies: the first is the controlling object and the second is the rotating mass which accelerates and decelerates depending on demand. The reaction system creates torque acting on the machine. This torque is controllable. This system is self-sufficient so it does not need any external object from environment to operate. It can be hermetically put in box and fitted into machine. This solution is perfect to implement to any inverted pendulum-like machines which have to balance near unstable equilibrium point (walking robots [41, 99, 106], traveling robots on wheels [28, 29, 107] and others). It is perfect to implement to the bicycle robot which is also an inverted pendulum. It is possible to stabilize an unmanned bicycle with zero velocity using the reaction wheel.

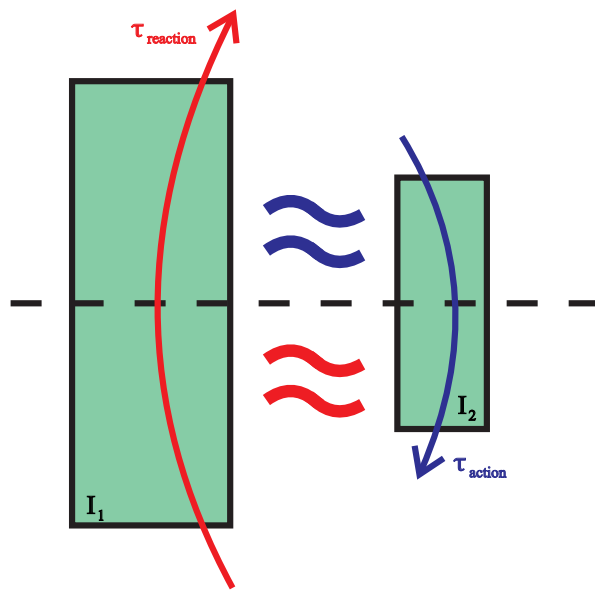


Figure 3.2: Rotating reaction system

Reaction wheel systems are often used in geostationary satellites which are in a state of weightlessness (it is worth look at the article [70] where this concept can be found). During theirs operation in the space, they have to correct its orientation regularly. Three reaction wheels can do this job in all three dimensions. Another example of taking an advantage of the reaction actuation is walking a tightrope with a pole. A human with a pole in his hands

is capable to keep the balance. His muscles produce the torque which accelerates the inertia and thanks to this the inertia acts on the human by stabilizing reaction torque. This could be promising technology of closed-loop control systems. In general, such actuation systems are not often used in the nonzero gravity places by the electromechanical engineering. Today it is worth to see things different and to explore new opportunities of robotic systems. This dissertation is intended to give a little piece of such kind of thinking.

This Chapter is based on several big theories which are essential to prepare mathematics presented here. It is based on analytical mechanics [43, 46, 97], control theory [5, 52] and differential equations theory [60, 61]. A lot of useful information can be found in book [8] in which is described the reaction wheel effect.

3.2 Mathematical modelling

In this Section, the full mathematical model of the reaction wheel pendulum is presented. A good way to describe a balancing system is to use the inverted pendulum structure. The aim is to stabilize it in unstable equilibrium point which is the vertical position when the center of mass of this construction is in the highest position. The general kinematic scheme is presented in Figure 3.3. In this Figure, two state-space x_1 and x_3 can be found and arrows which tell if the rotation has positive or negative value. These symbols represents two degrees of freedom and they are described as follows: x_1 is the angle of the robot from the vertical and x_3 is the rotation angle of the reaction wheel. The rest of them are their derivatives: x_2 is the angular velocity of the robot and x_4 is the rotation angle of the reaction wheel.

The pendulum has two degrees of freedom which are placed in two rotating joints. The first rotating joint is exactly where main part of the robot rotates relatively to the ground. The reaction wheel accelerates if resultant torque differs from zero and can be described as

$$\tau_r = \tau_g + \tau_{\text{reaction}} - \mu_r , \quad (3.1)$$

where τ_r is the torque acting on the robot, τ_g is gravity torque acting on the robot, τ_{reaction} is the reaction torque and μ_r is the friction torque acting on the robot from the environment. The second joint is in a place where the reaction wheel rotates. It accelerates under the resultant torque

$$\tau_I = \tau_{\text{action}} - \mu_I , \quad (3.2)$$

where τ_I is the torque acting on the reaction wheel, τ_{action} is the action torque and μ_I is the friction torque acting on the reaction wheel from the environment. The relation between action and reaction torques can be formulated as

$$\tau_{\text{action}} = -\tau_{\text{reaction}} . \quad (3.3)$$

Finally, the reaction torque (decreased by the friction) is produced only by the electric motor

$$\tau_{\text{action}} = \tau_m - \mu_m , \quad (3.4)$$

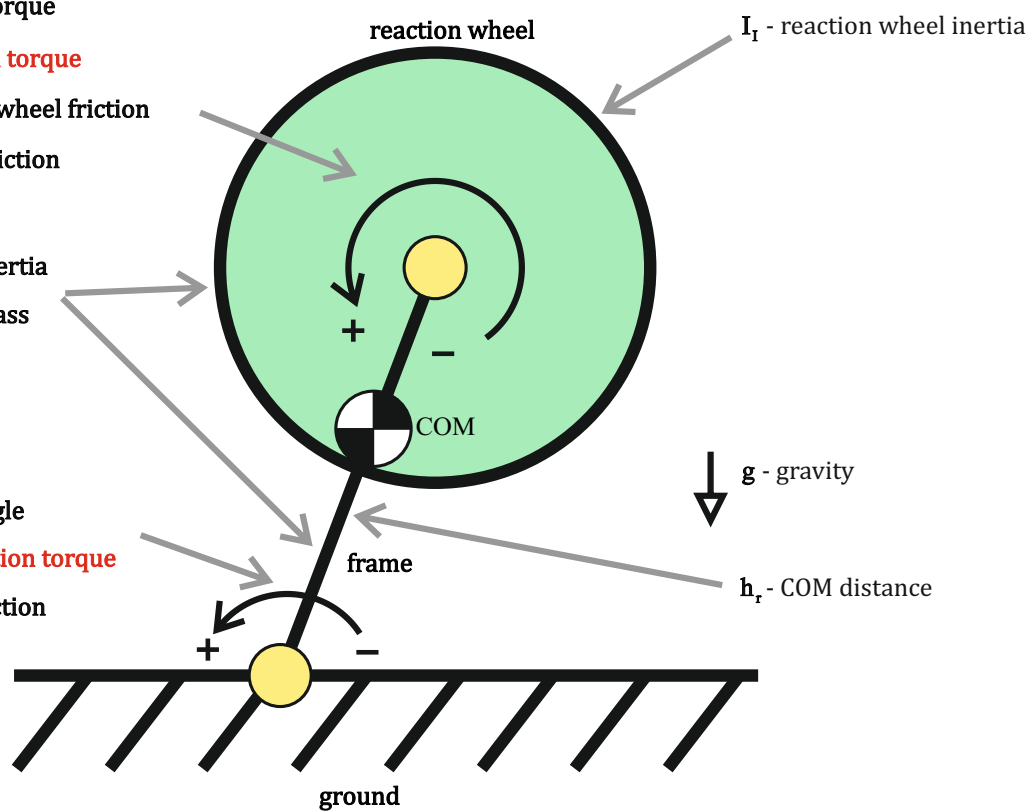
second joint x_3 - reaction wheel angle τ_m - motor torque (control) τ_g - gravity torque τ_{action} - action torque μ_I - reaction wheel friction μ_m - motor friction I_{rg} - robot inertia m_r - robot massfirst joint x_1 - robot angle τ_{reaction} - reaction torque μ_r - robot friction

Figure 3.3: Reaction wheel pendulum – kinematic scheme

where τ_m is the electric motor torque and μ_m is the friction torque acting on the electric motor shaft. The most important torques are marked in Figure 3.3.

To have a full mathematical model of the reaction wheel pendulum it is necessary to describe all mentioned symbols:

$$\tau_r = I_{rg}\dot{x}_2, \quad (3.5)$$

$$\tau_I = I_I\dot{x}_4, \quad (3.6)$$

$$\tau_g = m_rgh_r \sin(x_1), \quad (3.7)$$

$$\tau_m = k_m u, \quad (3.8)$$

$$\mu_r = b_r x_2, \quad (3.9)$$

$$\mu_I = b_I x_4, \quad (3.10)$$

$$\mu_m = b_m (x_4 - x_2), \quad (3.11)$$

where:

- I_{rg} is the moment of inertia of the robot relative to the ground,
- I_I is the moment of inertia of the rotating mass,
- m_r is the weight of the robot,
- g is the gravity of the Earth,
- h_r is the distance from the ground to the center of mass of the robot,
- k_m is the electric motor constant,
- b_r is the coefficient of friction in the robot rotation,
- b_I is the coefficient of friction in the rotation of the reaction wheel,
- b_m is the coefficient of friction in the rotation of the electric motor,
- the difference $(x_4 - x_2)$ is the rotation speed of the motor shaft relative to the ground.

The moment of inertia of the rotating mass is

$$I_I = I_{\text{reaction_wheel}} + I_{mr}, \quad (3.12)$$

where $I_{\text{reaction_wheel}}$ is the moment of inertia of the reaction wheel and I_{mr} is the moment of inertia of the rotor of the motor.

The mathematical model is needed to simulate the system and prepare appropriate control law to stabilize it in the unstable equilibrium point (vertical pose).

It was decided to use the state-space representation in the form

$$\dot{\underline{x}}(t) = \underline{f}(t, \underline{x}(t), \underline{u}(t)), \quad (3.13)$$

$$\underline{y}(t) = \underline{h}(t, \underline{x}(t), \underline{u}(t)). \quad (3.14)$$

where the state vector $\underline{x} \in \mathcal{R}^n$, the output vector $\underline{y} \in \mathcal{R}^p$, the control vector is $\underline{u} \in \mathcal{R}^m$, the algorithm describing changes in state vector $\underline{f}, \underline{h}$ is the output function.

The system is presented by the following equations (henceforth, time indices are omitted for brevity):

$$\dot{x}_1 = x_2, \quad (3.15)$$

$$\dot{x}_2 = \frac{gh_r m_r \sin(x_1)}{I_{rg}} - \frac{b_r x_2}{I_{rg}} - \frac{b_m x_2}{I_{rg}} + \frac{b_m x_4}{I_{rg}} - \frac{k_m u}{I_{rg}}, \quad (3.16)$$

$$\dot{x}_3 = x_4, \quad (3.17)$$

$$\dot{x}_4 = \frac{k_m u}{I_I} + \frac{b_m x_2}{I_I} - \frac{b_I x_4}{I_I} - \frac{b_m x_4}{I_I}. \quad (3.18)$$

The above model takes centrifugal force, gravitation force and also reaction momentum from reaction wheel into account.

Each physical parameter can be found in Section 3.8. This Section describes the real construction in detail.

It is possible to find the linear control law for this system ensuring its stability. To do so it is necessary to linearize the nonlinear system presented before. It was decided to use the Jacobian matrix method which is capable to linearize in any point of state [18].

Derivative of the state needs to be described by the new function f :

$$\dot{\underline{x}} = [\dot{x}_1, \dot{x}_2, \dot{x}_3, \dot{x}_4]^T = [f_1, f_2, f_3, f_4]^T, \quad (3.19)$$

similarly, the output y must be expressed by the new function h :

$$\underline{y} = [x_1, x_2, x_3, x_4]^T = [h_1, h_2, h_3, h_4]^T, \quad (3.20)$$

where f and h are differentiable. The linear system is presented by

$$\dot{\underline{x}} = \mathbf{A}\underline{x} + \mathbf{B}\underline{u}, \quad (3.21)$$

$$\underline{y} = \mathbf{C}\underline{x}, \quad (3.22)$$

where $\mathbf{A} \in \mathcal{R}^{n \times n}$, $\mathbf{B} \in \mathcal{R}^{n \times p}$ and $\mathbf{C} \in \mathcal{R}^{q \times n}$.

Every matrix of the state-space model: \mathbf{A} , \mathbf{B} , \mathbf{C} and \mathbf{D} can be expressed by Jacobian matrix

$$\mathbf{A} = \left[\begin{array}{cccc} \frac{\partial f_1}{\partial x_1} & \frac{\partial f_1}{\partial x_2} & \frac{\partial f_1}{\partial x_3} & \frac{\partial f_1}{\partial x_4} \\ \frac{\partial f_2}{\partial x_1} & \frac{\partial f_2}{\partial x_2} & \frac{\partial f_2}{\partial x_3} & \frac{\partial f_2}{\partial x_4} \\ \frac{\partial f_3}{\partial x_1} & \frac{\partial f_3}{\partial x_2} & \frac{\partial f_3}{\partial x_3} & \frac{\partial f_3}{\partial x_4} \\ \frac{\partial f_4}{\partial x_1} & \frac{\partial f_4}{\partial x_2} & \frac{\partial f_4}{\partial x_3} & \frac{\partial f_4}{\partial x_4} \end{array} \right]_{\substack{x=x_0 \\ u=u_0}}, \quad (3.23)$$

$$\mathbf{B} = \left[\begin{array}{c} \frac{\partial f_1}{\partial U_1} \\ \frac{\partial f_2}{\partial U_1} \\ \frac{\partial f_3}{\partial U_1} \\ \frac{\partial f_4}{\partial U_1} \end{array} \right]_{\substack{x=x_0 \\ u=u_0}}, \quad (3.24)$$

$$\mathbf{C} = \left[\begin{array}{cccc} \frac{\partial h_1}{\partial x_1} & \frac{\partial h_1}{\partial x_2} & \frac{\partial h_1}{\partial x_3} & \frac{\partial h_1}{\partial x_4} \\ \frac{\partial h_2}{\partial x_1} & \frac{\partial h_2}{\partial x_2} & \frac{\partial h_2}{\partial x_3} & \frac{\partial h_2}{\partial x_4} \\ \frac{\partial h_3}{\partial x_1} & \frac{\partial h_3}{\partial x_2} & \frac{\partial h_3}{\partial x_3} & \frac{\partial h_3}{\partial x_4} \\ \frac{\partial h_4}{\partial x_1} & \frac{\partial h_4}{\partial x_2} & \frac{\partial h_4}{\partial x_3} & \frac{\partial h_4}{\partial x_4} \end{array} \right]_{\substack{x=x_0 \\ u=u_0}}. \quad (3.25)$$

After solving these matrices the system is linearized in one point of state and control space. This point is indicated by: \underline{x}_0 and \underline{u}_0 and is called the equilibrium point (zero in this case). Replacing the derivatives, the \mathbf{A} matrix takes the form

$$\mathbf{A} = \begin{bmatrix} 0 & 1 & 0 & 0 \\ \frac{gh_r m_r}{I_{rg}} \cos(x_1) & -\frac{b_m + b_r}{I_{rg}} & 0 & \frac{b_m}{I_{rg}} \\ 0 & 0 & 0 & 1 \\ 0 & \frac{b_m}{I_I} & 0 & -\frac{b_I + b_m}{I_I} \end{bmatrix}_{\substack{x=x_0 \\ \underline{u}=\underline{u}_0}}, \quad (3.26)$$

which still has a nonlinear part which is cos function. Using the equilibrium point value

$$\mathbf{A} = \begin{bmatrix} 0 & 1 & 0 & 0 \\ \frac{gh_r m_r}{I_{rg}} \cos(x_{10}) & -\frac{b_m + b_r}{I_{rg}} & 0 & \frac{b_m}{I_{rg}} \\ 0 & 0 & 0 & 1 \\ 0 & \frac{b_m}{I_I} & 0 & -\frac{b_I + b_m}{I_I} \end{bmatrix}. \quad (3.27)$$

If it is necessary, it is possible to implement this matrix in the real system and linearize it in many points in state space. If the equilibrium point is a zero vector, then system matrices are:

$$\mathbf{A}_{\substack{\underline{x}_0=0 \\ \underline{u}_0=0}} = \begin{bmatrix} 0 & 1 & 0 & 0 \\ \frac{gh_r m_r}{I_{rg}} & -\frac{b_m + b_r}{I_{rg}} & 0 & \frac{b_m}{I_{rg}} \\ 0 & 0 & 0 & 1 \\ 0 & \frac{b_m}{I_I} & 0 & -\frac{b_I + b_m}{I_I} \end{bmatrix}, \quad (3.28)$$

$$\mathbf{B} = \begin{bmatrix} 0 \\ -\frac{k_m}{I_{rg}} \\ 0 \\ \frac{k_m}{I_I} \end{bmatrix}, \quad (3.29)$$

$$\mathbf{C} = \begin{bmatrix} 1 & 0 & 0 & 0 \\ 0 & 1 & 0 & 0 \\ 0 & 0 & 1 & 0 \\ 0 & 0 & 0 & 1 \end{bmatrix}. \quad (3.30)$$

The discrete-time system is formulated by equations (3.38) and (3.39).

It is possible to find the constant matrices: \mathbf{A}_d , \mathbf{B}_d and \mathbf{C}_d of discrete-time model: (3.40)-

(3.42), and after calculations:

$$\mathbf{A}_d = \begin{bmatrix} 1.0004 & 0.0033 & 0 & 0 \\ 0.2464 & 1.0004 & 0 & 0 \\ 0 & 0 & 1.0000 & 0.0033 \\ 0 & 0 & 0 & 1.0000 \end{bmatrix}, \quad (3.31)$$

$$\mathbf{B}_d = \begin{bmatrix} -0.0000 \\ -0.0146 \\ 0.0003 \\ 0.1566 \end{bmatrix}, \quad (3.32)$$

$$\mathbf{C}_d = \begin{bmatrix} 1 & 0 & 0 & 0 \\ 0 & 1 & 0 & 0 \\ 0 & 0 & 1 & 0 \\ 0 & 0 & 0 & 1 \end{bmatrix}. \quad (3.33)$$

The discretization period T_d is equal to 0.003 s. This discrete-time model is necessary to complete control law calculations presented below. Further decrease in the T_d does not change the final result of Riccati solution (it was tested by computer calculations). The remaining details can be found in the next Chapter.

3.3 Control algorithm design

3.3.1 Overview of stabilization techniques

There are several possible ways to design the control law which is able to stabilize the reaction wheel pendulum using feedback signals from sensors. Basic PID controller [10] is certainly insufficient to deal with this task, because it has one input and one output. In this case, it is necessary to stabilize all state-space variables simultaneously. The plant is undoubtedly nonlinear therefore the control system needs to be correctly designed. There are advanced techniques which are specially designed for nonlinear systems such us: sliding mode control [57], Lyapunov redesign [94], Feedback Linearization (FBL) [32], fuzzy logic control [14, 36], neural control [73] and some kinds of predictive control [69]. There is also a control algorithm based on Lyapunov theory which is the Backstepping method invented in 1990 by Petar V. Kokotović and well described in [59]. It was tested in the real application of the reaction wheel pendulum in [81, 83] however result was not satisfactory. It is necessary to describe the plant in the strict feedback form which is impossible for underactuated systems – like reaction wheel pendulum. For this reason the backstepping algorithm is not able to control the whole state vector.

In this dissertation, it is decided to use the LQR method to control the reaction wheel pendulum. As is described below this algorithm is able to stabilize considered nonlinear object. The Linear Quadratic Regulator (LQR – well described in [48, 68]) was originally developed for a linear systems description. Based on this the control law is optimal. The main goal is to minimize the quadratic cost function what is possible by solving the Riccati equations. This algorithm is also very useful for nonlinear systems since it nonlinear systems can be linearized for any state and can be controlled by linear regulator near the linearization point. If it is necessary, this action can be performed of many points of the state-space. The results of calculations can be fixed and stored or the whole calculation can be done on-line (interactively).

It is worth to mention that the real application of the reaction wheel pendulum was tested with FBL algorithm with results published in [109, 110]. Application of the FBL method slightly improved the control process (decreased the performance indices) in comparison with the LQR.

3.3.2 Fundamentals of quadratic control

The main purpose of the classic LQR controller is stabilization. The fundamental block diagram is presented in Figure 3.4. The system is described by state-space differential equations (3.21)-(3.22).

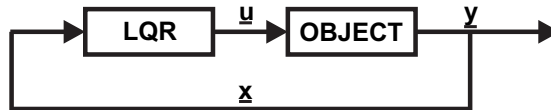


Figure 3.4: Block diagram of the LQR control system

It is possible to solve the LQR problem for the system to find the infinite-horizon, continuous-time LQR law. First of all, the control law is presented by

$$\underline{u}_c = -\mathbf{K}_c \underline{x}, \quad (3.34)$$

where $\mathbf{K}_c \in \mathcal{R}^{p \times n}$ is the state-feedback matrix.

It guarantees minimizing the quadratic cost function

$$J_c = \int_0^{\infty} [\underline{x}^T \mathbf{Q}_c \underline{x} + \underline{u}^T \mathbf{R}_c \underline{u}] dt, \quad (3.35)$$

where $\mathbf{R}_c > 0$ is the input weighting matrix and $\mathbf{Q}_c \geq 0$ is the state weighting matrix.

In short, it is of prime importance to find the \mathbf{K}_c matrix analytically. To reach this goal it is necessary to solve the Continuous-time Algebraic Riccati Equation (CARE)

$$\mathbf{A}^T \mathbf{P}_c + \mathbf{P}_c \mathbf{A} - \mathbf{P}_c \mathbf{B} \mathbf{R}_c^{-1} \mathbf{B}^T \mathbf{P}_c + \mathbf{Q}_c = \mathbf{0}, \quad (3.36)$$

and then to obtain the \mathbf{K}_c matrix

$$\mathbf{K}_c = \mathbf{R}_c^{-1} \mathbf{B}^T \mathbf{P}_c. \quad (3.37)$$

The solution of the CARE is the $\mathbf{P}_c > 0$ matrix.

Unfortunately, the computation of CARE is difficult especially by embedded microcontroller system in the real time [1, 21]. There is the alternative version of LQR control addressed to discrete-time systems. In this case, the Riccati equation looks different and is calculated on-line. This kind of approach is much easier to implement on digital machines. The final result of these two methods (for small discretization period T_d) should be almost the same. In other words, the matrix \mathbf{K} calculated by discrete time version of Riccati equation should tend to the \mathbf{K}_c calculated by the continuous-time version of Riccati equation after a finite number of iterations. This number is usually between one hundred and one thousand.

The discrete-time model of the system is presented by the following equations

$$\underline{x}_{k+1} = \mathbf{A}_d \underline{x}_k + \mathbf{B}_d \underline{u}_k, \quad (3.38)$$

$$\underline{y}_k = \mathbf{C}_d \underline{x}_k, \quad (3.39)$$

where index k is the discrete time.

Discretization of the continuous-time state-space model can be done by infinite series expansion (the sum of infinite series of components) [104]. This solution can be easily implemented in the real time computing machine. The matrices: \mathbf{A} and \mathbf{B} are discretized by following equations:

$$\mathbf{A}_d \approx \mathbf{I} + \mathbf{A} \left(\mathbf{I} T_d + \frac{\mathbf{A} T_d^2}{2!} + \frac{\mathbf{A}^2 T_d^3}{3!} + \dots + \frac{\mathbf{A}^{m-1} T_d^m}{m!} \right), \quad (3.40)$$

$$\mathbf{B}_d \approx \left(\mathbf{I} T_d + \frac{\mathbf{A} T_d^2}{2!} + \frac{\mathbf{A}^2 T_d^3}{3!} + \dots + \frac{\mathbf{A}^{m-1} T_d^m}{m!} \right) \mathbf{B}, \quad (3.41)$$

where \mathbf{I} is the identity matrix, m is the number of elements of the sequence, $m \in \mathbb{N}$, $m > 0$.

Discrete-time comparison of \mathbf{C} is more straightforward to compute

$$\mathbf{C}_d = \mathbf{C}. \quad (3.42)$$

The finite-horizon discrete-time LQR controller minimizes the following cost function:

$$J = \sum_{i=0}^n [\underline{x}_i^T \mathbf{Q} \underline{x}_i + \underline{u}_i^T \mathbf{R} \underline{u}_i]. \quad (3.43)$$

In this case,

$$\mathbf{K} = (\mathbf{R} + \mathbf{B}_d^T \mathbf{P} \mathbf{B}_d)^{-1} \mathbf{B}_d^T \mathbf{P} \mathbf{A}_d. \quad (3.44)$$

Finally, it is necessary to solve the Riccati equation. The discrete-time dynamic Riccati equation (DARE) is represented by the formula:

$$\mathbf{P}_{j-1} = \mathbf{Q} + \mathbf{A}_d^T \left(\mathbf{P}_j - \mathbf{P}_j \mathbf{B}_d (\mathbf{R} + \mathbf{B}_d^T \mathbf{P}_j \mathbf{B}_d)^{-1} \mathbf{B}_d^T \mathbf{P}_j \right) \mathbf{A}_d, \quad (3.45)$$

where j is the iteration index. As can be seen, the solution of this equation can be reached iteratively what means it is well implementable.

3.3.3 General control law

Designing an effective control law for the reaction wheel pendulum is quite complex. There are many constraints that need to be taken into account as an example the limited torque produced by the main electric motor which accelerates the rotating mass. The maximum velocity of rotating mass is also limited. Additionally, the angle from the vertical position of pendulum is limited by the ground level. In other words, the state-space and the admissible control space is constrained by many factors. This is quite typical for underactuated systems and the reaction wheel is a good example of it. When the control law is designed properly (matrices \mathbf{R} and \mathbf{Q} are correctly estimated), it keeps balance, and it is difficult to force the robot to fall on the ground, it is resistant to external disturbances and it uses low amount of electric energy to operate. Usually, it is worth to keep a proper distance to forbidden states of machine (like limit values of velocities or currents) to decrease demand for electric energy.

The reaction wheel pendulum is a nonlinear dynamical system. To control it well it is possible to use a nonlinear control techniques or linear control based on linearized description in the properly selected point. In this dissertation, several control strategies are proposed. Generally, it is based on linear quadratic regulation or backstepping regulation. Below, detailed derivation is presented which describe series of solutions.

It is possible to use a full mathematical model (3.15)-(3.18) to design the control law based on the LQR design procedure. The system can be expressed by (3.21)-(3.22). The system has only one control input u with its impact defined by vector \underline{b} . The linear quadratic control law is the result of a product of a multiplication of two vectors

$$u = -\underline{k}^T \underline{x}, \quad (3.46)$$

where \underline{k} is a new vector which consists of four scalar values

$$\underline{k} = [k_1, k_2, k_3, k_4]^T. \quad (3.47)$$

Linear quadratic controller design parameters are specified by R and \mathbf{Q} . For the considered system and based on [62]:

$$R = 100, \mathbf{Q} = \begin{bmatrix} 1 & 0 & 0 & 0 \\ 0 & 1 & 0 & 0 \\ 0 & 0 & 1 & 0 \\ 0 & 0 & 0 & 1 \end{bmatrix}. \quad (3.48)$$

Riccati equations, gives the following solution:

$$\underline{k} = [123.97, 17.67, -0.10, -0.67]^T. \quad (3.49)$$

Such a regulator can be tested both by means of simulation and on a real robot (which is described in Section 3.8). Having calculated the controller it is possible to describe the new closed-loop system

$$\dot{\underline{x}} = (\mathbf{A} - \underline{b}\underline{k}^T)\underline{x}. \quad (3.50)$$

It can be written in a simpler form, which is a typical linear system

$$\dot{\underline{x}} = \mathbf{A}_z \underline{x}. \quad (3.51)$$

Using symbols from a full linear model (3.28), matrix \mathbf{A}_z is equal to

$$\mathbf{A}_z = \begin{bmatrix} 0 & 1 & 0 & 0 \\ \frac{k_1 k_m}{I_{rg}} + \frac{g h_r m_r}{I_{rg}} & \frac{k_2 k_m}{I_{rg}} - \frac{b_m + b_r}{I_{rg}} & \frac{k_3 k_m}{I_{rg}} & \frac{b_m}{I_{rg}} + \frac{k_4 k_m}{I_{rg}} \\ 0 & 0 & 0 & 1 \\ -\frac{k_1 k_m}{I_I} & \frac{b_m}{I_I} - \frac{k_2 k_m}{I_I} & -\frac{k_3 k_m}{I_I} & -\frac{b_I + b_m}{I_I} - \frac{k_4 k_m}{I_I} \end{bmatrix}, \quad (3.52)$$

and consequently, it includes model symbols mixed with a regulator symbols. Replacing the symbols with scalar values from physical model yields

$$\mathbf{A}_z = \begin{bmatrix} 0 & 1 & 0 & 0 \\ -237.4090 & -36.2257 & -0.1389 & -0.8920 \\ 0 & 0 & 0 & 1 \\ 3331.3500 & 387.5210 & 1.4859 & 9.4328 \end{bmatrix}. \quad (3.53)$$

The closed-loop system needs to be stable, what means that the eigenvalues of matrix \mathbf{A}_z must have non-positive real values.

3.3.4 Tracking modification

Previously, the classic LQR was proposed. Its task was to stabilize the system in the equilibrium point and to minimize the cost function. This solution allows to reach only one point in the state space – the fixed equilibrium point. There is often a need to follow the desired trajectory by tracking control. The following equations explain how to modify the classic LQR control to get the tracking form.

The main idea is to translate the origin of the state-space by coordinates vectors \underline{x}_d and u_d of the desired point. It is formulated in the following way:

$$\dot{\underline{x}} = \mathbf{A}(\underline{x} - \underline{x}_d) + \underline{b}(u - u_d). \quad (3.54)$$

The cost function also needs to be modified to the following form:

$$J_d = \int_0^\infty \left[(\underline{x} - \underline{x}_d)^T \mathbf{Q} (\underline{x} - \underline{x}_d) + R(u - u_d)^2 \right] dt. \quad (3.55)$$

Finally, the control law for the tracking control becomes

$$u = -\underline{k}^T (\underline{x} - \underline{x}_d). \quad (3.56)$$

At any time, the desired state \underline{x}_d can be changed and the system must follow the desired trajectory. The optimal control guarantees the minimum quadratic cost reflecting designer's preferences matrices: R and Q .

The desired state \underline{x}_d is

$$\underline{x}_d = [x_{d1}, x_{d2}, x_{d3}, x_{d4}]^T. \quad (3.57)$$

The stabilizing control needs to be corrected by

$$u_{d1} = \frac{gh_r m_r}{k_m} \sin(x_{1d}) - \frac{b_r}{k_m} x_{2d} - \frac{b_m}{k_m} x_{2d} + \frac{b_m}{k_m} x_{4d}. \quad (3.58)$$

This equation can be obtained from (3.16) after replacing \underline{x} with \underline{x}_d and a few algebraic transformations.

3.3.5 State integration system LQI

Linear quadratic regulator can be transformed into yet another form. It is possible to create additional feedback which includes integrated state vector \underline{x}_i with the reference state vector (Fig. 3.5). Such a control algorithm is called the Linear Quadratic Integral (LQI) [31]. Using the integrated state vector can give the another capabilities to the system. Sometimes it is necessary to control the integrated state even if integration needs to be done numerically instead of performing direct measurement by sensors. The proposed block diagram shows how to make the reference state for yet another tracking control using the linear quadratic control theory. This approach proved to be useful to control the real reaction wheel pendulum (see results of experiments in Section 3.8) with only gyroscope sensor to measure the angle from the vertical position and the angular velocity of the pendulum. Such measurement device is relatively accurate compared to the other types but it has some crucial imperfections that need to be properly corrected. This is widely explained in Section 3.5.

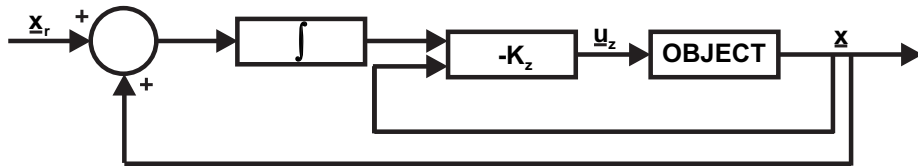


Figure 3.5: Block diagram of the LQI control system

The system is described by state-space equation (3.13). The difference \underline{x}_r and \underline{x} is integrated over time giving \underline{x}_i

$$\underline{x}_i = \int_0^\infty (\underline{x}_r - \underline{x}) dt, \quad (3.59)$$

where \underline{x}_r is the reference state. Let us define the new extended state vector

$$\underline{z} = [\underline{x}^T, \underline{x}_i^T]^T. \quad (3.60)$$

Expressing by the z label as above allows to use a typical quadratic regulator equations. A new \mathbf{K}_z matrix is given by

$$\mathbf{K}_z = [\underline{k}^T, \underline{k}_i^T]^T, \quad (3.61)$$

and the final control law becomes

$$\underline{u}_z = -\mathbf{K}_z \underline{z}, \quad (3.62)$$

It minimizes the following cost function

$$J = \int_0^\infty [\underline{z}^T \mathbf{Q} \underline{z} + R u_z^2] dt, \quad (3.63)$$

It is possible to check the stability of a new dynamic system which is described with parameters of a linear model and regulator

$$\dot{\underline{z}} = (\mathbf{A} - \mathbf{B} \mathbf{K}_z) \underline{z}, \quad (3.64)$$

and it can be simplified to

$$\dot{\underline{z}} = \mathbf{A}_z \underline{z}. \quad (3.65)$$

Stability of the system (3.65) relies on the eigenvalues of matrix $\mathbf{A}_z \in \mathcal{R}^{n \times n}$. Conclusions from this analysis can be used in many cases especially in identification and tuning process.

The aim is to solve the LQI control law of the reaction wheel. The system is described by equations (3.21)-(3.22). In this case \underline{k} and \underline{k}_i vectors have four elements:

$$\underline{k} = [k_1, k_2, k_3, k_4]^T, \quad (3.66)$$

$$\underline{k}_i = [k_{i1}, k_{i2}, k_{i3}, k_{i4}]^T. \quad (3.67)$$

The same applies to the \underline{x}_i vector

$$\underline{x}_i = [x_{i1}, x_{i2}, x_{i3}, x_{i4}]^T. \quad (3.68)$$

After a few substitutions A_z matrix for the reaction wheel pendulum

$$A_z = \begin{bmatrix} 0 & 1 & 0 & 0 \\ \frac{k_1 k_m}{I_{rg}} + \frac{g h_r m_r}{I_{rg}} & \frac{k_2 k_m}{I_{rg}} - \frac{b_m + b_r}{I_{rg}} & \frac{k_3 k_m}{I_{rg}} & \frac{b_m}{I_{rg}} + \frac{k_4 k_m}{I_{rg}} \\ 0 & 0 & 0 & 1 \\ -\frac{k_1 k_m}{I_I} & \frac{b_m}{I_I} - \frac{k_2 k_m}{I_I} & -\frac{k_3 k_m}{I_I} & -\frac{b_I + b_m}{I_I} - \frac{k_4 k_m}{I_I} \\ 1 & 0 & 0 & 0 \\ 0 & 1 & 0 & 0 \\ 0 & 0 & 1 & 0 \\ 0 & 0 & 0 & 1 \\ \dots & & & \\ 0 & 0 & 0 & 0 \\ \frac{k_{i1} k_m}{I_{rg}} & \frac{k_{i2} k_m}{I_{rg}} & \frac{k_{i3} k_m}{I_{rg}} & \frac{k_{i4} k_m}{I_{rg}} \\ 0 & 0 & 0 & 0 \\ -\frac{k_{i1} k_m}{I_I} & -\frac{k_{i2} k_m}{I_I} & -\frac{k_{i3} k_m}{I_I} & -\frac{k_{i4} k_m}{I_I} \\ 0 & 0 & 0 & 0 \\ 0 & 0 & 0 & 0 \\ 0 & 0 & 0 & 0 \\ 0 & 0 & 0 & 0 \\ \dots & & & \end{bmatrix}, \quad (3.69)$$

and

$$\underline{k}_i = [0, 0, 0.01, 0]^T. \quad (3.70)$$

In this research, it has been verified how a relatively small value in integral feedback can affect the system. In the rest of this dissertation results of various computer simulations (Section 3.6) and experiments on the real machine (Section 3.8) are presented which show effect of this kind of control law.

After substitution with scalar,

$$\mathbf{A}_z = \begin{bmatrix} 0 & 1 & 0 & 0 & 0 & 0 & 0 & 0 \\ -237.4090 & -36.2257 & -0.1389 & -0.8920 & 0 & 0 & 0.4391 & 0 \\ 0 & 0 & 0 & 1 & 0 & 0 & 0 & 0 \\ 3331.3500 & 387.5210 & 1.4859 & 9.4328 & 0 & 0 & -4.6987 & 0 \\ 1 & 0 & 0 & 0 & 0 & 0 & 0 & 0 \\ 0 & 1 & 0 & 0 & 0 & 0 & 0 & 0 \\ 0 & 0 & 1 & 0 & 0 & 0 & 0 & 0 \\ 0 & 0 & 0 & 1 & 0 & 0 & 0 & 0 \end{bmatrix}. \quad (3.71)$$

This is a great opportunity to verify if the considered closed-loop system is stable or not. Further information concerning the stability of the reaction wheel pendulum stabilized by LQI controller can be found in Section 3.4.

3.4 Stability of the system with reaction wheel

It is important to check the stability of the reaction wheel system especially when the real machine is constructed. In the control theory, there are various methods which allow to check the stability of the system. It can give a lot of meaningful information such as weighting and size of the elements, minimum and maximum control signals, phase margin and many others. In this dissertation two methods are used: eigenvalues analysis and step response.

The eigenvalues analysis is a well-known method in mathematics of dynamical systems theory which gives information about stability of linear systems. It can be used both to open-loop and closed-loop systems with the regulator. According to the first principle of Lyapunov it is possible to investigate stability of the nonlinear system based on its linear model obtained for the particular point of state. In this case, the machine is the inverted pendulum with the reaction wheel linearized in a vertical pose state. This method is based on the analysis of the location of eigenvalues on the complex plane. There are several rules that tell about the stability based on that location. If the absolute value of the real root becomes bigger, the damping of oscillations increases. When at least one complex root is bigger than zero, then the system oscillates. When the complex roots increase, also the oscillation increases. When there is one zero value real root, then the system is marginally stable.

Necessary equations needed to calculate the eigenvalues of the considered systems are presented in Table 3.1. The first system is the open-loop reaction wheel pendulum. The second and the third one apply to a control feedback are, respectively, the following algorithms: LQR and LQI. The λ symbolizes the eigenvalues. Table 3.2 presents eigenvalues of three considered systems.

Table 3.1: Characteristic equation depending on the type of the reaction wheel system

System type	Characteristic equation
open-loop	$\det(\underline{I}\lambda - \underline{A}) = 0$
LQR, LQI	$\det(\underline{I}\lambda - \underline{A}_z) = 0$

Table 3.2: Eigenvalues of different types of reaction wheel systems

System type	Eigenvalues λ
open-loop	0.0000
	8.5872
	– 8.6081
	– 0.2232
LQR	– 10.3796
	– 8.1276 + 0.9352 <i>i</i>
	– 8.1276 – 0.9352 <i>i</i>
	– 0.1581
LQI	0.0000
	0.0000
	0.0000
	– 10.6115
	– 7.9197 + 0.7319 <i>i</i>
	– 7.9197 – 0.7319 <i>i</i>
	0.5684
	– 0.9104

First of all, the inverted pendulum without any control is unstable. One of its root has a positive real part therefore collapsing from the unstable equilibrium point is inevitable for nonzero \underline{x}_0 . Because in this case every complex value is zero, there are no oscillations at all – the pendulum smoothly falls to the ground. As can be noticed, only the reaction wheel system with LQR controller is truly stable in infinite time horizon – each pole has a non-positive real part. This time the inverted pendulum is able to balance vertically in the vicinity of the equilibrium point. It is worth to mention is that it has two poles with nonzero complex parts and negative real parts, thus the pendulum stabilizes with oscillating damping motion. The third system with LQI controller is unstable. It has one pole with positive real part and two poles with negative real parts and nonzero complex parts. This means that the system is unstable and also its movements tend to have damping oscillation nature. This unstable positive real part pole is equal to: 0.5684. These stable poles have more than fourteen times bigger modules than this unstable one. This probably means, that instability tendency is much smaller than stability one. This also may provide, that movement of only one of degree of freedom is unstable such as rotating of the reaction wheel. This may not cause immediate fall. These observations are corrected later in this dissertation with the computer simulations.

Another well-known method to analyze the stability of linear systems is step response. It is suitable to SISO type objects thus it is usually worth to have a transfer function-type model of the system. There are as many transfer functions as the exact rank of \mathbf{A} matrix multiplied by rank of \mathbf{B} matrix (actually it gives the transfer function matrix). In this case, the full description of the open-loop and the LQR systems need four transfer functions and the LQI system needs eight transfer functions. These transfer functions have the control signal u as an input and output which does not always reflect a real physical parameter of the machine. However, the stability analysis based on the step responses is valuable to find if the system is stable and gives the estimated regulation time. Generally, in this stability analysis step response of the open-loop system is based on state space linear model (3.21) and (3.22). Inputs are defined by \mathbf{B} and outputs are defined by \mathbf{C} . When the system is stabilized by LQR or LQI is defined by following equation

$$\dot{\underline{x}} = (\mathbf{A} - \mathbf{B}\mathbf{K})\underline{x} + \mathbf{B}u \quad (3.72)$$

and (3.22). This time (like in open-loop system) inputs and outputs are defined by \mathbf{B} and \mathbf{C} , however it includes feedback defined by \mathbf{K} . Such step response analysis of the closed-loop system can give additional information about dynamics of the system like resistance to external disturbances. With the help of computing power of the program Matlab these transfer functions are calculated and listed in Table 3.3.

Table 3.3: Transfer functions of different types of reaction wheel systems

System type	Transfer function
Open-loop	$G_1(s) = \frac{-4.391s^2 - 0.4901s + 1.499 \cdot 10^{-14}}{s^4 + 0.2441s^3 - 73.92s^2 - 16.5s}$
	$G_2(s) = \frac{-4.391s^3 - 0.4901s^2}{s^4 + 0.2441s^3 - 73.92s^2 - 16.5s}$
	$G_3(s) = \frac{46.99s^2 + 0.4901s - 3473}{s^4 + 0.2441s^3 - 73.92s^2 - 16.5s}$
	$G_4(s) = \frac{46.99s^3 + 0.4901s^2 - 3473s}{s^4 + 0.2441s^3 - 73.92s^2 - 16.5s}$
LQR	$G_1(s) = \frac{-4.391s^2 - 0.4901s + 3.804 \cdot 10^{-14}}{s^4 + 26.79s^3 + 239.9s^2 + 732s + 109.8}$
	$G_2(s) = \frac{-4.391s^3 - 0.4901s^2 + 1.313 \cdot 10^{-15}s}{s^4 + 26.79s^3 + 239.9s^2 + 732s + 109.8}$
	$G_3(s) = \frac{46.99s^2 + 0.4901s - 3473}{s^4 + 26.79s^3 + 239.9s^2 + 732s + 109.8}$
	$G_4(s) = \frac{46.99s^3 + 0.4901s^2 - 3473s}{s^4 + 26.79s^3 + 239.9s^2 + 732s + 109.8}$
LQI	$G_1(s) = \frac{-4.391s^6 - 0.4901s^5 + 3.173 \cdot 10^{-14}s^4 + 5.504 \cdot 10^{-32}s^3}{s^8 + 0.2441s^7 - 73.92s^6 - 16.5s^5}$
	$G_2(s) = \frac{-4.391s^7 - 0.4901s^6}{s^8 + 0.2441s^7 - 73.92s^6 - 16.5s^5}$
	$G_3(s) = \frac{46.99s^6 + 0.4901s^5 - 3473s^4 + 1.299 \cdot 10^{-14}s^3 + 5.978 \cdot 10^{-32}s^2}{s^8 + 0.2441s^7 - 73.92s^6 - 16.5s^5}$
	$G_4(s) = \frac{46.99s^7 + 0.4901s^6 - 3473s^5}{s^8 + 0.2441s^7 - 73.92s^6 - 16.5s^5}$
	$G_5(s) = \frac{-4.391s^5 - 0.4901s^4 + 4.73 \cdot 10^{-14}s^3 - 1.01 \cdot 10^{-16}s^2 + 4.83 \cdot 10^{-31}s + 1.575 \cdot 10^{-48}}{s^8 + 0.2441s^7 - 73.92s^6 - 16.5s^5}$
	$G_6(s) = \frac{-4.391s^6 - 0.4901s^5 + 1.844 \cdot 10^{-13}s^4 - 3.869 \cdot 10^{-13}s^3 - 6.711 \cdot 10^{-31}s^2}{s^8 + 0.2441s^7 - 73.92s^6 - 16.5s^5}$
	$G_7(s) = \frac{46.99s^5 + 0.4901s^4 - 3473s^3 - 1.315 \cdot 10^{-14}s^2 - 2.028 \cdot 10^{-29}s - 3.765 \cdot 10^{-49}}{s^8 + 0.2441s^7 - 73.92s^6 - 16.5s^5}$
	$G_8(s) = \frac{46.99s^6 + 0.4901s^5 - 3473s^4 - 8.74 \cdot 10^{-15}s^3 - 7.072 \cdot 10^{-22}s^2}{s^8 + 0.2441s^7 - 73.92s^6 - 16.5s^5}$

The transfer function is the ratio of the Laplace transform of the output signal and the Laplace transform of the input signal. By using the inverse Laplace transform, the step response can be obtained according to the formula

$$y(t) = \mathcal{L}^{-1} \left\{ \frac{G(s)}{s} \right\} = h(t). \quad (3.73)$$

Figure 3.6 presents all step responses of different types of reaction wheel systems which are based on all transfer functions from Table: 3.3. This time only the reaction wheel stabilized by LQR controller (Fig. 3.6(b)) is stable and rest of systems are unstable (Fig. 3.6(a) and 3.6(c)). The same conclusion comes from eigenvalues analysis from Table 3.2.

Figure 3.6(a) presents four step responses of the open-loop reaction wheel system. As can be noticed, each step response proves, that the system is unstable – after 8 s the step values reaches enormously big numbers. This means that values tends to infinity and the system is unstable. The same can be noticed in LQI system in Figure 3.6(c). There are eight step responses that also reach infinite values after 8 s. Figure 3.6(b) presents four step responses of stable LQR system. Each of them shows that values reaches finite levels. This is sufficient to prove BIBO (Bounded Input Bounded Output) stability.

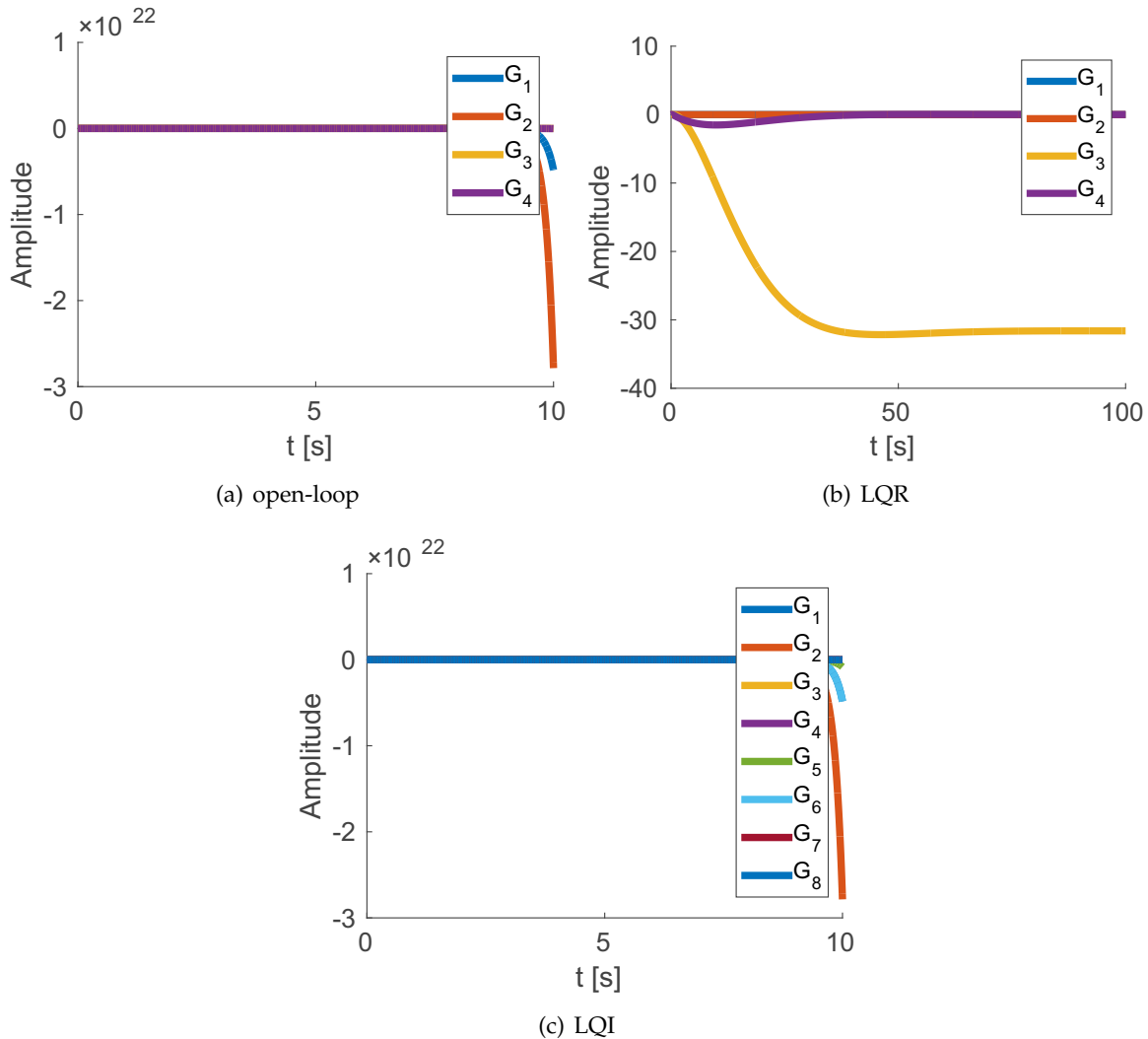


Figure 3.6: Step responses of different reaction wheel systems

This is important to know if the considered object is stable or not for assumed parameters. However, in order to improve knowledge about this subject it is worth to try how changes of important parameters can affect the stability.

This time five crucial parameters are chosen and taken into account. The result can be found in Figure 3.7. It presents the real parts of the eigenvalues as functions of selected parameters: r_I , m_I , h_I , b_r and b_I . Each examined parameter is in its own range of values (all

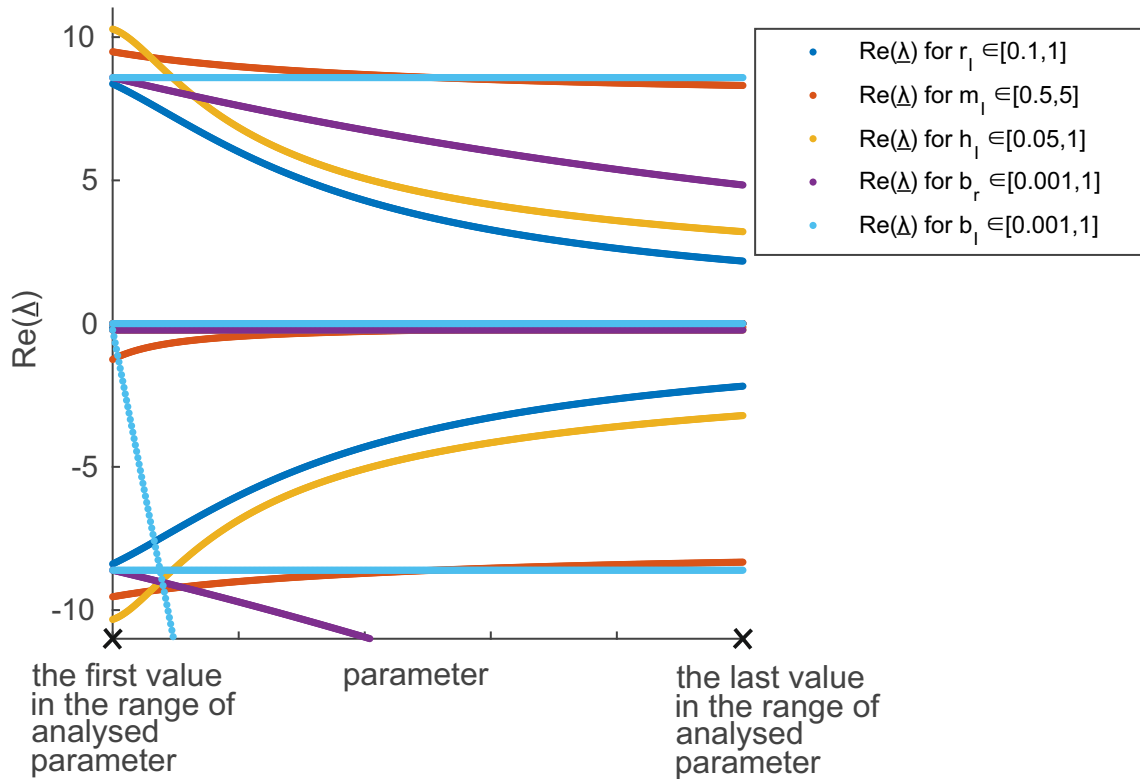


Figure 3.7: Real parts of the eigenvalues as functions of selected parameters: r_I , m_I , h_I , b_r and b_I

necessary details are in Figure 3.7). The system is unstable in every considered experiment.

The first parameter is the radius of the reaction wheel r_I . It starts from 0.1 m and ends at 1 m. As presented in Figure there are positive and negative roots. As the radius increases the absolute values of these roots decreases. When the positive real part of root decreases, the damping of the oscillations of the system increases. When the radius of the reaction wheel increases the moment of inertia grows. This means that it is more difficult to accelerate or decelerate this rotating mass and the dynamics of this part changes. Assuming that the friction in the electric motor is nonzero then this inertia also influence the whole structure and changes its dynamics. This is the explanation why making the radius r_I bigger causes increase of damping of oscillations in the system.

In general increasing rest of parameters also increases damping of oscillations in the system. The most important thing is that the positive roots fall and negative roots stay negative. When the reaction wheel weight m_I finally reaches 5 kg (from 0.5 kg at the beginning), the positive eigenvalue slightly decreases. In other words, the reaction wheel weight has a small impact on the values of roots. Different situation applies to the distance from the ground to the center of mass of the inertia h_I . Relatively small changes of this parameters results in a huge changes in roots especially it applies for initial range of values. For the biggest value the average distance from the imaginary axis of the roots is the biggest. Consequently, if the height of the inverted pendulum with the reaction wheel at the top rises the damping of the

oscillations of the system increases.

Linear increase of the coefficient of friction b_r causes a linear decrease of the positive root of the system. It may be obvious that when the b_r tends to infinity, then the inverted pendulum tends to be rigidly fixed to the ground. In this case it is not able to do any movements and is undoubtedly stable.

The second considered coefficient of friction b_I has a different effect on the position of roots. This is the coefficient of friction in the rotation of the reaction wheel – in other words the friction of the electric motor which accelerates the rotating mass. Figure shows that generally this factor has no effect on position of roots of the whole system – one of unstable positive root stays at the same level. It can also be noticed that one root tends from almost zero value to minus infinity.

All presented observations of the impact of the physical parameters of the pendulum with reaction wheel are of great value in designing process of the real machine. In conclusion, it is worth to focus especially on three parameters: radius of the reaction wheel r_I , distance from the ground to the center of mass of the inertia h_I and coefficient of friction in the robot rotation b_r . Increasing each of these parameters increases dumping of unwanted oscillations of the system.

3.5 Angle estimation with gyroscopic sensor

The implementation of the control algorithms in the real machine often causes multiple problems. The big challenge is to measure the state-space vector correctly with sufficient sampling frequency. In this Section, it is described how to measure deflection angle from the vertical position of the reaction wheel pendulum using mainly the gyroscopic sensor.

Nowadays, gyroscopic sensors are commonly used in many applications [19] (flying machines, walking robots, space satellites, mobile phones and many others). Currently they are mainly manufactured in MEMS (Microelectromechanical System) technology [67]. They are small, reliable, and energy efficient. The times that used rotating masses are long gone. The output of these sensors is the angular velocity. Unfortunately, they have one big drawback, which greatly complicates control algorithms – the drift. If the sensor does not rotate for a long time it should indicate zero angular velocity. The reality is different and every gyroscope output changes into nonzero value which is called the drift value. The control algorithm must compensate this effect using filters or proper techniques. In the course of research on this dissertation the Kalman filter was used. The estimation was used based on the angle from vertical position and the angular velocity of the robot based on the fusion of data from the two sensors: the gyroscope and the accelerometer. The accelerometer does not have a drift problem so it is perfect to get the appropriate reference. Today this is the classical approach to deal with the problem of gyroscopic drift compensation. Like any filtering as the Kalman filter brought an additional delay in the feedback loop. The robot stabilized properly however the reaction delay was clearly noticeable. Then it was decided to look for another method, which might be faster. The computer simulations (presented in the Section 3.6) and the experiments (Section 3.8) have led to the better solution. It has been noted that the com-

bination of the data from the gyroscope (with its imperfection) with selected features of the LQR optimal control algorithm gives a great and promising result using exactly this machine – the reaction wheel pendulum.

The greatest idea appeared after analysing the quadratic cost function (3.43). The aim of the LQR regulator is to minimize this cost as much as possible. Generally, the algorithm must leads each state value to zero: $\underline{x} \rightarrow 0$. During the research it turned out that sometimes is better to increase positively one state value and increase negatively some other state value to reach lower cost. In this case the conception is to let being increased the angle from vertical of the pendulum and the angle of the steering wheel at the same time. Of course this refers to the measured state not for the real state. Therefore, in this consideration a new symbol need to be introduced: the measured state $\underline{x}_m = [x_{m1}, x_{m2}, x_{m3}, x_{m4}]^T$. The measured state is used in control feedback in the real machine. The biggest problem is that it differs from the real state \underline{x} . In order to simplify the content presented here, it is assumed that the sensors measure the state continuously (with no discretization). It is also assumed that the angle of rotation of the reaction wheel and its angular velocity are measured without any errors. The angle with respect to the vertical position is the result of the integration of the gyroscope sensor output. The accelerometer which measures the acceleration (also the gravity) is used only once right after starting the robot and it gives the reference state.

To gather the most important assumptions mentioned above:

1. The accelerometer is used only once right after turning the robot on and it gives the reference angle from the vertical position.
2. The gyroscope sensor is used to get the angle from the vertical and the angular velocity of the robot. The velocity is integrated giving the angle.
3. The control law is designed using the LQR algorithm.
4. The controlled object is the reaction wheel pendulum.

At the beginning, two integrals can be introduced using the real state

$$x_1(t) = \int_0^\infty x_2(t)dt, \quad (3.74)$$

$$x_3(t) = \int_0^\infty x_4(t)dt. \quad (3.75)$$

The angular velocity measured by this sensor

$$x_{m2} = x_2 + \xi, \quad (3.76)$$

where ξ is the gyroscope drift and it is the source of all complications considered in this Section. When the real velocity is zero, the measured value is equal to ξ . When the computing unit integrates the nonzero gyroscope drift the result increases instead of being constant. It means that the LQR cost function (3.43) increases. To compensate this, the new symbol ω is

put into angular velocity intentionally

$$x_{m4} = x_4 + \omega . \quad (3.77)$$

It means that the reaction wheel becomes nonzero and rotates with the velocity equal to ω . In other words, the gyroscope drift ξ causes the reaction wheel velocity ω . The nonzero ξ is the cause and the increase in ω is the effect. This gives a balance in the cost function when the robot is stable. This is proved by computer simulations and experiments on the real object with results presented in Sections 3.6 and 3.8.

Now it is possible to formulate exact equations to describe how the computing unit calculates measured angles

$$\begin{aligned} x_{m1}(t) &= \int_0^\infty x_{m2}(t)dt = \int_0^\infty (x_2(t) + \xi(t))dt = \int_0^\infty x_2(t)dt + \int_0^\infty \xi(t)dt = \\ &= x_1(t) + \xi(t)t + c_1 , \end{aligned} \quad (3.78)$$

$$\begin{aligned} x_{m3}(t) &= \int_0^\infty x_{m4}(t)dt = \int_0^\infty (x_4(t) + \omega(t))dt = \int_0^\infty x_4(t)dt + \int_0^\infty \omega(t)dt = \\ &= x_4(t) + \omega(t)t + c_2 . \end{aligned} \quad (3.79)$$

As can be seen, these measured angles increases proportionally to ξ and ω . The result of these integrations are also constant coefficients: c_1 and c_2 which determine the initial state of the machine. The c_1 is the initial angle from the vertical and it can be measured by the accelerometer once right after starting of the robot. The c_2 is the initial angle of the steering wheel. Usually, it is assumed to be equal to zero. From now both these coefficients are ignored to avoid any confusion. They are irrelevant in presentation of the main idea of this Section. Finally, the measured state is equal to

$$\underline{x}_m = \begin{bmatrix} x_1 + \xi t \\ x_2 + \xi \\ x_3 + \omega t \\ x_4 + \omega \end{bmatrix} . \quad (3.80)$$

To make this case clear it is worth to use four new symbols. The machine starts from the real initial state \underline{x}_0 and after the infinite time the state is equal to the real final state \underline{x}_∞ .



Figure 3.8: Time horizon

The computing unit of the machine starts from the measured initial state \underline{x}_{m0} and after the infinite time the measured final state is $\underline{x}_{m\infty}$.

$$\underline{x}_0 = \begin{bmatrix} 0 \\ 0 \\ 0 \\ 0 \\ 0 \end{bmatrix} \implies \underline{x}_\infty = \begin{bmatrix} 0 \\ 0 \\ wt \\ \omega \end{bmatrix} = \begin{bmatrix} 0 \\ 0 \\ \varepsilon \\ \omega \end{bmatrix}, \quad (3.81)$$

$$\underline{x}_{m0} = \begin{bmatrix} 0 \\ \xi \\ 0 \\ 0 \end{bmatrix} \implies \underline{x}_{m\infty} = \begin{bmatrix} \xi t \\ \xi \\ wt \\ \omega \end{bmatrix} = \begin{bmatrix} \varepsilon \\ \xi \\ \varepsilon \\ \omega \end{bmatrix}, \quad (3.82)$$

where $\varepsilon \rightarrow \pm\infty$. Figure 3.8 symbolically shows change of time from zero to the infinity. The equations (3.81) and (3.82) describe how the real and measured states evolve from the starting moment to the infinite time. As can be seen, in (3.81) the reaction wheel permanently rotates with the velocity ω and the angle reaches the infinite value. The angle from vertical of the machine x_1 and its angular velocity x_2 are zero. The pendulum is stable in upright position. Another thing happens in the computing unit – both angles x_{m1} and x_{m3} go to the infinity and angular velocities x_{m2} and x_{m4} are nonzero (ξ and ω).

Now the question is: what is the relation between ξ and ω and what parameters affects it? To answer this question it is necessary to use equation from the mathematical model of the reaction wheel pendulum (3.17). Assuming that the acceleration of the robot is zero, $\dot{x}_2 = 0$, and using the equation (3.81)

$$0 = \frac{k_m u_{m\infty}}{I_I} + \frac{b_m \cdot 0}{I_I} - \frac{b_I \omega}{I_I} - \frac{b_m \omega}{I_I}, \quad (3.83)$$

and, finally,

$$u_{m\infty} = -\frac{b_I + b_m}{k_m} \omega. \quad (3.84)$$

This gives the control value $u_{m\infty}$ of the real machine from the mathematical model. The same control can be calculated using the LQR control law (3.34) and the measured state $\underline{x}_{m\infty}$

$$u_{m\infty} = -K \underline{x}_{m\infty}. \quad (3.85)$$

This allows to use (3.82), (3.84) and (3.85) giving

$$k_1\xi t + k_2\xi + k_3\omega t + k_4\omega = -\frac{b_I + b_m}{k_m}\omega, \quad (3.86)$$

which can be transformed into

$$\xi = -\frac{k_3 t + k_4 + \frac{b_I + b_m}{k_m}}{k_1 t + k_2} \omega. \quad (3.87)$$

This is actually the answer to the question stated above. The problem is the time variable t which increases to the infinity and is still in equation (3.87). To solve this problem it is necessary to calculate the limit of this function as time t approaches infinity

$$\lim_{t \rightarrow \infty} \xi = - \left(\lim_{t \rightarrow \infty} \frac{k_3 t}{k_1 t + k_2} + \lim_{t \rightarrow \infty} \frac{k_4}{k_1 t + k_2} + \lim_{t \rightarrow \infty} \frac{\frac{b_I + b_m}{k_m}}{k_1 t + k_2} \right) \omega = \quad (3.88)$$

$$= - \lim_{t \rightarrow \infty} \frac{k_3 t}{k_1 t + k_2} \omega = -\frac{k_3}{k_1} \omega. \quad (3.89)$$

The end result is as follows

$$\omega = -\frac{k_1}{k_3} \xi. \quad (3.90)$$

This is the final relation between ξ and ω . It depends only on LQR control law coefficients: k_1 and k_3 . In other words, it is possible to calculate the drift of the gyroscope sensor in the real machine when the velocity of the steering wheel is known – and vice versa.

Now yet another question: is it possible to make any modification in the control law to reduce the reaction wheel velocity to zero despite the gyroscope drift ξ exists?

In the previous consideration (mainly expressed by (3.81) and (3.82)), the angle of the reaction wheel constantly increases while the pendulum is in the stable position. To control the whole state, the additional integration in feedback loop is often used which is called the LQI control algorithm. This algorithm is more precisely described in Section 3.3.5. As it is presented there, the state of the machine \underline{x} is extended by its integration which finally gives the state \underline{z} . Observations of results of computer simulations and experiments on the real machine (presented in Sections: 3.6 and 3.8) prove, that the measured extended state \underline{z}_m is equal to

$$\underline{z}_m = \begin{bmatrix} x_1 + \xi t \\ x_2 + \xi \\ x_3 + \sigma \\ x_4 \\ x_{i1} \\ x_{i2} \\ x_{i3} + \sigma t \\ x_{i4} \end{bmatrix}, \quad (3.91)$$

where σ is the angle of the steering wheel when the pendulum is stabilized in the vertical position. As can be noticed, there is no ω in this equation like it is in previous solution in (3.80). It means that LQI control allows to stabilize the reaction wheel pendulum in the vertical position and reduce all velocities to zero even if the gyroscope sensor has a drift ξ .

A good way to explain how the LQI control algorithm stabilizes the reaction wheel pendulum is to express two states: initial state and state with time tending to infinity. There is a need to use the following symbols: \underline{z}_0 – the real initial LQI state, \underline{z}_∞ – the real LQI state with time tending to infinity, \underline{z}_{m0} – the measured initial LQI state and $\underline{z}_{m\infty}$ – the measured LQI state with time tending to infinity. These symbols are expressed in equation (3.92) and (3.93).

$$\underline{z}_0 = \begin{bmatrix} 0 \\ 0 \\ 0 \\ 0 \\ 0 \\ 0 \\ 0 \\ 0 \end{bmatrix} \implies \underline{z}_\infty = \begin{bmatrix} 0 \\ 0 \\ \sigma \\ 0 \\ 0 \\ 0 \\ \sigma t \\ 0 \end{bmatrix} = \begin{bmatrix} 0 \\ 0 \\ \sigma \\ 0 \\ 0 \\ 0 \\ \pm\infty \\ 0 \end{bmatrix}, \quad (3.92)$$

$$\underline{z}_{m0} = \begin{bmatrix} 0 \\ \xi \\ 0 \\ 0 \\ 0 \\ 0 \\ 0 \\ 0 \end{bmatrix} \implies \underline{z}_{m\infty} = \begin{bmatrix} \xi t \\ \xi \\ \sigma \\ 0 \\ 0 \\ 0 \\ \sigma t \\ 0 \end{bmatrix} = \begin{bmatrix} \pm\infty \\ \xi \\ \sigma \\ 0 \\ 0 \\ 0 \\ \pm\infty \\ 0 \end{bmatrix}. \quad (3.93)$$

The equation (3.92) describes how the real state changes in time when the machine is stabilized by LQI control algorithm. Initially, the whole state is zero. The gyroscope drift causes the reaction wheel to rotate by angle σ . The integral of it (which is the z_7) grows to infinity. Finally, no mechanical parts of the pendulum move at all. The measured LQI state (equation (3.93)) describes measured LQI state changes in time. Initially, every state variable is zero except the velocity z_{m2} which is equal to the drift ξ . After some period of time the LQI stabilizes the system, and the cost (3.63) is at the lowest possible level. In computing unit the measured angle from the vertical z_{m1} constantly grows and it is compensated by constantly growing z_{m7} . States z_{m2} and z_{m3} end with constant values ξ and σ .

Now it is worth to know what is the relation between ξ and σ . When the machine is stabilized by the LQI controller it does not move so the control value is zero (based on the equation (3.16)). Values from (3.93) can be put into the LQI control law (3.63) giving

$$0 = k_1\xi t + k_2\xi + k_3\sigma + k_{i3}\sigma , \quad (3.94)$$

and, finally,

$$\xi = -\frac{k_{i3}t + k_3}{k_1t + k_2}\sigma . \quad (3.95)$$

Once again the limit of the function as $t \rightarrow \infty$ needs to be calculated as below

$$\lim_{t \rightarrow \infty} \xi = -\left(\lim_{t \rightarrow \infty} \frac{k_{i3}t}{k_1t + k_2} + \lim_{t \rightarrow \infty} \frac{k_3}{k_1t + k_2}\right)\sigma = -\frac{k_{i3}}{k_1}\sigma . \quad (3.96)$$

Finally, the relation between ξ and σ becomes

$$\sigma = -\frac{k_1}{k_{i3}}\xi . \quad (3.97)$$

To sum up, the LQR control algorithm can be used to stabilize the reaction wheel pendulum using only gyroscope sensor. With the additional integrating feedback loop (LQI) it is possible to reduce all velocities to zero even if the drift of the gyroscope sensor is nonzero. This result can be achieved in the inverted pendulum machine.

3.6 Computer simulations

This Section includes series of computer simulations of the reaction wheel system. The detailed analysis of presented results describes how the reaction wheel pendulum works with a several different control strategies. Each simulation is based on the Euler integration method [27] and uses differential equations of motion of the object (3.15)-(3.18) from Section 3.2. The Euler integration method (forward Euler) is based on the following algorithm

$$\underline{x}_{n+1} = \underline{x}_n + \Delta t \underline{f}(\underline{x}_n, t_n) , \quad (3.98)$$

$$t_{n+1} = t_n + \Delta t , \quad (3.99)$$

where Δt is the time step, \underline{x}_n is the state in the current moment, \underline{x}_{n+1} is the state in the next step of integration, $\underline{f}(\underline{x}_n, t_n)$ is the differential equation $\underline{f} \in \mathcal{R}^{n+1}$. The equation (3.99) describes how the time increment is calculated. This algorithm allows to calculate every state space variable by computer program.

A full list of computer simulations can be found in Tables: 3.4-3.6.

Table 3.4: A full list of computer simulations of the inverted wheel pendulum – description of each test

Number	Description
1	free swinging
2	getting up
3	constant external torque disturbance
4	short strong external torque disturbance
5	following the reference signal
6	following the reference signal
7	the drift of the gyroscope sensor
8	the drift of the gyroscope sensor
9	following the reference signal
10	following the reference signal

Table 3.5: A full list of computer simulations of the inverted wheel pendulum – controller type and initial state

Number	Controller	Initial state \underline{x}_0
1	uncontrolled	$[0.0873 \text{ rad}, 0 \text{ rad/s}, 0 \text{ rad}, 0 \text{ rad/s}]^T$
2	LQR	$[0.0873 \text{ rad}, 0 \text{ rad/s}, 0 \text{ rad}, 0 \text{ rad/s}]^T$
3	LQR	$\underline{0}$
4	LQR	$\underline{0}$
5	LQR tracking	$\underline{0}$

Table 3.5 – continued

Number	Controller	Initial state \underline{x}_0
6	LQR tracking	$\underline{0}$
7	LQR	$[0.0873 \text{ rad}, 0 \text{ rad/s}, 0 \text{ rad}, 0 \text{ rad/s}]^T$
8	LQI	$[0.0873 \text{ rad}, 0 \text{ rad/s}, 0 \text{ rad}, 0 \text{ rad/s}]^T$
9	LQI tracking	$[0.0873 \text{ rad}, 0 \text{ rad/s}, 0 \text{ rad}, 0 \text{ rad/s}]^T$
10	LQI tracking	$[0.0873 \text{ rad}, 0 \text{ rad/s}, 0 \text{ rad}, 0 \text{ rad/s}]^T$

Table 3.6: A full list of computer simulations of the inverted wheel pendulum – additional specification of each test

Number	Specification
1	—
2	—
3	—
4	—
5	from $t = 5 \text{ s}$ the reference state: $\underline{x}_{d_I} = [0 \text{ rad}, 0 \text{ rad/s}, 5 \text{ rad}, 0 \text{ rad/s}]^T$ and from $t = 50 \text{ s}$ the reference state is: $\underline{x}_{d_{II}} = [0 \text{ rad}, 0 \text{ rad/s}, \text{var rad}, 1 \text{ rad/s}]^T$
6	reference state is: $\underline{x}_{d_{III}} = [0.0349 \text{ rad}, 0 \text{ rad/s}, \text{var rad}, \text{var rad/s}]^T$
7	real state \underline{x} and measured state \underline{x}_m
8	real state \underline{x} and measured state \underline{x}_m
9	in from $t = 50 \text{ s}$ the reference state is: $\underline{x}_{r_I} = [0 \text{ rad}, 0 \text{ rad/s}, 5 \text{ rad}, 0 \text{ rad/s}]^T$
10	from $t = 50 \text{ s}$ the reference state is: $\underline{x}_{r_{II}} = [0 \text{ rad}, 0 \text{ rad/s}, \text{var rad}, 20 \text{ rad/s}]^T$

Simulation 1 concerns the uncontrolled inverted pendulum with the reaction wheel. This Figure shows how state values of the object change in period of 25 s. The initial state is $\underline{x}_0 = [0.0873 \text{ rad}, 0 \text{ rad/s}, 0 \text{ rad}, 0 \text{ rad/s}]^T$ so it starts from almost vertical position. After that the pendulum starts to swing. The friction causes that the oscillation amplitude decreases with time. The initial angle and velocity of the steering wheel is zero and after a short time it also oscillates which is again caused by the friction. After 20 s the angle x_3 rises from zero to 1.6 rad. If the friction in the rotation of the reaction wheel b_I were zero and there were no electric motor torque τ_m , the steering wheel would never rotate. This illustrates how the pendulum and the reaction wheel interact during the motion.

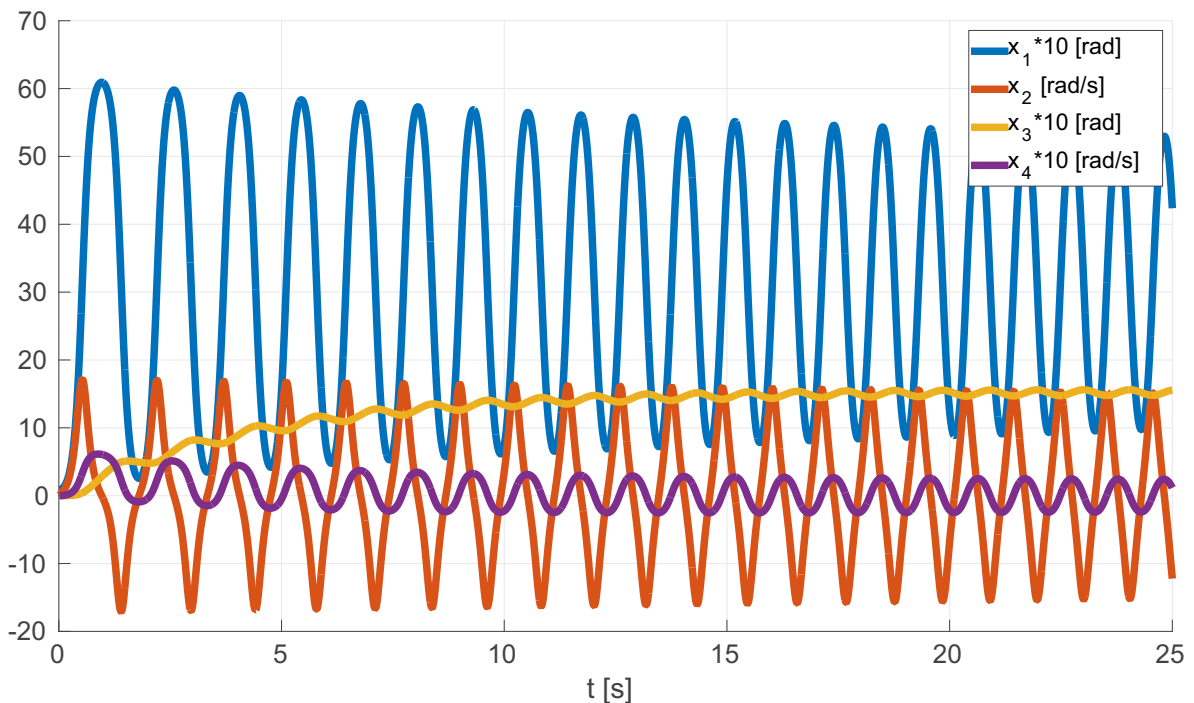


Figure 3.9: **Simulation 1** (specified in Tables: 3.4-3.6)

Simulation 2 applies to the pendulum with LQR control. The control law is consistent with (3.46) and parameters from (3.49) all presented in Section 3.3.3. The LQR controller stabilizes the system correctly – it is capable to keep the vertical pose. The system starts from the initial state like in previous example. Right after the beginning the controller quickly increases applied torque and each state value sharply and rapidly change. Three states: x_1 , x_2 and x_4 reach the desired level (zero) after a little more than 5 s. The angle of rotation of the steering wheel x_3 needs more than 20 s to get zero level. This disproportion guarantees minimizing the cost function (3.35) defined by weight matrix Q (3.48). It is worth to mention that every state value has the same weight and yet there are such differences in regulation time.

Simulation 3 concerns the case when the constant external torque acts on the object. The

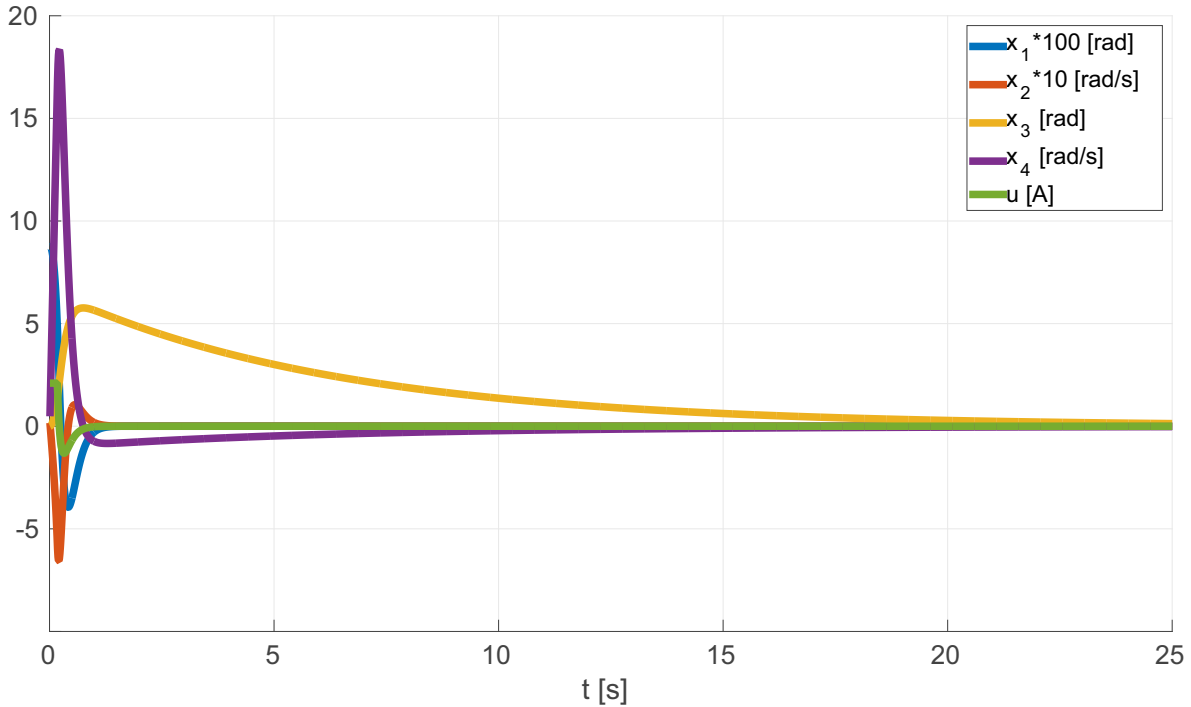
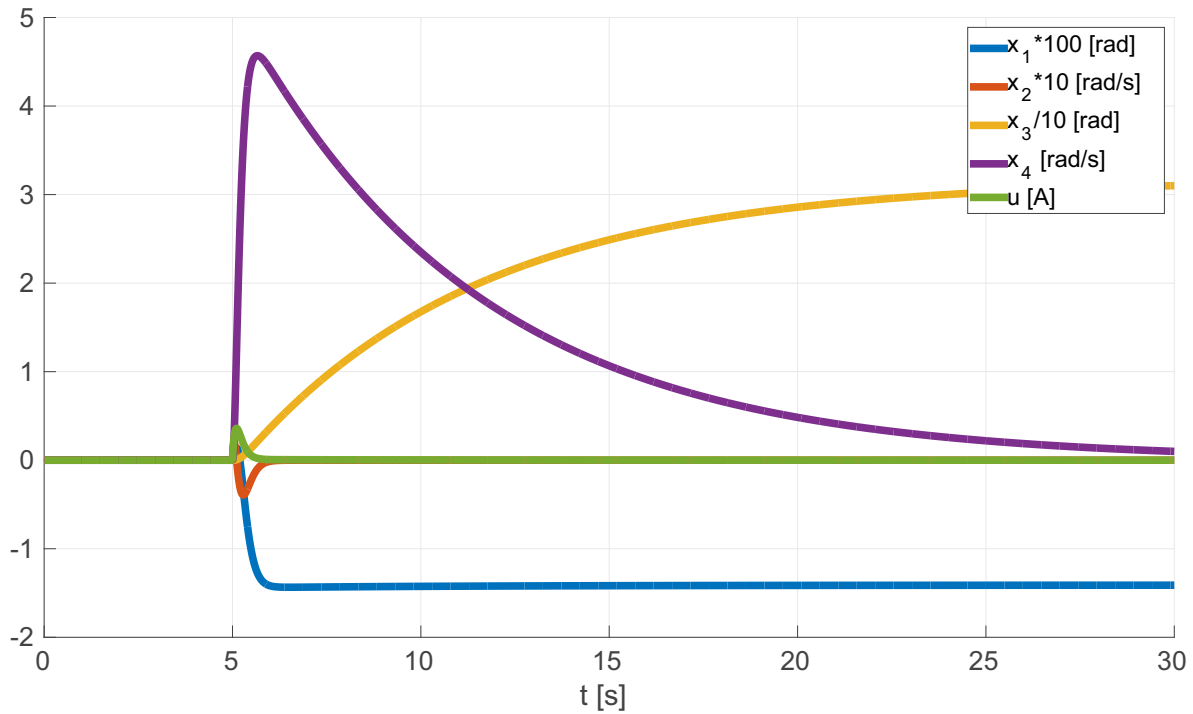
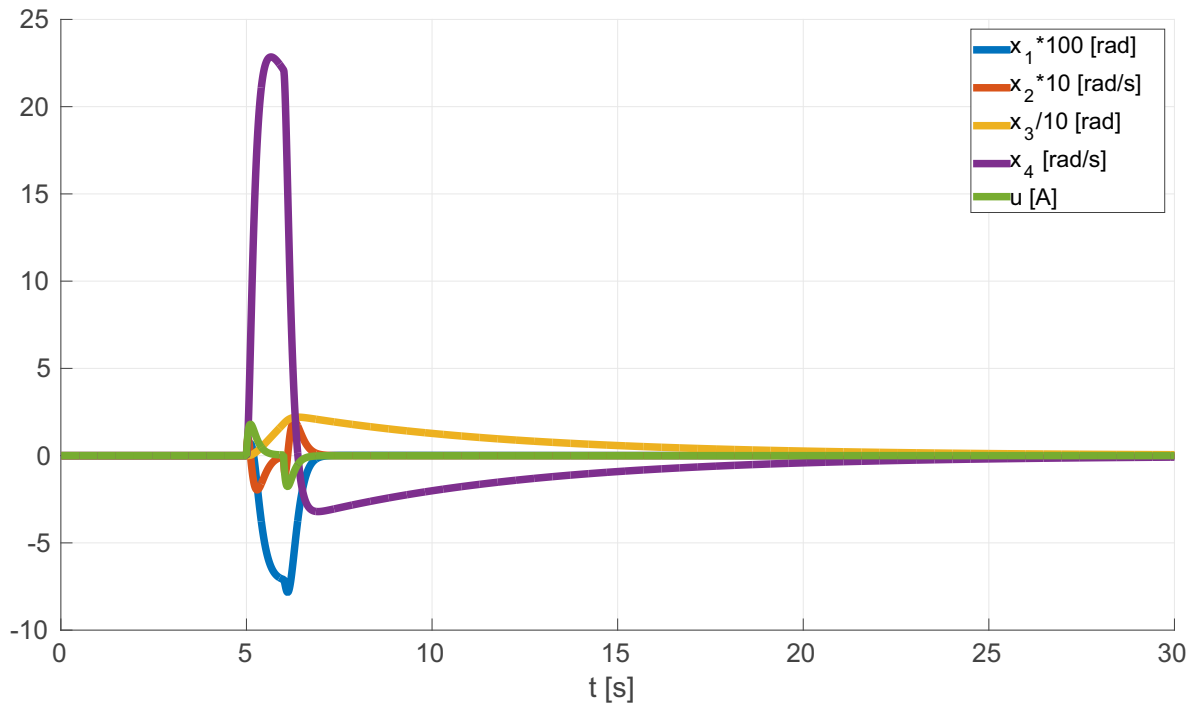


Figure 3.10: **Simulation 2** (specified in Tables: 3.4-3.6)

same control law is used as previously. The question is: is this closed-loop system capable of finding new stable point in the state-space when the additional torque is applied? This external disturbance causes rotation in the axis of rotation of the robot in the first degree of freedom. An analogical phenomenon appears when the additional mass is attached to the machine asymmetrically which significantly translates the center of gravity. The simulation starts from the stable state (zero level). Next 5 s of simulation show that system is stable in its equilibrium point. Suddenly, exactly from $t = 5$ s, the external torque (0.1 Nm) starts to act the machine. The system is able to keep balance despite this disturbance. There are noticeable changes in final values of x_1 and x_3 which are far from the zero level. Finally, this machine with LQR control finds a new stable point of state when it is under the influence of this torque. In other words, it is possible to install some additional mass (not to heavy, of course) anywhere in the machine and still maintain stability properly. Consequently, the machine changes its angle x_1 a little from the vertical position and rotates its steering wheel x_3 at some angle (different from zero).

Simulation 4 represents the case, when there is five times stronger (0.5 Nm) external disturbance than in **Simulation 3**. This time the additional torque appears in 5 s and after next 1 s it disappears. Once again the system remains stable. If this torque were last a few seconds more the pendulum would fall down (it was tested but the result of this study is not included in this dissertation). In other words, the torque is relatively strong, causes a temporary imbalance and after this the state values returns to the desired zero level $\underline{x} = [0 \text{ rad}, 0 \text{ rad/s}, 0 \text{ rad}, 0 \text{ rad/s}]^T$.

Figure 3.11: **Simulation 3** (specified in Tables: 3.4-3.6)Figure 3.12: **Simulation 4** (specified in Tables: 3.4-3.6)

Simulation 5 represents LQR tracking control presented in Subsection 3.3.4. The reaction wheel pendulum starts from stable zero state. After 5 s the reference state changes into $\underline{x}_{dI} = [0 \text{ rad}, 0 \text{ rad/s}, 5 \text{ rad}, 0 \text{ rad/s}]^T$. The LQR tracking control changes the state of the machine correctly. States: x_1 and x_2 reach the stable level much faster (1 s) than states x_3 and x_4 (25 s). After $t = 30$ s of simulation the desired state returns to zero level and $t = 5$ s the desired state $\underline{x}_{dII} = [0 \text{ rad}, 0 \text{ rad/s}, \text{var rad}, 1 \text{ rad/s}]^T$. In this case, the control law causes that the velocity of the reaction wheel x_4 reaches a constant nonzero level. This means that the angle x_3 can not remain in zero level and can not increase the quadratic cost function (3.55). This is the reason, why the desired x_{d3} is marked as var. The result of this algorithm is correct – the velocity of the reaction wheel reaches desired level in relatively short time (1 s). To sum up the LQR tracking control is appropriate to change states of the reaction wheel pendulum without loosing the stability.

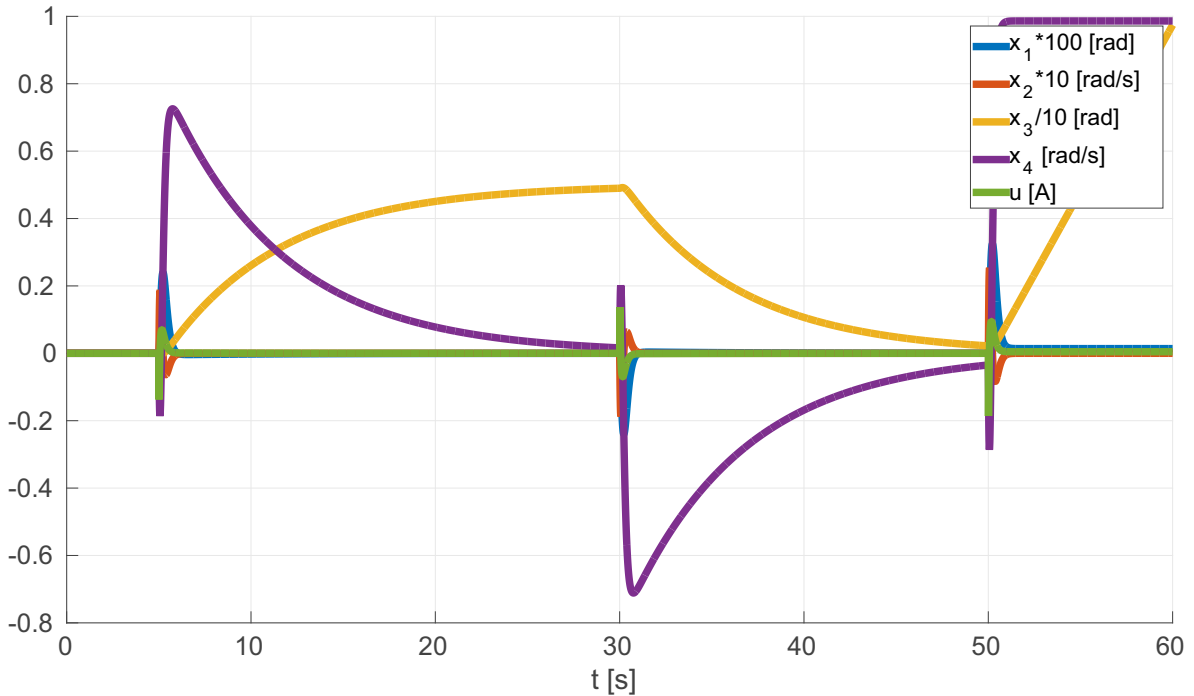


Figure 3.13: **Simulation 5** (specified in Tables: 3.4-3.6)

The LQR control algorithm can be also tested to track the x_1 state value – the angle from the vertical position of the pendulum. The result is in **Simulation 6**. Being in state x_1 different than zero (0.0349 rad) costs the energy and causes acceleration of the reaction wheel. Greater reaction wheel velocity x_4 means bigger friction torque μ_m so bigger control u . Finally, after 13 s the velocity of steering wheel is so high and produces so big friction what results in saturation of control. The machine loses the controlability and falls down. The important thing is that it is possible to use the tracking control to change the main angle of the pendulum x_1 for a short moment and then return to the optimal energy equilibrium point.

In the real machine the fact that needs to be taken into account is that the measured state \underline{x}_m differs from the real state \underline{x} . In Section 3.5 the state measurement technique is proposed

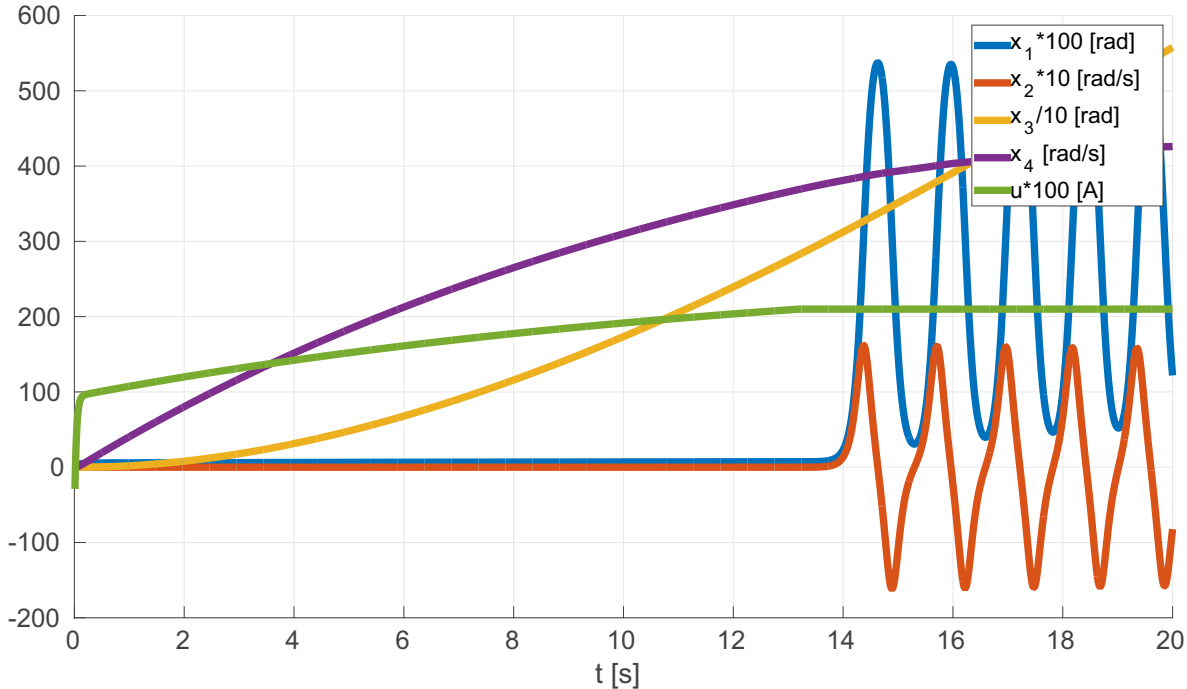
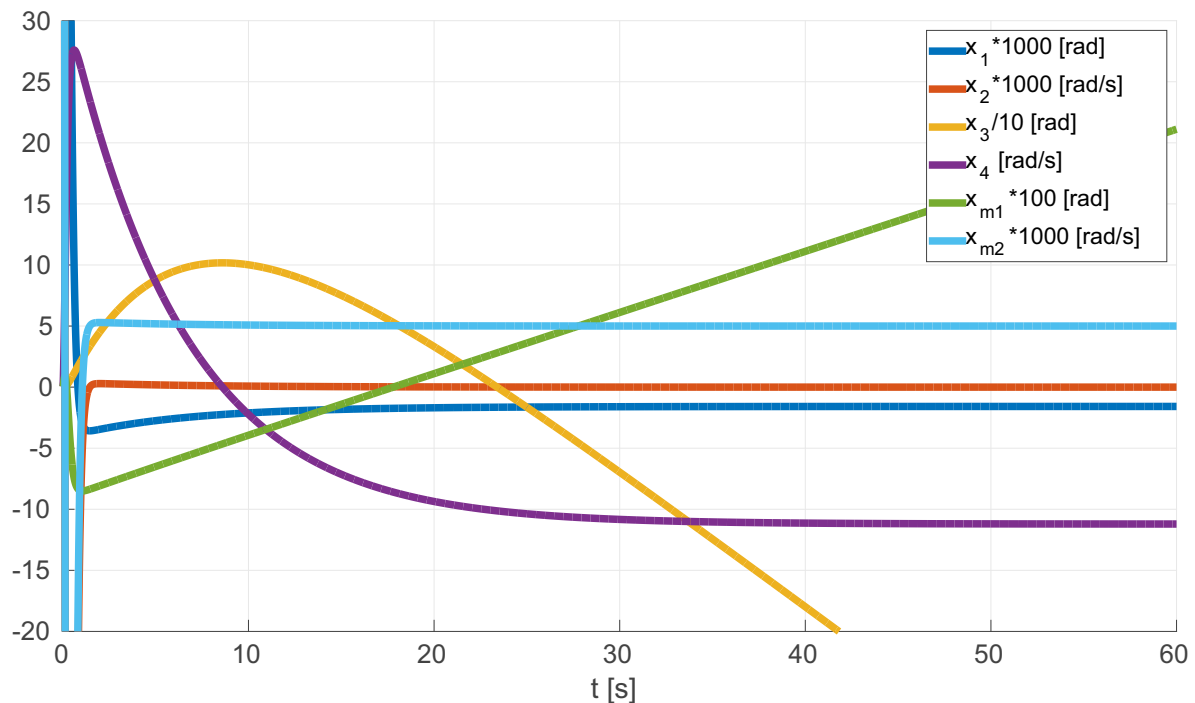
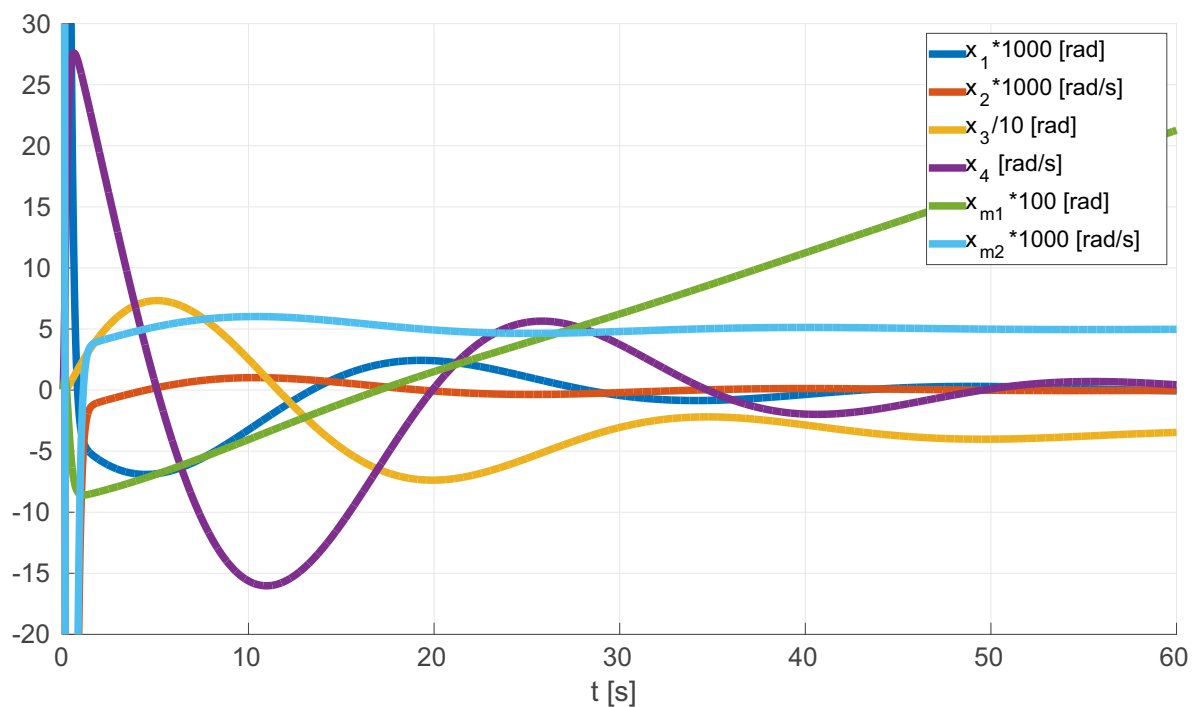


Figure 3.14: **Simulation 6** (specified in Tables: 3.4-3.6)

and it is based only on the gyroscope sensor. As already mentioned, this sensor has a drift. When the drift is integrated it endlessly increases. In this case the gyroscope measures x_{m2} which is integrated what results in x_{m1} . These two measurements are used in control feedback in LQR control. The result can be found in **Simulation 7**. The machine starts from the state $[0.0873 \text{ rad}, 0 \text{ rad/s}, 0 \text{ rad}, 0 \text{ rad/s}]^T$. First of all, what is very interesting, the system is BIBO stable even if the x_{m1} constantly rises. The real angle x_1 remains constant but it is slightly different from zero – this is also explainable. To minimize the cost function (3.35), rising x_{m1} needs to be compensated by rising the real reaction angle x_3 . Constantly rotating steering wheel creates the constant friction torque μ_m which finally changes the optimal energy point of the pendulum. As can be noticed, the x_{m2} stabilizes in the drift ξ level. Summarizing using only gyroscope sensor to measure states x_{m1} and x_{m2} with LQR controller can stabilize the reaction wheel pendulum, but drift imperfection results in permanent rotation of the steering wheel.

As it is mentioned in Section 3.5 the appropriate solution to cope with continuously rotating reaction wheel is the LQI control method. The result is presented in **Simulation 8**. After 60 s the pendulum completely stops to rotate – each angle is constant, each velocity is zero. The initial state is the same as in Figure 3.15. As can be noticed, the main stabilizing process is still fast – it needs about 1 s to stabilize the angle x_1 . On the other hand the angle x_3 significantly oscillates by 60 s and finally stops. Additional integrating loop accurately described in Section 3.3.5 gives promising results in controlling the reaction wheel system with gyroscope sensor used to measure angle x_1 and velocity x_2 .

At the end there are two computer simulations more: **Simulations 9** and **10**. Both of them

Figure 3.15: **Simulation 7** (specified in Tables: 3.4-3.6)Figure 3.16: **Simulation 8** (specified in Tables: 3.4-3.6)

show the tracking ability of the LQI control algorithm. Both of these simulations starts from the initial state $[0.0873 \text{ rad}, 0 \text{ rad/s}, 0 \text{ rad}, 0 \text{ rad/s}]^T$ where the reference state \underline{x}_r is zero. From $t = 50 \text{ s}$ the reference changes. In the first one the reference changes into $\underline{x}_{rI} = [0 \text{ rad}, 0 \text{ rad/s}, 5 \text{ rad}, 0 \text{ rad/s}]^T$. In this case the control law is defined by (3.62). In the second simulation the reference state changes from zero into $\underline{x}_{rII} = [0 \text{ rad}, 0 \text{ rad/s}, \text{var rad}, 20 \text{ rad/s}]^T$ and exceptionally for this case the control law is defined by: $[0, 0, 0, 0.01]$ (analogically to (3.70) but the this time x_4 is integrated). In both simulations the system is stable and reaches the reference states. The tracking dynamics is much slower than in LQR tracking method (**Simulation 5**) but there is a huge advantage – it causes much lower accelerations and also much lower jerks. This is much safer for the real applications.

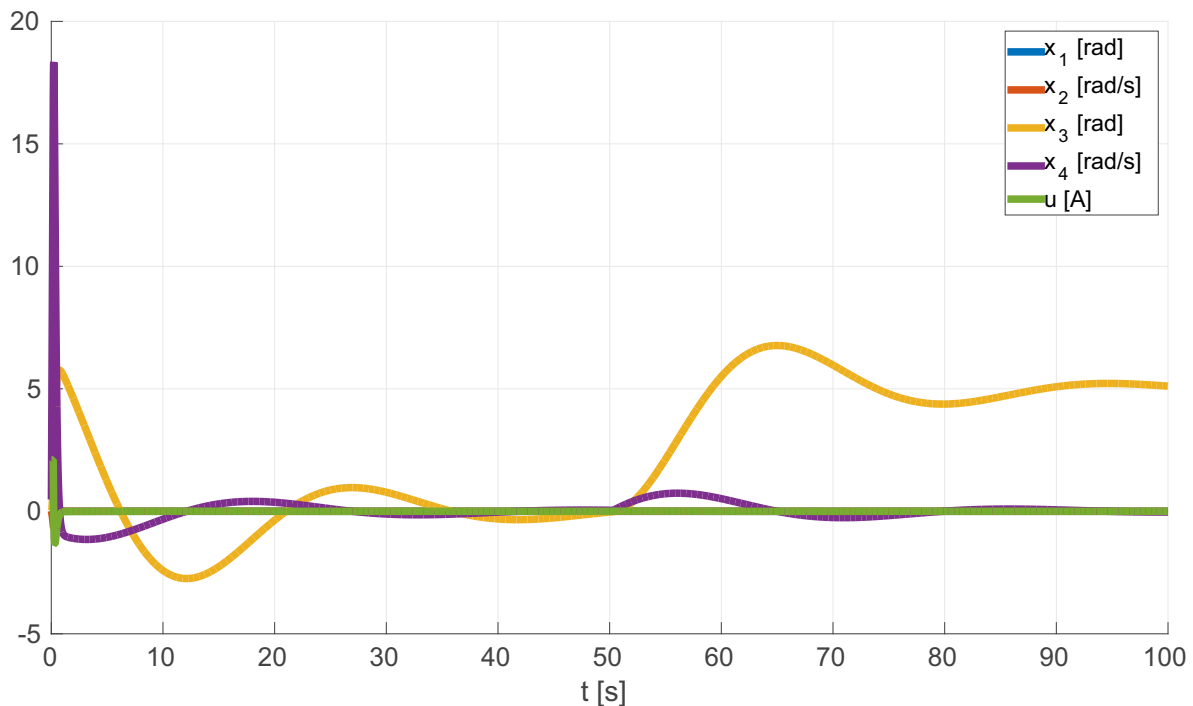


Figure 3.17: **Simulation 9** (specified in Tables: 3.4-3.6)

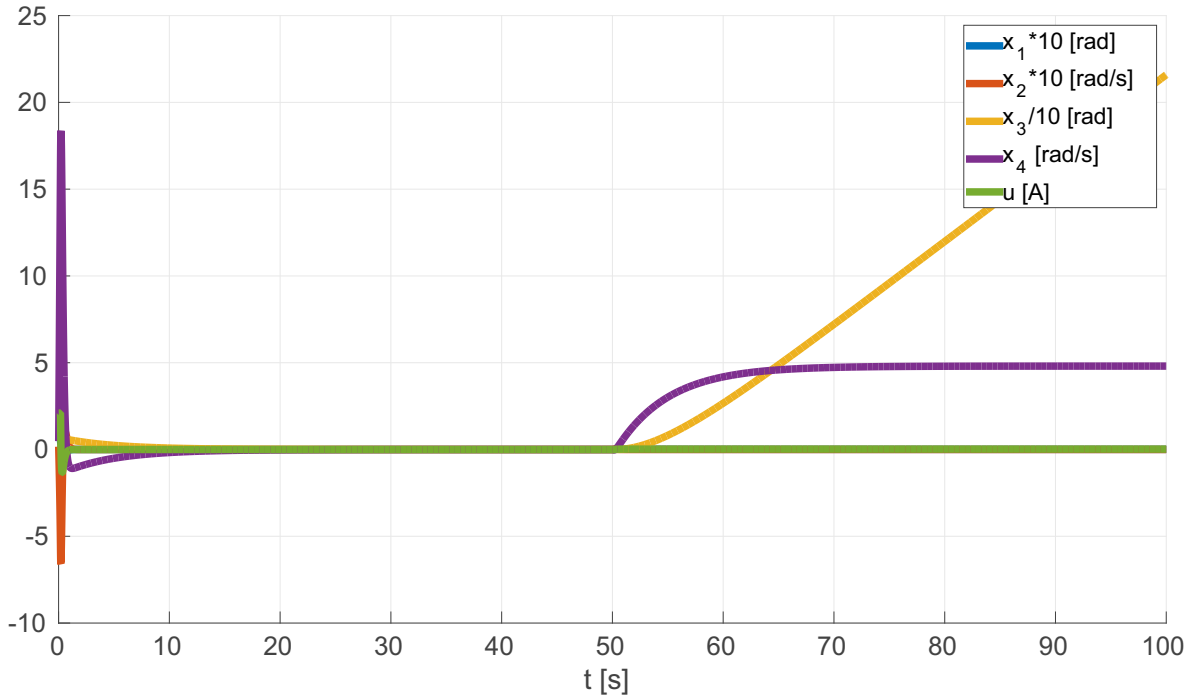


Figure 3.18: **Simulation 10** (specified in Tables: 3.4-3.6)

3.7 Energy efficiency considerations

To fully understand the principle of operation of the reaction wheel it is important to know where the energy flows and how the energy is converted into its other forms. In this Section it is explained why the reaction wheel is energetically efficient and why it is worth to use it as an actuating device.

The following types of energy should be considered: kinetic, potential, dissipation and the work done by the electric energy source. In this case the sum of kinetic, potential and dissipation energies is constant if the external electric energy source is turned off. Otherwise, when the electric potential of the battery causes the rotation of the motor then the total sum of the energy of the system increases.

The energy equations are based on [88]. At the beginning the kinetic energy is equal to

$$K = \frac{I_{rg}x_2^2}{2} + \frac{I_Ix_4^2}{2}, \quad (3.100)$$

and it consists of two components which are related with two main rotating parts of the reaction wheel: the main frame and the steering wheel. Each component includes the moment of inertia and the squared angular velocity divided by two. Next is the potential energy

$$P = m_rgh_r [1 + \cos(x_1)]. \quad (3.101)$$

It is proportional to the weight of the robot m_r , the gravity of the Earth g , distance h_r and nonlinear part with angle x_1 . The potential energy reaches the highest level exactly for the

equilibrium point of the pendulum. This is the point where the center of mass of the robot is at its highest position. The minimum potential energy (actually zero energy) is when the pendulum hangs down. Typically in swinging pendulum when there is no friction kinetic energy is transformed into potential energy and vice versa. This process is periodical with the frequency of the physical pendulum. In these conditions when there is no external forces and the friction can be neglected according to the first Newton's laws of motion the rotating mass velocity is always zero. The totally different situation is when the friction exists in the system. The dissipation energy can be calculated from

$$D = 2 \int_0^T \left[\frac{b_r x_2^2}{2} + \frac{b_I x_4^2}{2} + \frac{b_m(x_4 - x_2)^2}{2} \right] dt \quad (3.102)$$

and after simplifying

$$D = \int_0^T [b_r x_2^2 + b_I x_4^2 + b_m(x_4 - x_2)^2] dt, \quad (3.103)$$

where T is the period of observation. Generally, the dissipation is the integral of the squared velocity multiplied by the coefficient of friction. There are three different velocities in this system, that need to be taken into account: x_2 , x_4 and the relative velocity $(x_4 - x_2)$. In this dissertation, it is assumed that the electric energy loss is omitted, what allows to focus on the most important part here which is the mechanics of movement. As can be noticed, the dissipation energy consists of main three components. Two of them describe how the energy dissipates by the contact with the external environment. In other words, the system loses the energy when the first joint rotates with the nonzero friction and also when the steering wheel rotates and is slowed down by the air resistance. The third component of the whole dissipation is not related with the relation with the outside world of this system. This is based on the relative angular velocity of two rotating joints of the system: $(x_4 - x_2)$. This is the velocity of the electric motor which drives the steering wheel. It is worth to mention that there are some applications where these frictions are intentionally used to create useful torques for short moments [34]. This can be achieved by a mechanical brake which can increase the friction b_m immediately and enormously.

The work done by the electric energy source is equal to

$$W = \int_0^T U u(t) dt, \quad (3.104)$$

where U is voltage of the battery and $u(t)$ is current which flows in motor coils. In the studied system it is equal to $U = 24V$. The work W is the external source of energy. It directly creates the control – the current which flows in motor coils. It is assumed that the motor driver is capable to recuperate energy when the motor brakes. As a consequence of this the energy can go out and return to the power source. In other words, it is normal that work W increases and decreases during the operation of the machine.

Finally, the sum of energies can be formulated as

$$S = K + P + D + W. \quad (3.105)$$

Using the computer simulation is possible to verify if energy transformations are correct. Figure 3.19 presents the first computer simulation of uncontrolled reaction wheel system. Each coefficient of friction is intentionally increased one hundred times

$$\{b_m = 0.001, b_r = 0.001, b_I = 0.001\} \rightarrow \{b_m = 0.1, b_r = 0.1, b_I = 0.1\},$$

what allows to show energy transformations better. The rest of physical parameters are unchanged. The pendulum starts from the point of state: $\underline{x}_0 = [0.52 \text{ rad}, 0 \text{ rad/s}, 0 \text{ rad}, 0 \text{ rad/s}]^T$. After that it swings a couple of times and after near 4 s ends hanging down at the state $\underline{x}_{end} = [3.14 \text{ rad}, 0 \text{ rad/s}, 1.63 \text{ rad}, 0 \text{ rad/s}]^T$. The sum of energy S is constant during the whole simulation. At the beginning, the whole energy is concentrated in the potential energy. At this moment the kinetic energy is zero and dissipation energy is also zero. Right after the beginning, the potential energy quickly decreases and kinetic energy and dissipation rises. When the kinetic energy reaches the local maximum, the potential energy reaches zero and vice versa. The amplitude of oscillation of the pendulum decreases with time. Finally, the pendulum stops, the kinetic energy is zero and the whole initial potential energy transforms into dissipation. It is worth to mention that the rotation angle of the reaction wheel x_3 begins from zero and ends at the angle 1.63 rad. It moves because of nonzero friction torques.

The second computer simulation concerns the reaction wheel system with LQR controller and is presented in Figure 3.20. This time each coefficient of friction is increased ten times

$$\{b_m = 0.001, b_r = 0.001, b_I = 0.001\} \rightarrow \{b_m = 0.01, b_r = 0.01, b_I = 0.01\}.$$

Using the coefficients from the original model in computer simulation generates small energy of dissipation which may be difficult to see from the plot. Computer simulation shows 15 s of the stabilization process. In Figure 3.20(a) presents energies and Figure 3.20(b) presents state-space variables \underline{x} and the control u . The initial state is the same as before: $\underline{x}_0 = [0.52 \text{ rad}, 0 \text{ rad/s}, 0 \text{ rad}, 0 \text{ rad/s}]^T$. Feedback system works correctly and the simulation ends at the desired state: $\underline{x}_0 = [0 \text{ rad}, 0 \text{ rad/s}, 0 \text{ rad}, 0 \text{ rad/s}]^T$. The initial energy of the whole system S is equal to the initial potential energy P . After that the velocities x_2 and x_4 increase which generates dissipation. The current strongly flows from the battery so the energy of the system rises – especially at the beginning of the simulation. Right after first strong jerk of the robot the lot of energy returns to the battery. Finally, after the simulation the work done by the electric energy source is clearly bigger than zero, the dissipation is also bigger than zero and the sum of energies is bigger than the initial state. Since this moment the machine does not need any energy to keep balance. In other words, this simulation proves a huge advantage of stabilization method based on reaction wheel. It only coasts the energy when the machine is far from the equilibrium point.

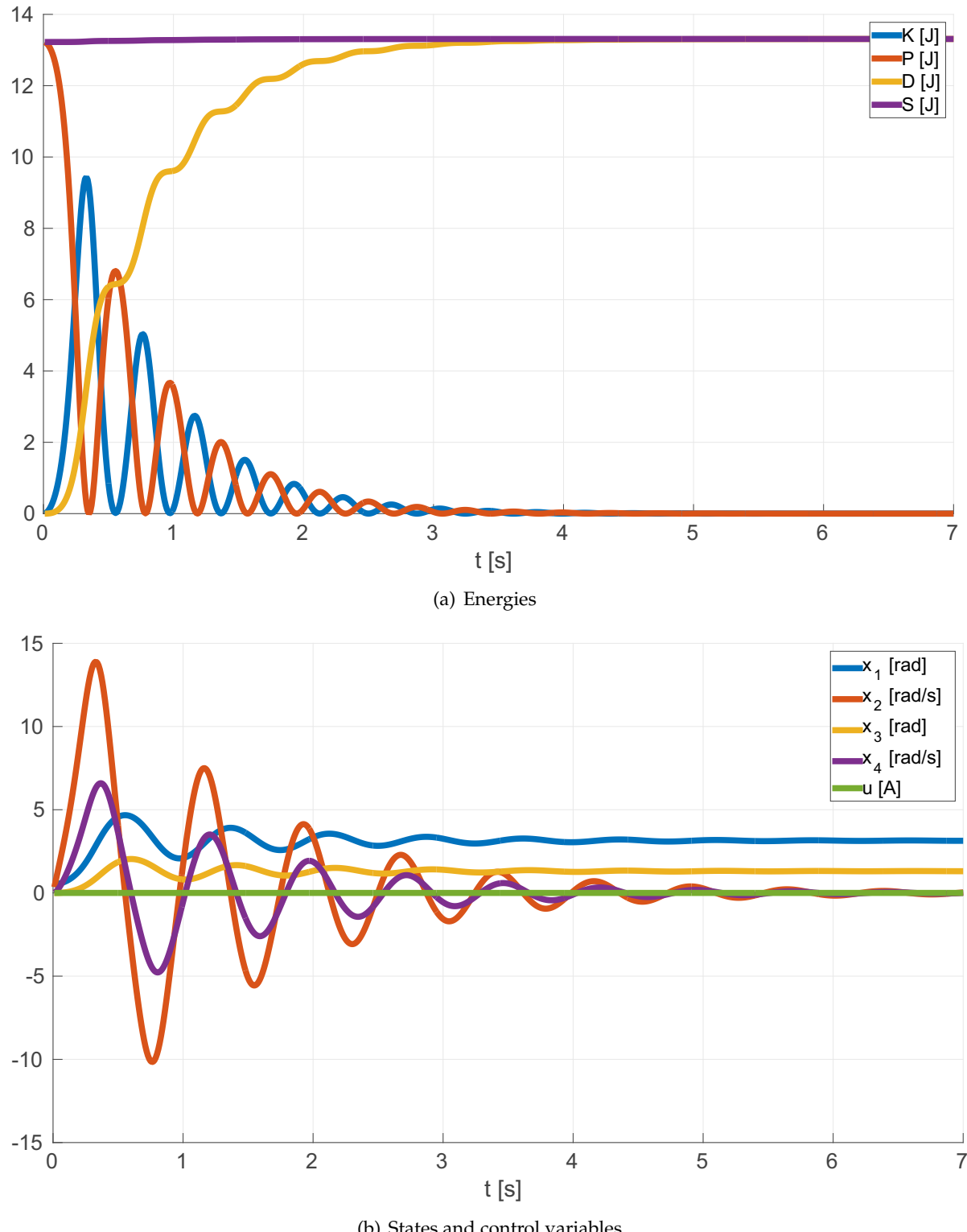
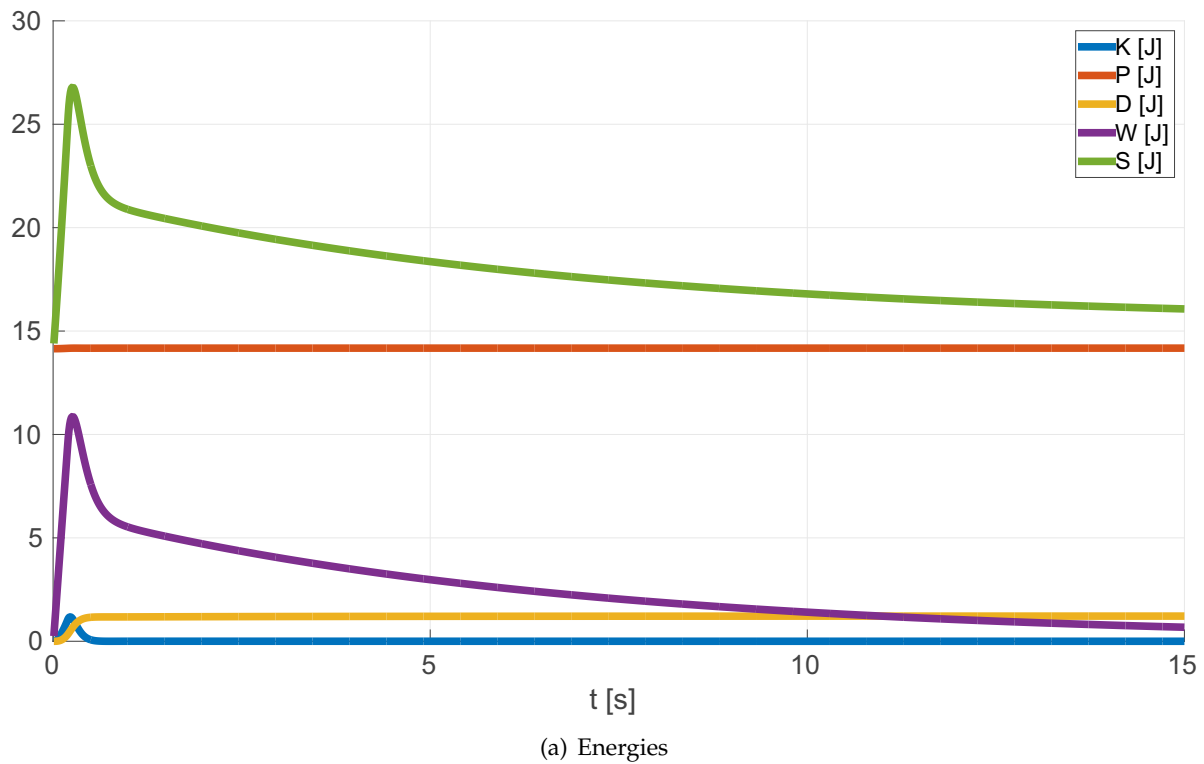
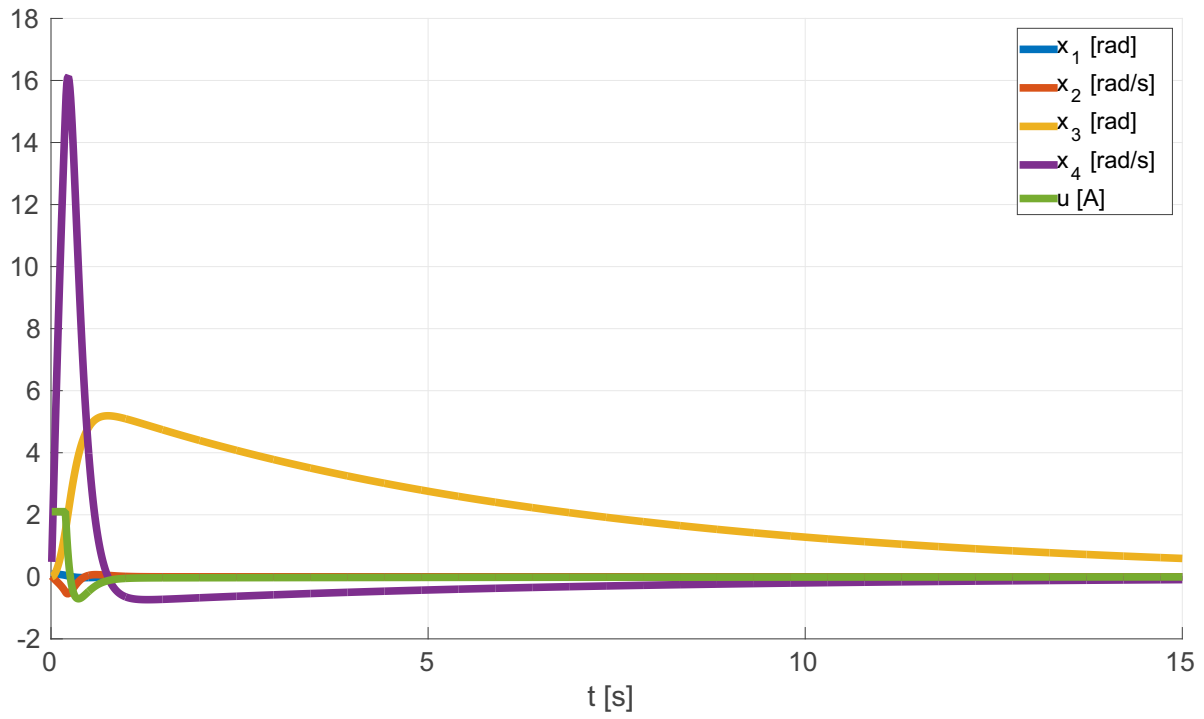


Figure 3.19: Simulation of the uncontrolled reaction wheel system – energies, states and control



(a) Energies



(b) States and control variables

Figure 3.20: Simulation of the reaction wheel system with the LQR controller – energies, states and control

3.8 Tests on a real robot

3.8.1 Reaction wheel robot description

The reaction wheel system with several control algorithms was tested on the real machine and results are presented in this Section. The experiments confirm the correctness of the chosen control strategies and give a confirmation for many inertial actuation analysis from this Chapter.

In this Subsection the real machine is described – it was used to perform a series of experiments which refer to many parts of this Chapter.

The robot is presented in Figures: 3.21 and 3.22. The construction was developed and made during master thesis in 2011 [38]. This was the beginning of the research on the reaction wheel. The first tests of this machine have been carried out and conclusions drawn. Finally, it was obvious that this subject gives a perfect area for further research on this object and results are presented in this dissertation.

The construction is made mainly from aluminium profiles. At the top of it there is a reaction wheel made from steel. This is the heaviest element. It is mounted on the DC motor shaft. There is no gearbox in this solution what guarantees no additional disturbances which usually appear when changing of direction of the motor torque. It was decided to use the classical high torque low-speed brushed electric motor. Generally, sampling frequency for control law generation is 300 Hz. The tracking control of the current which flows in motor coils is calculated with the frequency of 20 kHz. The measurements of are performed with the same frequency. Further information about torque control can be found in [38]. Here it is important to say, that there is an additional control loop which controls the motor current and is made by specially designed electronic circuit. Some conclusions from stability analysis from Section 3.4 were used to optimise this real construction (such as: proportion between radius of the reaction wheel and its weight).

The main processing unit is the microcontroller STM32F407VGT6 from STMicroelectronics Company. It is responsible for gathering measurements and control two control loops: current control loop and robot stabilizing control loop. As was tested this robot uses 70 % of computing power of this microcontroller for a typical work.

The incremental encoder was used to measure the angle of rotation of the steering wheel x_{m3} and the velocity x_{m4} . It gives 1800 impulses per one rotation. This type of sensor does not give the absolute position of the rotation, but it is negligible in this research.

Another very important sensor is the IMU (Inertial Measurement Unit). Its purpose is to measure angle x_{m1} from the vertical position of the robot and the velocity x_{m2} . Here decided to use the following model: ADIS16300PCBZ from Analog Devices Company. The products from this company are known to be relatively precise compared with available components on the market. It has the 1-axis gyroscope and the 3-axis accelerometer. As described in Section 3.5 the most important here is the gyroscope. It has the crucial role in stabilizing process of the robot. It measures the velocity at the output 300 times per second. The accelerometer is used only once right after turning on the machine as a reference angle from the vertical. The data transfer between sensor and microcontroller is digital so there is no risk to loose or

damage any measurement.

Additionally, the FIR (Finite Impulse Response) filter is implemented in the software of the microcontroller. Actually this is the 5-th order low-pass digital filter. Its task is block the high frequency noise. The cut-off frequency has been set to 60 Hz and has been found by an experiment. Actually, it has given the best final result on the machine – the smallest oscillations. A several of similar filters have been tested and analysed.

The whole robot is placed on two wheels. It is an inverted pendulum-like single-track mechanism – the same as the bicycle. It can not accelerate by itself and it needs to be pushed to travel. Moving forward and backward in this case is not important because it gives additional degree of freedom. To be compatible with the mathematical model defined by differential equations (3.15)-(3.15) only two degrees of freedom are taken into account.

It was decided to mount two pneumatic shock absorbers (one for each side of it) to prevent the whole device from the sudden and danger contact with the ground and to support the robot when it is turned off.

All necessary physical parameters have been identified and can be found in Table 3.7.

Table 3.7: Physical parameters of the reaction wheel robot

Name	Value	Unit
m_r	5.16	kg
r_w	0.03	m
h_r	0.14	m
$I_{reaction_wheel}$	0.3500	kg m ²
I_{mr}	0.0008	kg m ²
I_{rg}	0.7877	kg m ²
k_m	0.421	Nm/A
b_r	0.001	N m s
b_I	0.001	N m s
b_m	0.001	N m s
g	9.80665	m/s ²
u_{max}	±2.1	A

Table 3.7 – continued

Name	Value	Unit
x_{4max}	± 66	rad/s
U	24	V

Also two limit values can be found in this table: the maximum current u_{max} and the maximum DC motor velocity x_{4max} . There is also the nominal power supply voltage of the electric motor U .

The robot is powered from the external power supply. The battery is optional and it was not used for tests. It is worth to mention that Figure 3.22 actually presents the experiment, when the robot gets up from the initial state $x_1 \neq 0$. Finally, after the stabilization process it maintains the vertical position.

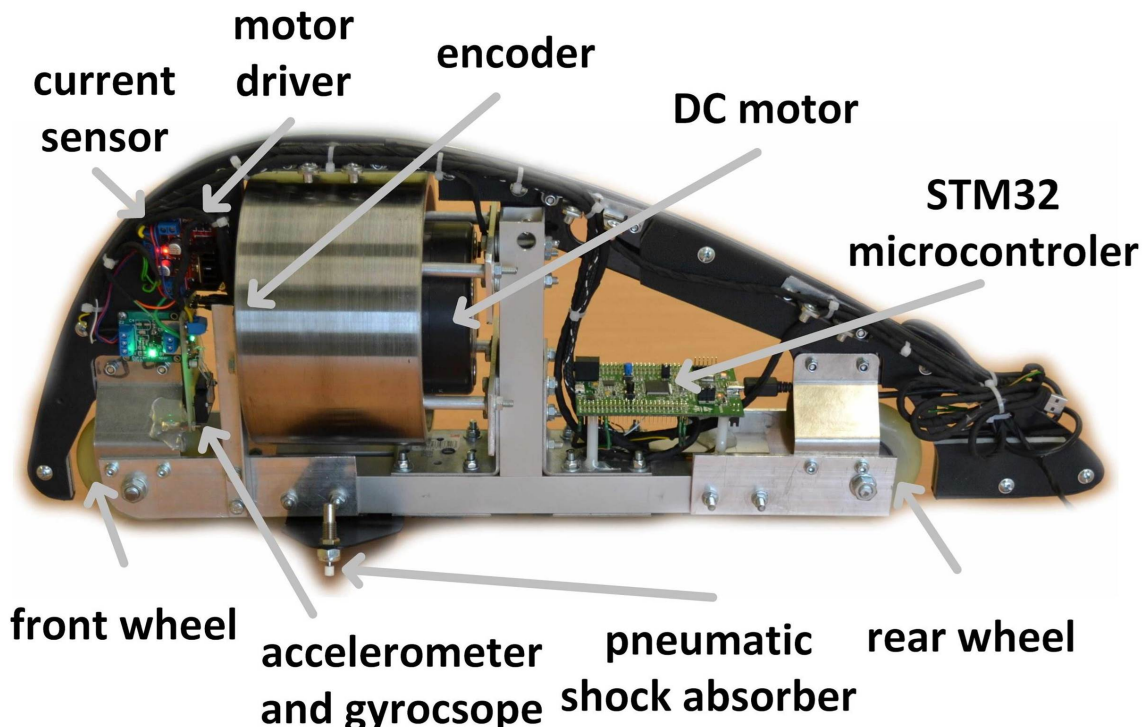


Figure 3.21: Reaction wheel robot – side view. Description of main parts

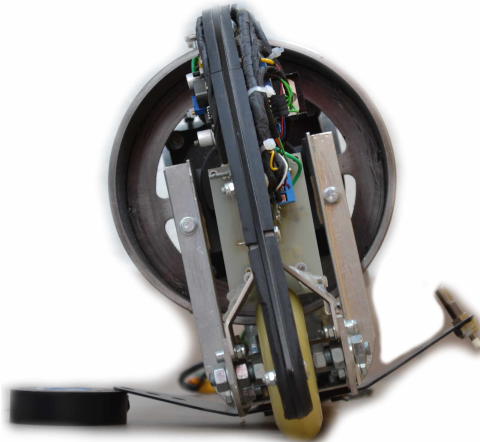


Figure 3.22: Reaction wheel robot – front view

3.8.2 Results of experiments

Many of experiments have conducted and their results are presented in this Subsection to give additional insight into principle of operation of the reaction wheel.

Each state value is marked as a measured value \underline{x}_m – not real value \underline{x} . It is mentioned in Section 3.5 the real values are unknown.

A list of conducted experiments can be found in Table 3.8.

Table 3.8: A full list of experiments of the inverted wheel pendulum

Number	Controller	Description
1	LQR	external torque disturbance
2	LQR	external short and strong torque disturbances
3	LQR	getting up
4	LQR	the drift of the gyroscope
5	LQI	the drift of the gyroscope
6	LQI	the drift of the gyroscope and high-gain integration feedback

Experiment 1 presents the reaction wheel pendulum stabilized by LQR controller. The control law is defined by (3.46) and parameters given by (3.49). Between 1 s and 6 s the external torque acts on the object. This disturbance is created by attaching additional mass to the machine during its work. As can be seen, it is stable and keeps the vertical position during the whole experiment. The disturbance torque in this case changes the angle from the vertical position of the object from zero to -0.07 rad what is easy to see by human observer. To minimise the cost function (3.35) any changes in angle x_1 need to be compensated by changes in angle x_3 – this was described in detail with computer simulations in Section 3.6. Consequently, in **Experiment 1** can be noticed that x_{m3} strongly rises which is caused by changing the x_{m1} . As the computer **Simulation 3** shows that x_{m3} would stop at same finite level after about 30 s. Nevertheless at the end of the experiment (after 14 s) the angle of rotation of the steering wheel returns to the initial state (approximately).

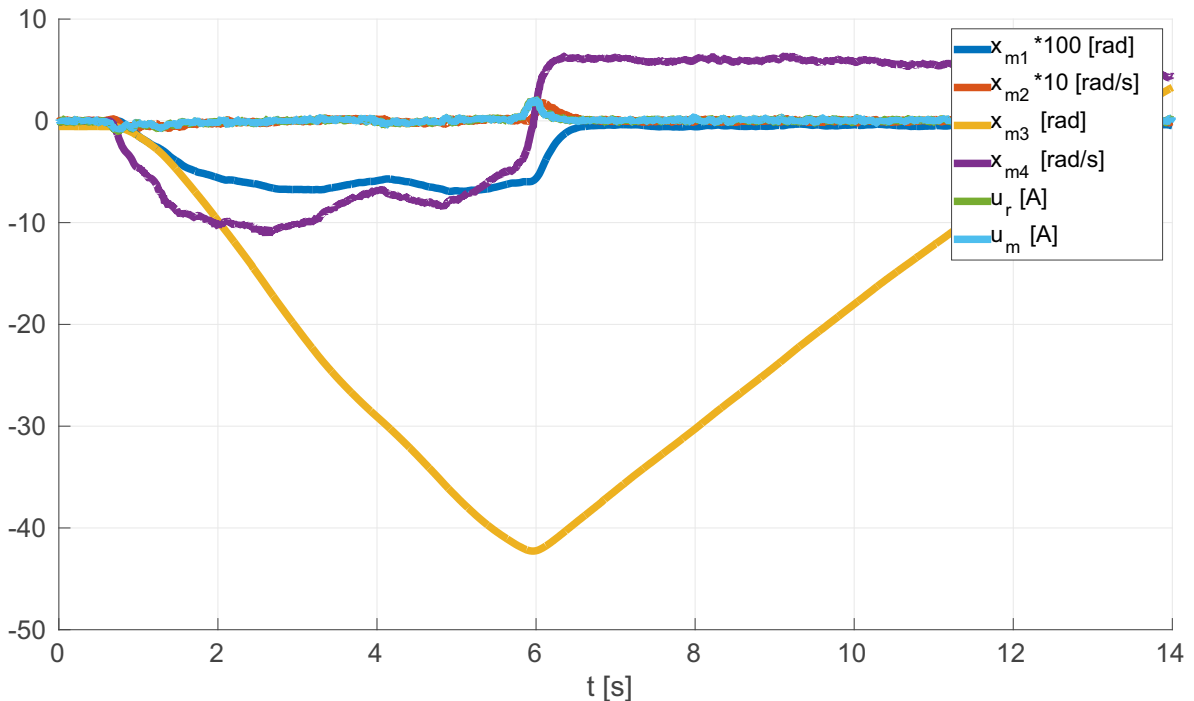


Figure 3.23: **Experiment 1** (specified in Table 3.8)

In **Experiment 2** the machine is put to the test of short and strong torque disturbances. The control system reacts very quickly and sometimes the control value (the current in electric motor coils) saturates. The symbol u_m is the measured current and u_r is the reference current. As can be seen, in **Experiment 2** u_r sometimes is greater than maximum possible current u_{max} . The closed-loop system is stable through the whole experiment. Every time the disturbance torque is in the same direction, therefore the angle of the reaction wheel x_{m3} is significantly different than zero. In other words, the mean value of the disturbance is bigger than zero thus the mean value of x_{m1} is bigger than zero what needs to be compensated by x_{m3} bigger than zero.

Experiment 3 shows how the robot gets up from the angle x_1 different than zero. An

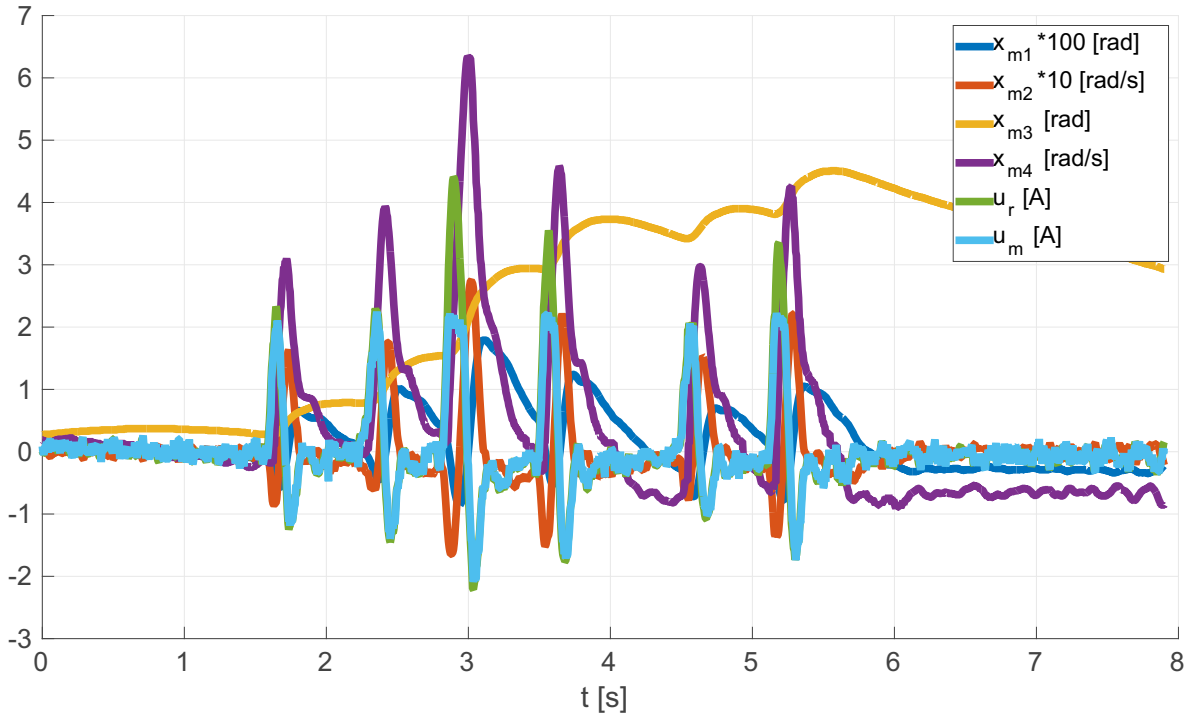


Figure 3.24: Experiment 2 (specified in Table 3.8)

analogous situation can be found in computer **Simulation 2**. The real object starts from the state $[0.06 \text{ rad}, 0 \text{ rad/s}, 0 \text{ rad}, 0 \text{ rad/s}]^T$ and after about 1 s reaches the vertical position. First 0.2 s the control value saturates on its limit. After reaching the vertical position, the angle x_{m3} slowly tends to zero.

Another **Experiment 4** presents the gyroscope drift problem. Through all tested time the robot is stable and the velocity x_{m2} is near to zero. The measured angle from the vertical position x_{m1} decreases. This needs to be compensated by decreasing the x_{m3} to minimise the cost function (3.35). The machine is controlled by the LQR regulator what means that the reaction wheel constantly rotates (angle x_{m3} decreases and tends to minus infinity). The same situation can be found in the computer **Simulation 7**.

In previous experiment the nonzero gyroscope drift causes the nonzero reaction wheel velocity x_{m4} in steady-state. To bring every velocity in the machine to zero it is advantageous to use LQI control algorithm instead of LQR. As it is deeply described in Sections 3.3.5 and 3.5 the LQI has additional integration block in feedback loop. It integrates the whole state and modifies the cost function. **Experiment 5** presents how this method works in practise. The velocity x_{m4} oscillates near to the zero level. The angle x_{m3} does not increase to infinity (or minus infinity) – it oscillates around some constant level (this level is analytically solved in Section 3.5). Originally \underline{K}_i vector is defined by (3.70). In this experiment this vector is multiplied ten times to give the integration effect stronger than in **Simulation 8**. The oscillations have higher frequencies and the compensation effect is quicker. Generally, this integration process is slow and it is difficult to measure in real machine – this is the reason

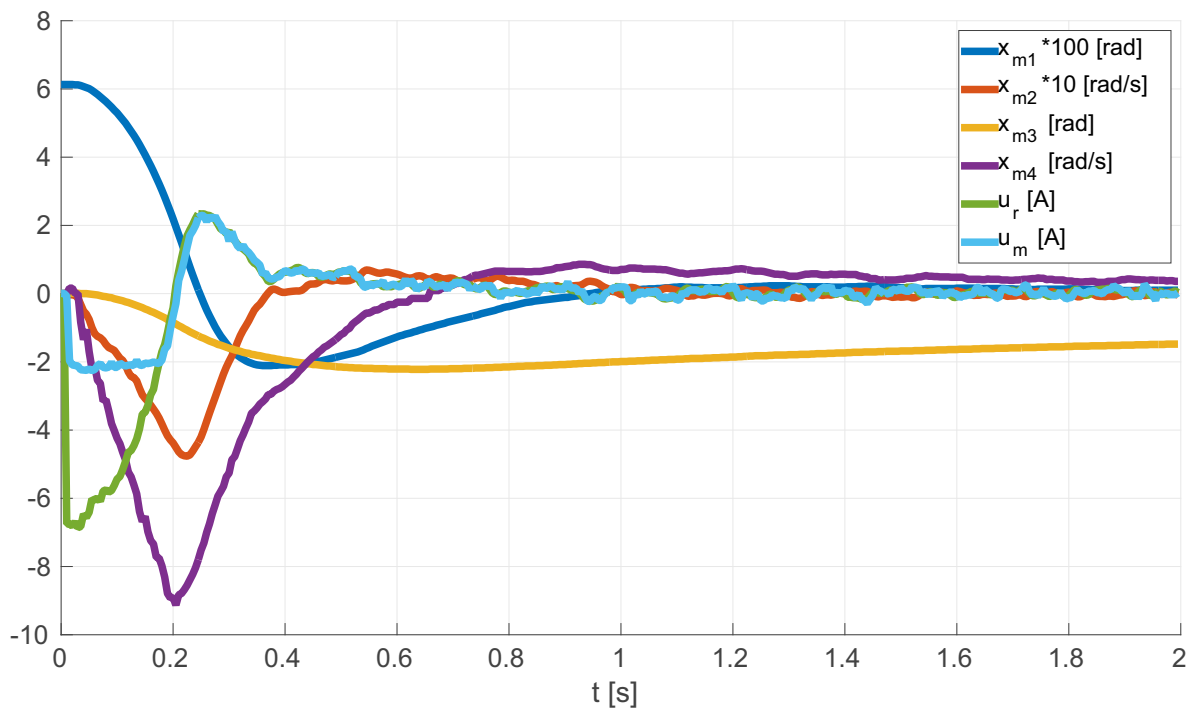


Figure 3.25: Experiment 3 (specified in Table 3.8)

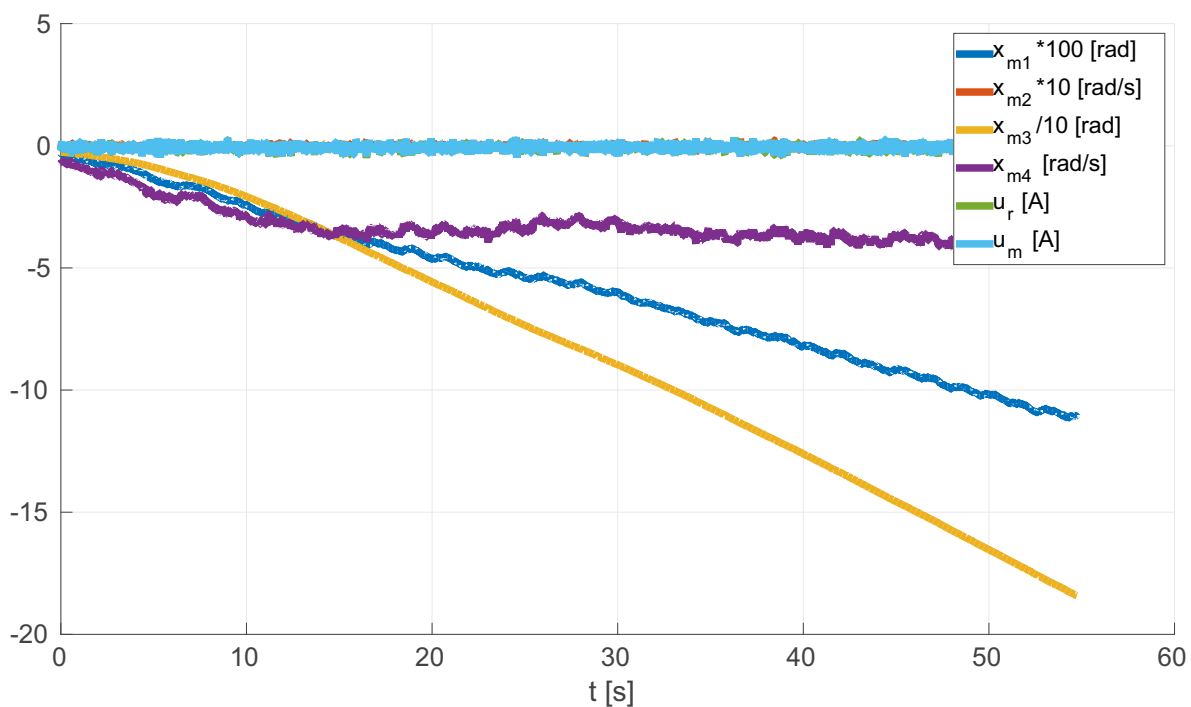


Figure 3.26: Experiment 4 (specified in Table 3.8)

why \underline{K}_i is bigger than in (3.70). However, this results helped to find exact \underline{K}_i settings for the real machine.

The last **Experiment 6** is analogical to the previous one. This time the \underline{K}_i vector is one hundred times bigger than in (3.70). This setting of LQI control shows bad effect of stabilisation caused by too strong integration feedback. The oscillations of x_{m3} and x_{m4} are dangerously strong. This solution is unacceptable to the real application.

All these experiments on the real machine give a good overview on the stabilisation process based on reaction wheel. It also proves that mathematical model proposed in Section 3.2 and later the computer simulations from Section 3.6 are correct. Simulations and experiments helped to design proper control strategies which decrease all velocities as much as possible in the real application.

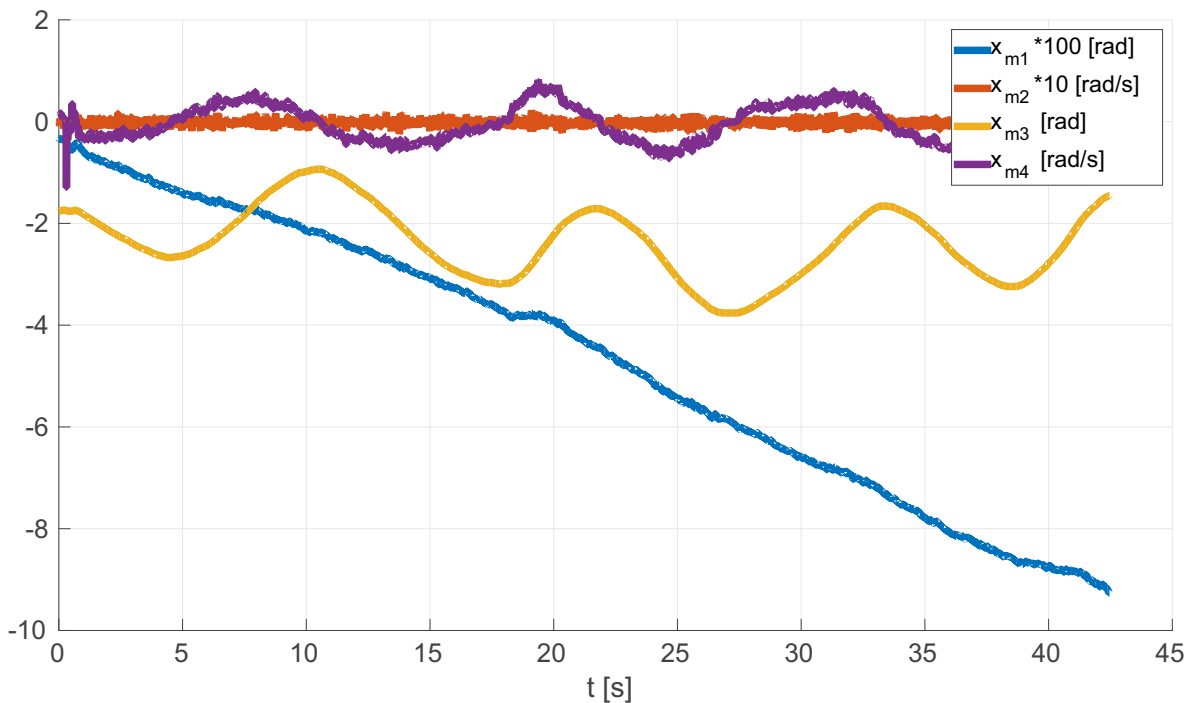


Figure 3.27: **Experiment 5** (specified in Table 3.8)

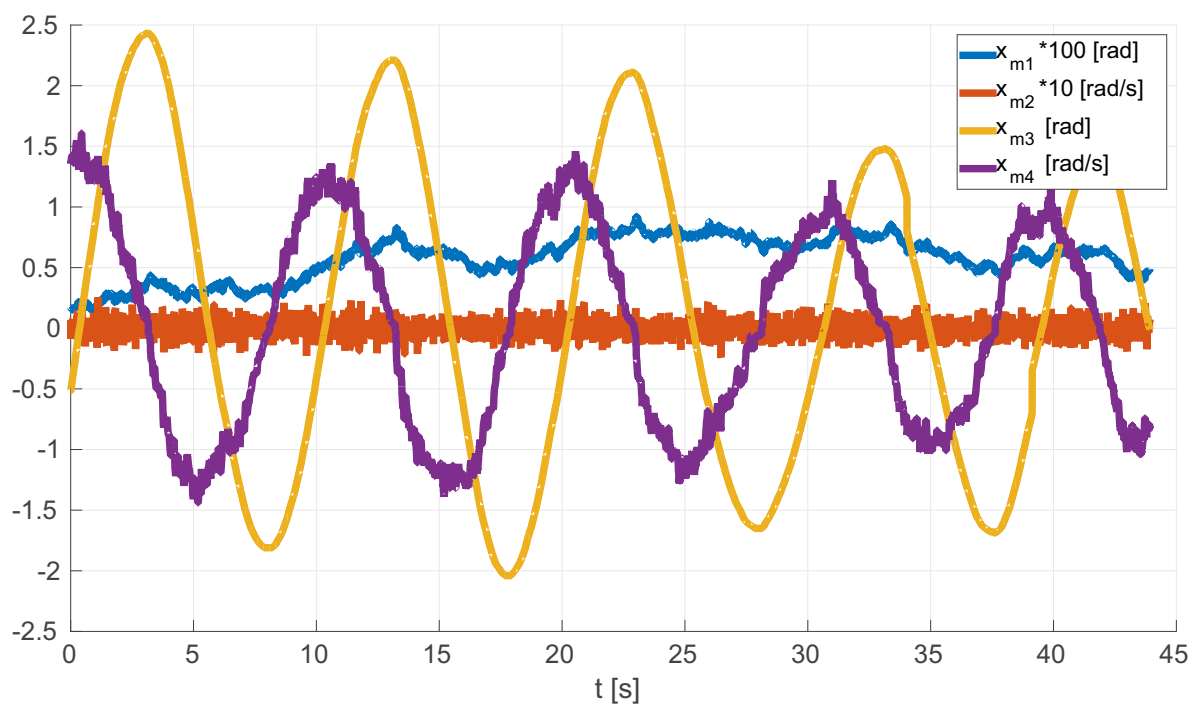


Figure 3.28: Experiment 6 (specified in Table 3.8)

Chapter 4

Bicycle with reaction wheel

4.1 Overview of bicycle mathematical models

Mathematical modeling of bicycles is complex. Many scientists have been struggling with it for a long time. Actually it started right after constructing the first bicycle which appeared in 1817 [42]. People did not understand why the bicycle keeps stability while riding. However, this mean of transport has been used for a very long time and most of people still can not explain the bicycle phenomenon. This has inspired scientists to solve this problem analytically. It is difficult to say if this task is solved at this moment. The full bicycle mathematical model is strongly nonlinear, nonholonomic with multiple inputs and multiple outputs. Many mathematical models are more or less simplified and they are usually sufficient to reflect the reality as much as it is needed for a particular purpose.

It is very important to perform computer simulations of the product that will be given to the market. It is necessary to predict if a new mean of transport will be efficient enough, strong enough or convenient enough for the human. This dissertation presents a new object which might be a new kind of mean of transport in the near future. Therefore, it is very important to test this object in detail by computer simulation. People always need new designs, shapes and styles in things they use, in things they touch. The new version of the bicycle with additional degree of freedom is certainly consistent with this modern trend. Currently, people more and more often use a new forms of transportation especially when it do not pollute the environment. Magnificent examples of creating fruitful results from the combination of fields of science like: physics, robotics and electronics are: bicycle with only one wheel¹, Segway² or Lit-C1³.

Nowadays, almost every machine is electronically-controlled. Big motorcycles companies try to improve their products. The innovation is in the predicting the trajectory of the motorcycle and control it to avoid crashes. This improves safety what actually encourage people to spend more money on it. To reach this goal it is necessary to have a good mathematical model implemented in computer simulation program. In this case, having the differential equations of motion of bicycle which explain the stability phenomenon is not everything. One of the biggest difficulty is to describe the physics of tyres which contacts with the ground. Many factors needs to be considered such as: elasticity, friction, shape, pressure and many others. Today this is the state-of-the-art in bicycle (motorcycle) research. Two authors need to be mentioned here: Sharp [91] and Vitorre Cossalter. There is a book [26] where

¹www.unicycle.com

²www.segway.com

³www.litmotors.com/c1

detailed description of the motorcycle dynamics can be found.

Generally, the history of bicycles began in 1817 when Karl von Drais constructed the first two wheel single-track vehicle which was stabilisable by steering the front wheel [42]. Next, in 1897 French mathematician Carvallo [23] created the general form of dynamic equations of the bicycle. After that in 1899 in the Cambridge University the great mathematician F. J. W. Whipple prepared the nonlinear differential equations of motion of the bicycle which were able to reflect the natural behaviour of a single-track vehicle. He published it in [100] and this was probably the first serious work about bicycles ever. It turned out that Whipple solved this problem as good as it is willingly used now in many cases. Whipple was not able to verify his model in computer simulation – it was long before computers. If he had been able to use computer simulation of his model, he would have been proud of it.

It is worth to use dynamic equations of motion of the bicycle from [30]. This article was published in 1955 by Döhring. The author used Whipple experience and combined it with the article of Klain and Sommerfeld [58] finally reaching corrected and well-prepared Whipple model. In 1970s there was a noticeable peak in interest in single-track vehicles. There were several reasons: firstly digital computers were becoming available to help to work with equations, rise in huge motorcycle popularity and naturally rise in motorcycles accidents, boom in environment friendly means of transportation thanks to bicycles. In 1985 [91] was published the full dynamic model of the motorcycle with elastic tyres.

In general, there are two main ways to prepare differential equations of motion of multi-body system: based on Newton's laws of motion or based on Lagrange method. When the number of degrees of freedom increases using these methods becomes more difficult and finally almost impossible to solve. It is worth to say that there is Kane's method [53] which can be used for complex systems and usually is able to handle with it. Nowadays bicycle models still improve and Kane's method is often taken [49, 76, 86].

There are also other increasingly approaches how to describe bicycle dynamics. Today Multibody Dynamics (MBD) software becomes popular. Suitable to perform simulations of almost any multibody object with many degrees of freedom. A few very popular software today are: Simscape Multibody⁴, Simpack⁵, Adams⁶, MBDyn⁷, COMSOL Multibody Dynamics Module⁸. There is also Bikesim⁹ which is dedicated for exploring motions of motorcycles. In spite of the fact that such a computer aid becomes more reliable, the practice proves that in many cases working with detailed mathematical model is inevitable. The MBD software is usually based on recursive algorithms giving only the approximate result which might be insufficient.

In this dissertation the linear Whipple model is chosen. It is decided to use the model proposed in [72]. Authors named it as: the canonical bicycle model. They describe that this model is able to reflect the most important states of the bicycle like: capsizing, weave and wobble

⁴www.mathworks.com/products/simmechanics

⁵www.simpack.com

⁶www.mscsoftware.com/product/adams

⁷www.mbdyn.org

⁸www.comsol.com/multibody-dynamics-module

⁹www.carsim.com/products/bikesim

(it is described in Section 4.4). In this case the tyre dynamics is omitted and it is assumed that the contact between wheels and ground is perfect (without slipping). This is the perfect version to extend it with the additional degree of freedom (the reaction wheel) and perform series of computer simulations. In this work, the canonical bicycle model is converted into a new form and then examined (see the rest of this Chapter).

4.2 Detailed mathematical modeling and bicycle modification

4.2.1 Complete model of the bicycle

This Section includes dynamic equations of the bicycle and the bicycle with the reaction wheel. Both of them are presented in different forms which are necessary in rest of analysis.

The full kinematic scheme of the bicycle is shown in Figure 4.1. Many of symbols are

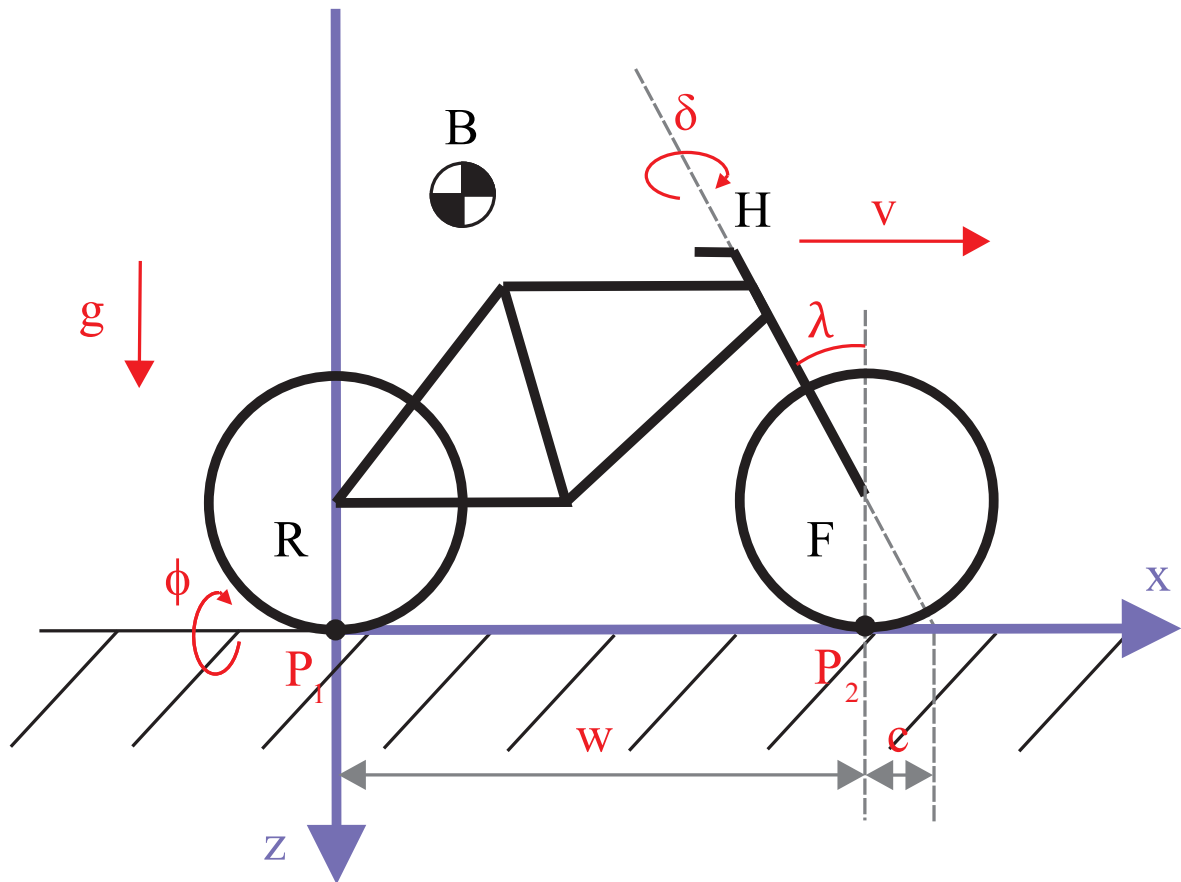


Figure 4.1: The kinematic scheme of the bicycle robot

taken from [72] and [66]. The kinematic scheme is also inspired on these papers. This makes the article more familiar for everyone who works on bicycles. There are four main parts: rear wheel R , front wheel F , body B and handlebar H . The body is the additional mass which can be attached to the whole structure and it usually refers to the human body.

The model has two degrees of freedom (generalized coordinates) marked on the scheme (see Figure 4.1): the handlebar angle δ and angle of the bicycle from the vertical ϕ . When these angles increases with arrowhead they are positive otherwise they are negative. When the bicycle goes straight and does not lean to the left or right side the number of degrees of freedom decreases to zero. Generally, it is assumed that there are two control signals (torques) which act the object in axes in accordance with location of degrees of freedom. δ and ϕ and its derivatives change over time. The rest of parameters are fixed. The bicycle velocity v is treated as a constant value. The time index (t) is omitted to assure clarity of presentation.

The main dynamic equation of the bicycle is:

$$\underline{M}\ddot{\underline{q}} + \underline{C}\dot{\underline{q}} + \underline{K}\underline{q} = \underline{f}, \quad (4.1)$$

where $\underline{M} \in \mathcal{R}^{n \times n}$ is the mass matrix, $\underline{C} \in \mathcal{R}^{n \times n}$ is the damping matrix, $\underline{K} \in \mathcal{R}^{n \times n}$ is the stiffness matrix, $\underline{f} \in \mathcal{R}^n$ is the control vector and $\underline{q} \in \mathcal{R}^n$ is the generalized variable vector. According to, [84] this equation can be formulated as

$$\underline{M}\ddot{\underline{q}} + v\underline{C}_1\dot{\underline{q}} + [g\underline{K}_0 + v^2\underline{K}_2]\underline{q} = \underline{f}. \quad (4.2)$$

The gravity of the Earth is expressed by g . Symbols: \underline{C}_1 , \underline{K}_0 and \underline{K}_2 are parts of \underline{C} and \underline{K} . Two angles (which represents two degrees of freedom) are put into \underline{q} vector

$$\underline{q} = [\phi, \delta]^T. \quad (4.3)$$

The control vector \underline{f} includes two torques

$$\underline{f} = \underline{u} = [u_1, u_2]^T = [T_\phi, T_\delta]^T \quad (4.4)$$

which act on the vehicle in corresponding axes.

Matrices from (4.1):

$$\underline{M} = \begin{bmatrix} M_{\phi\phi} & M_{\phi\delta} \\ M_{\delta\phi} & M_{\delta\delta} \end{bmatrix}, \quad (4.5)$$

$$\underline{C}_1 = \begin{bmatrix} C_{1\phi\phi} & C_{1\phi\delta} \\ C_{1\delta\phi} & C_{1\delta\delta} \end{bmatrix}, \quad (4.6)$$

$$\underline{K}_0 = \begin{bmatrix} K_{0\phi\phi} & K_{0\phi\delta} \\ K_{0\delta\phi} & K_{0\delta\delta} \end{bmatrix}, \quad (4.7)$$

$$\underline{K}_2 = \begin{bmatrix} K_{2\phi\phi} & K_{2\phi\delta} \\ K_{2\delta\phi} & K_{2\delta\delta} \end{bmatrix}, \quad (4.8)$$

represent parameters of the bicycle model. The physical parameters (which are taken from [72]) are equal to:

$$\mathbf{M} = \begin{bmatrix} 80.8172 & 2.3194 \\ 2.3194 & 0.2978 \end{bmatrix}, \quad (4.9)$$

$$\mathbf{C}_1 = \begin{bmatrix} 0.0000 & 33.8664 \\ -0.8504 & 1.6854 \end{bmatrix}, \quad (4.10)$$

$$\mathbf{K}_0 = \begin{bmatrix} -80.9500 & -2.5995 \\ -2.5995 & -0.8033 \end{bmatrix}, \quad (4.11)$$

$$\mathbf{K}_2 = \begin{bmatrix} 0.0000 & 76.5973 \\ 0.0000 & 2.6543 \end{bmatrix}. \quad (4.12)$$

These values came from detailed parameters of four parts: rear wheel, front wheel, body and handlebar, what is described precisely in [72]. Detailed equations and physical parameters are presented in Appendix A. This form of the bicycle model gives a great base for any further considerations in this case.

It is possible to use a specific method of analysis only when the system is represented in the right form. For example, in this case, the correct form allows to: make computer simulation, analyse stability, check controllability or observability, solve the control law and more. Every dynamic system represented by matrix equation (4.1) can be transformed into state-space representation

$$\dot{\underline{x}} = \mathbf{A}\underline{x} + \mathbf{B}\underline{u}, \quad (4.13)$$

$$\underline{y} = \mathbf{C}\underline{x}, \quad (4.14)$$

where $\mathbf{A} \in \mathcal{R}^{n \times n}$, $\mathbf{B} \in \mathcal{R}^{n \times p}$ and $\mathbf{C} \in \mathcal{R}^{q \times n}$. The state vector is equal to $\underline{x} = [\phi, \dot{\phi}, \delta, \dot{\delta}]^T$. After a few mathematical operations the matrices of the bicycle model become

$$\mathbf{A} = \begin{bmatrix} 0 & 1 \\ \frac{K_{0\phi\phi}M_{\delta\delta}g - K_{0\delta\phi}M_{\phi\delta}g + K_{2\phi\phi}M_{\delta\delta}v^2 - K_{2\delta\phi}M_{\phi\delta}v^2}{M_{\delta\phi}M_{\phi\delta} - M_{\delta\delta}M_{\phi\phi}} & -\frac{C_{\delta\phi}M_{\phi\delta}v - C_{\phi\phi}M_{\delta\delta}v}{M_{\delta\phi}M_{\phi\delta} - M_{\delta\delta}M_{\phi\phi}} \dots \\ 0 & 0 \\ -\frac{K_{0\phi\phi}M_{\delta\phi}g - K_{0\delta\phi}M_{\phi\phi}g + K_{2\phi\phi}M_{\delta\phi}v^2 - K_{2\delta\phi}M_{\phi\phi}v^2}{M_{\delta\phi}M_{\phi\delta} - M_{\delta\delta}M_{\phi\phi}} & \frac{C_{\delta\phi}M_{\phi\phi}v - C_{\phi\phi}M_{\delta\phi}v}{M_{\delta\phi}M_{\phi\delta} - M_{\delta\delta}M_{\phi\phi}} \\ 0 & 0 \\ \frac{K_{0\phi\delta}M_{\delta\delta}g - K_{0\delta\delta}M_{\phi\delta}g + K_{2\phi\delta}M_{\delta\delta}v^2 - K_{2\delta\delta}M_{\phi\delta}v^2}{M_{\delta\phi}M_{\phi\delta} - M_{\delta\delta}M_{\phi\phi}} & -\frac{C_{\delta\delta}M_{\phi\delta}v - C_{\phi\delta}M_{\delta\delta}v}{M_{\delta\phi}M_{\phi\delta} - M_{\delta\delta}M_{\phi\phi}} \dots \\ 0 & 1 \\ -\frac{K_{0\phi\delta}M_{\delta\phi}g - K_{0\delta\delta}M_{\phi\phi}g + K_{2\phi\delta}M_{\delta\phi}v^2 - K_{2\delta\delta}M_{\phi\phi}v^2}{M_{\delta\phi}M_{\phi\delta} - M_{\delta\delta}M_{\phi\phi}} & \frac{C_{\delta\delta}M_{\phi\phi}v - C_{\phi\delta}M_{\delta\phi}v}{M_{\delta\phi}M_{\phi\delta} - M_{\delta\delta}M_{\phi\phi}} \end{bmatrix}, \quad (4.15)$$

$$\mathbf{B} = \begin{bmatrix} 0 & 0 \\ -\frac{M_{\delta\delta}}{M_{\delta\phi}M_{\phi\delta} - M_{\delta\delta}M_{\phi\phi}} & \frac{M_{\phi\delta}}{M_{\delta\phi}M_{\phi\delta} - M_{\delta\delta}M_{\phi\phi}} \\ 0 & 0 \\ \frac{M_{\delta\phi}}{M_{\delta\phi}M_{\phi\delta} - M_{\delta\delta}M_{\phi\phi}} & -\frac{M_{\phi\phi}}{M_{\delta\phi}M_{\phi\delta} - M_{\delta\delta}M_{\phi\phi}} \end{bmatrix}. \quad (4.16)$$

Next, the state-space differential equations need to be found. The second derivatives of the generalized coordinates are

$$\begin{aligned} \dot{x}_2 = & x_1 \left(\frac{K_{0\phi\phi}M_{\delta\delta}g}{M_{\delta\phi}M_{\phi\delta} - M_{\delta\delta}M_{\phi\phi}} - \frac{K_{0\delta\phi}M_{\phi\delta}g}{M_{\delta\phi}M_{\phi\delta} - M_{\delta\delta}M_{\phi\phi}} + \frac{K_{2\phi\phi}M_{\delta\delta}v^2}{M_{\delta\phi}M_{\phi\delta} - M_{\delta\delta}M_{\phi\phi}} + \right. \\ & \left. - \frac{K_{2\delta\phi}M_{\phi\delta}v^2}{M_{\delta\phi}M_{\phi\delta} - M_{\delta\delta}M_{\phi\phi}} \right) + x_2 \left(\frac{C_{\phi\phi}M_{\delta\delta}v}{M_{\delta\phi}M_{\phi\delta} - M_{\delta\delta}M_{\phi\phi}} - \frac{C_{\delta\phi}M_{\phi\delta}v}{M_{\delta\phi}M_{\phi\delta} - M_{\delta\delta}M_{\phi\phi}} \right) + \\ & + x_3 \left(\frac{K_{0\phi\delta}M_{\delta\delta}g}{M_{\delta\phi}M_{\phi\delta} - M_{\delta\delta}M_{\phi\phi}} - \frac{K_{0\delta\delta}M_{\phi\delta}g}{M_{\delta\phi}M_{\phi\delta} - M_{\delta\delta}M_{\phi\phi}} + \frac{K_{2\phi\delta}M_{\delta\delta}v^2}{M_{\delta\phi}M_{\phi\delta} - M_{\delta\delta}M_{\phi\phi}} + \right. \\ & \left. - \frac{K_{2\delta\delta}M_{\phi\delta}v^2}{M_{\delta\phi}M_{\phi\delta} - M_{\delta\delta}M_{\phi\phi}} \right) + x_4 \left(\frac{C_{\phi\delta}M_{\delta\delta}v}{M_{\delta\phi}M_{\phi\delta} - M_{\delta\delta}M_{\phi\phi}} - \frac{C_{\delta\delta}M_{\phi\delta}v}{M_{\delta\phi}M_{\phi\delta} - M_{\delta\delta}M_{\phi\phi}} \right) + \\ & - u_1 \left(\frac{M_{\delta\delta}}{M_{\delta\phi}M_{\phi\delta} - M_{\delta\delta}M_{\phi\phi}} \right) + u_2 \left(\frac{M_{\phi\delta}}{M_{\delta\phi}M_{\phi\delta} - M_{\delta\delta}M_{\phi\phi}} \right), \end{aligned} \quad (4.17)$$

$$\begin{aligned}
\dot{x}_4 = & x_1 \left(\frac{K_{0\delta\phi}M_{\phi\phi}g}{M_{\delta\phi}M_{\phi\delta} - M_{\delta\delta}M_{\phi\phi}} - \frac{K_{0\phi\phi}M_{\delta\phi}g}{M_{\delta\phi}M_{\phi\delta} - M_{\delta\delta}M_{\phi\phi}} - \frac{K_{2\phi\phi}M_{\delta\phi}v^2}{M_{\delta\phi}M_{\phi\delta} - M_{\delta\delta}M_{\phi\phi}} + \right. \\
& \left. + \frac{K_{2\delta\phi}M_{\phi\phi}v^2}{M_{\delta\phi}M_{\phi\delta} - M_{\delta\delta}M_{\phi\phi}} \right) + x_2 \left(\frac{C_{\delta\phi}M_{\phi\phi}v}{M_{\delta\phi}M_{\phi\delta} - M_{\delta\delta}M_{\phi\phi}} - \frac{C_{\phi\phi}M_{\delta\phi}v}{M_{\delta\phi}M_{\phi\delta} - M_{\delta\delta}M_{\phi\phi}} \right) + \\
& + x_3 \left(\frac{K_{0\delta\delta}M_{\phi\phi}g}{M_{\delta\phi}M_{\phi\delta} - M_{\delta\delta}M_{\phi\phi}} - \frac{K_{0\phi\delta}M_{\delta\phi}g}{M_{\delta\phi}M_{\phi\delta} - M_{\delta\delta}M_{\phi\phi}} - \frac{K_{2\phi\delta}M_{\delta\phi}v^2}{M_{\delta\phi}M_{\phi\delta} - M_{\delta\delta}M_{\phi\phi}} + \right. \\
& \left. + \frac{K_{2\delta\delta}M_{\phi\phi}v^2}{M_{\delta\phi}M_{\phi\delta} - M_{\delta\delta}M_{\phi\phi}} \right) + x_4 \left(\frac{C_{\delta\delta}M_{\phi\phi}v}{M_{\delta\phi}M_{\phi\delta} - M_{\delta\delta}M_{\phi\phi}} - \frac{C_{\phi\delta}M_{\delta\phi}v}{M_{\delta\phi}M_{\phi\delta} - M_{\delta\delta}M_{\phi\phi}} \right) + \\
& + u_1 \left(\frac{M_{\delta\phi}}{M_{\delta\phi}M_{\phi\delta} - M_{\delta\delta}M_{\phi\phi}} \right) - u_2 \left(\frac{M_{\phi\phi}}{M_{\delta\phi}M_{\phi\delta} - M_{\delta\delta}M_{\phi\phi}} \right). \tag{4.18}
\end{aligned}$$

The symbolic state-space representation can be simplified by substitutions the fixed values (equations (4.5)-(4.8) and (4.9)-(4.12)). Finally,

$$A = \begin{bmatrix} 0.0000 & 1.0000 & 0.0000 & 0.0000 \\ 9.4898 & -1.0552 & -89.6913 & -3.3052 \\ 0.0000 & 0.0000 & 0.0000 & 1.0000 \\ 11.7195 & 36.7681 & -166.2630 & -30.8487 \end{bmatrix}, \tag{4.19}$$

$$B = \begin{bmatrix} 0.0000 & 0.0000 \\ -0.1241 & 0.0159 \\ 0.0000 & 0.0000 \\ 4.3238 & -0.1241 \end{bmatrix}, \tag{4.20}$$

and the differential equations:

$$\begin{aligned}
\dot{x}_2 = & 9.48977x_1 - 1.05522x_2 - 89.6913x_3 - 3.30515x_4 + 0.015935u_1 + \\
& - 0.124092u_2, \tag{4.21}
\end{aligned}$$

$$\begin{aligned}
\dot{x}_4 = & 11.7195x_1 + 36.7681x_2 - 166.263x_3 - 30.8487x_4 - 0.124092u_1 + \\
& + 4.32384u_2. \tag{4.22}
\end{aligned}$$

The bicycle mathematical model presented here is ready for further computer analysis.

4.2.2 Full model of bicycle with reaction wheel

Section 4.1 presents the background for the mathematical modeling of single-track vehicles. Several important publications are mentioned there which give consideration for various approaches to solving this complex problem. Finally, the canonical model of the bicycle (named so by the authors of the reference) is chosen from [72]. This is the linear version of the Whipple model. Next, in Subsection 4.2.1 this model is transformed into the state-space representation (4.15)-(4.16) and differential equations (4.17)-(4.18). These conversions are necessary to simulate and analyse the bicycle using a computer model.

The main thesis of this dissertation refers to bicycle modification with additional degree of freedom which is the reaction wheel. Having a relatively good mathematical model of this new system is very important here. A description of the dynamics from the Subsection 4.2.1 is extended and, finally, the full mathematical model of the bicycle with the reaction wheel is presented here. This is definitely the novelty. There is no literature available which concerns such combination: the bicycle and the reaction wheel.

In Figure 4.2, the kinematic scheme of the bicycle robot with the reaction wheel is presented.

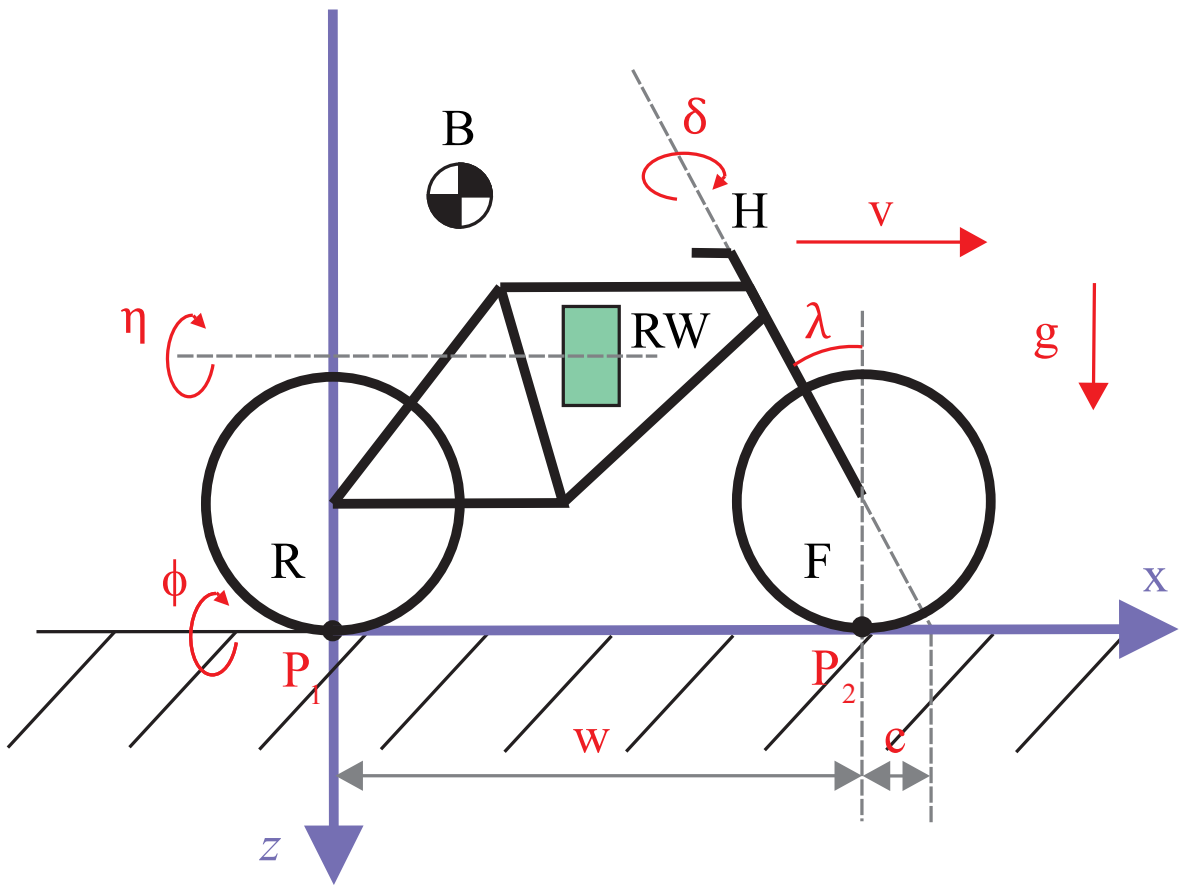


Figure 4.2: The kinematic scheme of the bicycle robot with the reaction wheel

Actually, it is a modified version of the scheme from Figure 4.1. At the beginning the body mass m_B is increased by the reaction wheel mass m_I therefore the main dynamic equation of the bicycle (4.2) is modified into

$$\mathbf{M}_{RW}\ddot{\underline{q}} + v\mathbf{C}_{1RW}\dot{\underline{q}} + [g\mathbf{K}_{0RW} + v^2\mathbf{K}_{2RW}]\underline{q} = \underline{f}. \quad (4.23)$$

All four matrices: \mathbf{M}_{RW} , \mathbf{C}_{1RW} , \mathbf{K}_{0RW} and \mathbf{K}_{2RW} take the mass of the reaction wheel into account. The physical parameters of the reaction wheel mounted on the bicycle can be found in Appendix B.

This time the system has three degrees of freedom (generalized coordinates): the handlebar angle δ and angle of the bicycle from the vertical ϕ and the angle of the steering wheel η . The generalized coordinates vector \underline{q} is equal to

$$\underline{q} = [\phi, \delta, \eta]^T. \quad (4.24)$$

Naturally there is an additional part marked as: *RW* – Reaction Wheel.

The state vector

$$\underline{x} = [q_1, \dot{q}_1, q_2, \dot{q}_2, q_3, \dot{q}_3]^T, \quad (4.25)$$

and, after substitution,

$$\underline{x} = [\phi, \dot{\phi}, \delta, \dot{\delta}, \eta, \dot{\eta}]^T. \quad (4.26)$$

The control vector \underline{u} has composed of torques

$$\underline{u} = [u_1, u_2, u_3]^T = [T_\phi, T_\delta, T_\eta]^T, \quad (4.27)$$

which act on the vehicle in corresponding axes (marked by: ϕ , δ and η). This means that it is possible to control this system by torque applied to the whole bicycle or to the handlebar or to the reaction wheel.

The key thing is to combine two mathematical models (bicycle and reaction wheel) into one complete version capable of reflecting the behaviour of the complete system. At the beginning, the torque τ_r which acts on the bicycle in the main axis (axis ϕ)

$$\tau_r = \tau_{\text{bicycle}} + \tau_{\text{reaction}} - \mu_r, \quad (4.28)$$

where τ_{bicycle} is the torque from the original Whipple model [72] which acts on the bicycle (sum of torques that comes, from canonical bicycle model), τ_{reaction} is the reaction torque and μ_r is the friction torque acting on the vehicle from the environment. Next the steering wheel accelerates under the torque

$$\tau_I = \tau_{\text{action}} - \mu_I, \quad (4.29)$$

where τ_{action} is the action torque, and μ_I is the friction torque acting on the reaction wheel from the environment. The same as in the dynamic equations of the reaction wheel pendulum (3.3) action is equal to negative reaction

$$\tau_{\text{action}} = -\tau_{\text{reaction}}, \quad (4.30)$$

and the action torque τ_{action} is created by the electric motor which accelerates the rotating wheel according to the formula

$$\tau_{\text{action}} = T_\eta - \mu_m, \quad (4.31)$$

where T_η is the electric motor torque and μ_m is the friction torque acting on the electric motor shaft.

For further research it is necessary to convert equations: (4.2)-(4.8) and (4.26)-(4.31) into state-space form (4.13):

$$\begin{aligned}
 A = & \left[\begin{array}{cccccc}
 0 & & & & & & \\
 \frac{K_{0\phi\phi}M_{\delta\delta}g - K_{0\delta\phi}M_{\phi\delta}g + K_{2\phi\phi}M_{\delta\delta}v^2 - K_{2\delta\phi}M_{\phi\delta}v^2}{M_{\delta\phi}M_{\phi\delta} - M_{\delta\delta}M_{\phi\phi}} & & & & & & \\
 0 & & & & & & \\
 -\frac{K_{0\phi\phi}M_{\delta\phi}g - K_{0\delta\phi}M_{\phi\phi}g + K_{2\phi\phi}M_{\delta\phi}v^2 - K_{2\delta\phi}M_{\phi\phi}v^2}{M_{\delta\phi}M_{\phi\delta} - M_{\delta\delta}M_{\phi\phi}} & & & & & & \dots \\
 0 & & & & & & \\
 0 & & & & & & \\
 \hline
 1 & & & & & & \\
 \frac{M_{\delta\delta}b_r}{M_{\delta\phi}M_{\phi\delta} - M_{\delta\delta}M_{\phi\phi}} - \frac{M_{\delta\delta}b_m}{M_{\delta\phi}M_{\phi\delta} - M_{\delta\delta}M_{\phi\phi}} - \frac{C_{\delta\phi}M_{\phi\delta}v - C_{\phi\phi}M_{\delta\delta}v}{M_{\delta\phi}M_{\phi\delta} - M_{\delta\delta}M_{\phi\phi}} & & & & & & \\
 0 & & & & & & \\
 \dots & & & & & & \\
 \frac{C_{\delta\phi}M_{\phi\phi}v - C_{\phi\phi}M_{\delta\phi}v}{M_{\delta\phi}M_{\phi\delta} - M_{\delta\delta}M_{\phi\phi}} & & & & & & \dots \\
 0 & & & & & & \\
 \frac{b_m}{I_I} & & & & & & \\
 \hline
 0 & & & & & & \\
 \frac{K_{0\phi\delta}M_{\delta\delta}g - K_{0\delta\delta}M_{\phi\delta}g + K_{2\phi\delta}M_{\delta\delta}v^2 - K_{2\delta\delta}M_{\phi\delta}v^2}{M_{\delta\phi}M_{\phi\delta} - M_{\delta\delta}M_{\phi\phi}} & & & & & & \\
 0 & & & & & & \\
 \dots & & & & & & \\
 -\frac{K_{0\phi\delta}M_{\delta\phi}g - K_{0\delta\delta}M_{\phi\phi}g + K_{2\phi\delta}M_{\delta\phi}v^2 - K_{2\delta\delta}M_{\phi\phi}v^2}{M_{\delta\phi}M_{\phi\delta} - M_{\delta\delta}M_{\phi\phi}} & & & & & & \dots \\
 0 & & & & & & \\
 0 & & & & & & \\
 \hline
 0 & 0 & 0 & & & & \\
 -\frac{C_{\delta\delta}M_{\phi\delta}v - C_{\phi\delta}M_{\delta\delta}v}{M_{\delta\phi}M_{\phi\delta} - M_{\delta\delta}M_{\phi\phi}} & 0 & \frac{M_{\delta\delta}b_m}{M_{\delta\phi}M_{\phi\delta} - M_{\delta\delta}M_{\phi\phi}} & & & & \\
 \dots & & & & & & \\
 1 & 0 & 0 & & & & \\
 \frac{C_{\delta\delta}M_{\phi\phi}v - C_{\phi\delta}M_{\delta\phi}v}{M_{\delta\phi}M_{\phi\delta} - M_{\delta\delta}M_{\phi\phi}} & 0 & 0 & & & & \\
 0 & 0 & 1 & & & & \\
 0 & 0 & -\frac{b_I + b_m}{I_I} & & & & \\
 \end{array} \right], \tag{4.32}
 \end{aligned}$$

$$\mathbf{B} = \begin{bmatrix} 0 & 0 & 0 \\ -\frac{M_{\delta\delta}}{M_{\delta\phi}M_{\phi\delta}-M_{\delta\delta}M_{\phi\phi}} & \frac{M_{\phi\delta}}{M_{\delta\phi}M_{\phi\delta}-M_{\delta\delta}M_{\phi\phi}} & -\frac{M_{\delta\delta}}{M_{\delta\phi}M_{\phi\delta}-M_{\delta\delta}M_{\phi\phi}} \\ 0 & 0 & 0 \\ \frac{M_{\delta\phi}}{M_{\delta\phi}M_{\phi\delta}-M_{\delta\delta}M_{\phi\phi}} & -\frac{M_{\phi\phi}}{M_{\delta\phi}M_{\phi\delta}-M_{\delta\delta}M_{\phi\phi}} & 0 \\ 0 & 0 & 0 \\ 0 & 0 & \frac{1}{I_I} \end{bmatrix}. \quad (4.33)$$

In this case, the differential equations are

$$\begin{aligned} \dot{x}_2 &= x_1 \left(\frac{K_{0\phi\phi}M_{\delta\delta}g}{M_{\delta\phi}M_{\phi\delta}-M_{\delta\delta}M_{\phi\phi}} - \frac{K_{0\delta\phi}M_{\phi\delta}g}{M_{\delta\phi}M_{\phi\delta}-M_{\delta\delta}M_{\phi\phi}} + \frac{K_{2\phi\phi}M_{\delta\delta}v^2}{M_{\delta\phi}M_{\phi\delta}-M_{\delta\delta}M_{\phi\phi}} + \right. \\ &\quad \left. - \frac{K_{2\delta\phi}M_{\phi\delta}v^2}{M_{\delta\phi}M_{\phi\delta}-M_{\delta\delta}M_{\phi\phi}} \right) + x_2 \left(\frac{C_{\phi\phi}M_{\delta\delta}v}{M_{\delta\phi}M_{\phi\delta}-M_{\delta\delta}M_{\phi\phi}} - \frac{C_{\delta\phi}M_{\phi\delta}v}{M_{\delta\phi}M_{\phi\delta}-M_{\delta\delta}M_{\phi\phi}} + \right. \\ &\quad \left. + \frac{b_r M_{\delta\delta}}{M_{\delta\phi}M_{\phi\delta}-M_{\delta\delta}M_{\phi\phi}} + \frac{b_m M_{\delta\delta}}{M_{\delta\phi}M_{\phi\delta}-M_{\delta\delta}M_{\phi\phi}} \right) + x_3 \left(\frac{K_{0\phi\delta}M_{\delta\delta}g}{M_{\delta\phi}M_{\phi\delta}-M_{\delta\delta}M_{\phi\phi}} + \right. \\ &\quad \left. - \frac{K_{0\delta\delta}M_{\phi\delta}g}{M_{\delta\phi}M_{\phi\delta}-M_{\delta\delta}M_{\phi\phi}} + \frac{K_{2\phi\delta}M_{\delta\delta}v^2}{M_{\delta\phi}M_{\phi\delta}-M_{\delta\delta}M_{\phi\phi}} - \frac{K_{2\delta\delta}M_{\phi\delta}v^2}{M_{\delta\phi}M_{\phi\delta}-M_{\delta\delta}M_{\phi\phi}} \right) + \\ &\quad + x_4 \left(\frac{C_{\phi\delta}M_{\delta\delta}v}{M_{\delta\phi}M_{\phi\delta}-M_{\delta\delta}M_{\phi\phi}} - \frac{C_{\delta\delta}M_{\phi\delta}v}{M_{\delta\phi}M_{\phi\delta}-M_{\delta\delta}M_{\phi\phi}} \right) + x_6 \left(-\frac{b_m M_{\delta\delta}}{M_{\delta\phi}M_{\phi\delta}-M_{\delta\delta}M_{\phi\phi}} \right) + \\ &\quad + u_1 \left(-\frac{M_{\delta\delta}}{M_{\delta\phi}M_{\phi\delta}-M_{\delta\delta}M_{\phi\phi}} \right) + u_2 \left(\frac{M_{\phi\delta}}{M_{\delta\phi}M_{\phi\delta}-M_{\delta\delta}M_{\phi\phi}} \right) + \\ &\quad + u_3 \left(-\frac{M_{\delta\delta}}{M_{\delta\phi}M_{\phi\delta}-M_{\delta\delta}M_{\phi\phi}} \right), \end{aligned} \quad (4.34)$$

$$\begin{aligned} \dot{x}_4 &= x_1 \left(\frac{K_{0\delta\phi}M_{\phi\phi}g}{M_{\delta\phi}M_{\phi\delta}-M_{\delta\delta}M_{\phi\phi}} - \frac{K_{0\phi\delta}M_{\delta\phi}g}{M_{\delta\phi}M_{\phi\delta}-M_{\delta\delta}M_{\phi\phi}} - \frac{K_{2\phi\phi}M_{\delta\phi}v^2}{M_{\delta\phi}M_{\phi\delta}-M_{\delta\delta}M_{\phi\phi}} + \right. \\ &\quad \left. + \frac{K_{2\delta\phi}M_{\phi\delta}v^2}{M_{\delta\phi}M_{\phi\delta}-M_{\delta\delta}M_{\phi\phi}} \right) + x_2 \left(\frac{C_{\delta\phi}M_{\phi\phi}v}{M_{\delta\phi}M_{\phi\delta}-M_{\delta\delta}M_{\phi\phi}} - \frac{C_{\phi\phi}M_{\delta\phi}v}{M_{\delta\phi}M_{\phi\delta}-M_{\delta\delta}M_{\phi\phi}} \right) + \\ &\quad + x_3 \left(\frac{K_{0\delta\delta}M_{\phi\phi}g}{M_{\delta\phi}M_{\phi\delta}-M_{\delta\delta}M_{\phi\phi}} - \frac{K_{0\phi\delta}M_{\delta\phi}g}{M_{\delta\phi}M_{\phi\delta}-M_{\delta\delta}M_{\phi\phi}} - \frac{K_{2\phi\delta}M_{\delta\phi}v^2}{M_{\delta\phi}M_{\phi\delta}-M_{\delta\delta}M_{\phi\phi}} + \right. \\ &\quad \left. + \frac{K_{2\delta\delta}M_{\phi\phi}v^2}{M_{\delta\phi}M_{\phi\delta}-M_{\delta\delta}M_{\phi\phi}} \right) + x_4 \left(\frac{C_{\delta\delta}M_{\phi\phi}v}{M_{\delta\phi}M_{\phi\delta}-M_{\delta\delta}M_{\phi\phi}} - \frac{C_{\phi\delta}M_{\delta\phi}v}{M_{\delta\phi}M_{\phi\delta}-M_{\delta\delta}M_{\phi\phi}} \right) + \\ &\quad + u_1 \left(\frac{M_{\delta\phi}}{M_{\delta\phi}M_{\phi\delta}-M_{\delta\delta}M_{\phi\phi}} \right) + u_2 \left(-\frac{M_{\phi\phi}}{M_{\delta\phi}M_{\phi\delta}-M_{\delta\delta}M_{\phi\phi}} \right), \end{aligned} \quad (4.35)$$

$$\dot{x}_6 = x_2 \frac{b_m}{I_I} - x_6 \left(\frac{b_I}{I_I} + \frac{b_m}{I_I} \right) + u_3 \frac{1}{I_I}. \quad (4.36)$$

These equations are derivatives of the generalized coordinates vector q (4.24).

Equations (4.34)-(4.36) and (4.32)-(4.33) can be written in short by using scalar parameters instead of symbols. Physical parameters of reaction wheel can be found in Table 3.7 and

parameters of the bicycle can be found in Table B.1. Finally, the state-space representation with physical parameters of the bicycle with the reaction wheel is as follows:

$$\mathbf{A} = \begin{bmatrix} 0 & 1 & 0 & 0 & 0 & 0 \\ 9.6836 & -0.1031 & -1.6177 & -0.3282 & 0 & 0 \\ 0 & 0 & 0 & 1 & 0 & 0 \\ 11.4693 & 3.67365 & 34.3316 & -3.0879 & 0 & 0 \\ 0 & 0 & 0 & 0 & 0 & 1 \\ 0 & 0.0004 & 0 & 0 & 0 & -0.0008 \end{bmatrix}, \quad (4.37)$$

$$\mathbf{B} = \begin{bmatrix} 0 & 0 & 0 \\ 0.0137 & -0.1212 & 0.0137 \\ 0 & 0 & 0 \\ -0.1212 & 4.3201 & 0 \\ 0 & 0 & 0 \\ 0 & 0 & 0.4000 \end{bmatrix}, \quad (4.38)$$

and differential equations become:

$$\begin{aligned} \dot{x}_2 &= 9.6836 x_1 - 0.1031 x_2 - 1.6177 x_3 - 0.3281 x_4 - 0.0001 x_6 + 0.0137 u_1 + \\ &\quad -0.1212 u_2 + 0.0137 u_3, \end{aligned} \quad (4.39)$$

$$\dot{x}_4 = 11.7195 x_1 + 36.7681 x_2 - 166.2630 x_3 - 30.8487 x_4 - 0.1241 u_1 + 4.3238 u_2 \quad (4.40)$$

$$\dot{x}_6 = 0.1116 x_2 - 0.2232 x_6 + 46.9866 u_3. \quad (4.41)$$

It is important to show things as simple as possible. These final equations probably are presented in the shortest possible form – every constant has been replaced with the corresponding number to reduce symbols as many as possible.

4.3 Appropriate control system design

This Section presents control algorithms for the bicycle with the reaction wheel. At the beginning all six bicycle systems are specified in Table 4.1 which includes all bicycle systems considered in this dissertation. However, in this Section uncontrolled bicycles are omitted. Generally, the bicycle model presented in Subsection 4.2.1 includes two control inputs – two torques which act on the bicycle in the same axes as the general coordinates (degrees of freedom). It is assumed that only one control signal is used to stabilize the bicycle (when the reaction wheel is turned off): the handlebar torque. In this dissertation, the bicycle is considered as the unmanned autonomic robotic system. Thinking about the real bicycle robot,

it is usually controlled only by this one signal [8, 10, 37]. The second control signal (which is not analysed in this dissertation and is zero – left for further research) is the torque which acts on the bicycle laterally (this is T_ϕ symbol in equation (4.4)). Nevertheless a human who drives a bicycle can stabilize it using only his hands – this is probably obvious for all those who can ride a bicycle. When the reaction wheel is turned on the system is treated as if it has two inputs: the handlebar torque and the reaction wheel torque. Using T_ϕ is more typical for human balancing method which is not the aim of this research.

Table 4.1: Description of analysed bicycle systems

System	Description
Bicycle1	bicycle controlled by the handlebar
Bicycle2	bicycle with the reaction wheel controlled by the handlebar
Bicycle3	bicycle with the reaction wheel controlled by the reaction wheel
Bicycle4	bicycle with the reaction wheel controlled by the handlebar and the reaction wheel
Bicycle5	uncontrolled bicycle
Bicycle6	uncontrolled bicycle with the reaction wheel

There are many control algorithms which are able to stabilize the bicycle. Some recent examples include: fuzzy sliding mode control [50], model predictive control [3] and adaptive control [4]. There are some comparisons of stabilisation techniques in [80] and [82]. The bicycle is controlled only by the handlebar in this Subsection. The aim is to stabilize the bicycle modeled by differential dynamic equations (4.50)-(4.18) and decrease every acceleration and every velocity of the system to zero.

The linear quadratic regulator (LQR) is widely described in Section 3.3. The system is defined by (3.21)-(3.22). General form of the control law is (3.34). It guarantees minimum level of the cost function (3.35). The cost function J depends on the input weight matrix \mathbf{R} and on the state weight matrix \mathbf{Q} . These two parameters generally set the LQR regulator. In this case, the standard values [62] are chosen what can as in Table 4.2.

Table 4.2: LQR settings

System	R	Q
Bicycle1, Bicycle2, Bicycle3	1	diag {1, 1, 1, 1}
Bicycle4	diag {1, 1}	diag {1, 1, 1, 1}

At this moment the Algebraic Riccati Equation (3.36) and \mathbf{K} matrix equation (3.37) are possible to calculate. The result can be found in Table 4.3.

Table 4.3: The result of the Algebraic Riccati Equation for considered systems

System	\mathbf{K}
Bicycle1	$[k_{1_1}, k_{1_2}, k_{1_3}, k_{1_4}]^T =$ $= [-3.3299, -0.2242, 3.8968, 0.2127]^T$
Bicycle2	$[k_{2_1}, k_{2_2}, k_{2_3}, k_{2_4}, k_{2_5}, k_{2_6}]^T =$ $= [-2.4590, -0.3339, 4.8497, 0.4499, -0.3312, -1.0093]^T$
Bicycle3	$[k_{3_1}, k_{3_2}, k_{3_3}, k_{3_4}, k_{3_5}, k_{3_6}]^T =$ $= [0.6489, -0.0249, -1.5871, -0.1492, 1.0000, 1.0221]^T$
Bicycle4	$\begin{aligned} & \begin{bmatrix} k_{4_21} & k_{4_22} & k_{4_23} & k_{4_24} & k_{4_25} & k_{4_26} \\ k_{4_31} & k_{4_32} & k_{4_33} & k_{4_34} & k_{4_35} & k_{4_36} \end{bmatrix}^T = \\ & = \begin{bmatrix} -2.5042 & -0.3305 & 4.7667 & 0.4436 & -0.0230 & -0.0405 \\ 0.3969 & -0.0381 & -1.0223 & -0.1062 & 0.9997 & 1.0197 \end{bmatrix}^T \end{aligned}$

As can be noticed, only in the Bicycle4 matrix \mathbf{K} has two rows. This is equivalent to two control signals: the handlebar torque u_2 and the reaction wheel torque u_3 . Naturally, the

Bicycle1 has the smallest number of columns of the \mathbf{K} matrix because it has the smallest size of the state vector and the smallest number of degrees of freedom. The comparison of control laws of the Bicycle1 and the Bicycle2 is interesting. In the Bicycle2 the feedback is stronger (values of matrix \mathbf{K} are bigger) because the reaction wheel when turned off only increases the mass (inertia) of the whole object. Series of control laws presented here are tested and evaluated by computer simulations in Section 4.5. Finally, the autonomous closed-loop system can be formulated as

$$\dot{\underline{x}} = (\mathbf{A} - \mathbf{B}\mathbf{K})\underline{x} \quad (4.42)$$

and shorter by

$$\dot{\underline{x}} = \mathbf{A}_z \underline{x}. \quad (4.43)$$

Matrix \mathbf{A}_z defines the complete closed-loop system and at this moment can be fully expressed by symbols and next by physical parameters. To find this \mathbf{A}_z matrix of the bicycle, it is important to use the following equations: (4.4), (4.15), (4.16) and Table 4.3. The same holds in the case of the bicycle with the reaction wheel – this time formulas need to be used are: (4.27), (4.32), (4.33) and Table 4.3. All necessary physical parameters can be found in Table 3.7 and Table B.1. Finally, four systems can be expressed as follows:

- Bicycle1

$$\mathbf{A}_{1z} = \begin{bmatrix} 0 & & & \\ \frac{K_{0\phi\phi}M_{\delta\delta}g - K_{0\delta\phi}M_{\phi\delta}g + K_{2\phi\phi}M_{\delta\delta}v^2 - K_{2\delta\phi}M_{\phi\delta}v^2}{M_{\delta\phi}M_{\phi\delta} - M_{\delta\delta}M_{\phi\phi}} - \frac{M_{\phi\delta}k_1}{M_{\delta\phi}M_{\phi\delta} - M_{\delta\delta}M_{\phi\phi}} & \dots & & \\ 0 & & & \\ \frac{M_{\phi\phi}k_1}{M_{\delta\phi}M_{\phi\delta} - M_{\delta\delta}M_{\phi\phi}} - \frac{K_{0\phi\phi}M_{\delta\phi}g - K_{0\delta\phi}M_{\phi\delta}g + K_{2\phi\phi}M_{\delta\phi}v^2 - K_{2\delta\phi}M_{\phi\phi}v^2}{M_{\delta\phi}M_{\phi\delta} - M_{\delta\delta}M_{\phi\phi}} & & & \\ \hline 1 & & & \\ -\frac{C_{\delta\phi}M_{\phi\delta}v - C_{\phi\phi}M_{\delta\delta}v}{M_{\delta\phi}M_{\phi\delta} - M_{\delta\delta}M_{\phi\phi}} - \frac{M_{\phi\delta}k_2}{M_{\delta\phi}M_{\phi\delta} - M_{\delta\delta}M_{\phi\phi}} & \dots & & \\ \dots & & & \\ 0 & & & \\ \frac{C_{\delta\phi}M_{\phi\phi}v - C_{\phi\phi}M_{\delta\phi}v}{M_{\delta\phi}M_{\phi\delta} - M_{\delta\delta}M_{\phi\phi}} + \frac{M_{\phi\phi}k_2}{M_{\delta\phi}M_{\phi\delta} - M_{\delta\delta}M_{\phi\phi}} & & & \\ \hline 0 & & & \\ \frac{K_{0\phi\delta}M_{\delta\delta}g - K_{0\delta\delta}M_{\phi\delta}g + K_{2\phi\delta}M_{\delta\delta}v^2 - K_{2\delta\delta}M_{\phi\delta}v^2}{M_{\delta\phi}M_{\phi\delta} - M_{\delta\delta}M_{\phi\phi}} - \frac{M_{\phi\delta}k_3}{M_{\delta\phi}M_{\phi\delta} - M_{\delta\delta}M_{\phi\phi}} & \dots & & \\ \dots & & & \\ 0 & & & \\ \frac{M_{\phi\phi}k_3}{M_{\delta\phi}M_{\phi\delta} - M_{\delta\delta}M_{\phi\phi}} - \frac{K_{0\phi\delta}M_{\delta\phi}g - K_{0\delta\delta}M_{\phi\phi}g + K_{2\phi\delta}M_{\delta\phi}v^2 - K_{2\delta\delta}M_{\phi\phi}v^2}{M_{\delta\phi}M_{\phi\delta} - M_{\delta\delta}M_{\phi\phi}} & & & \end{bmatrix}$$

$$\left[\begin{array}{c} 0 \\ -\frac{C_{\delta\delta}M_{\phi\delta}v - C_{\phi\delta}M_{\delta\delta}v}{M_{\delta\phi}M_{\phi\delta} - M_{\delta\delta}M_{\phi\phi}} - \frac{M_{\phi\delta}k_4}{M_{\delta\phi}M_{\phi\delta} - M_{\delta\delta}M_{\phi\phi}} \\ \dots \\ 1 \\ \frac{C_{\delta\delta}M_{\phi\phi}v - C_{\phi\delta}M_{\delta\phi}v}{M_{\delta\phi}M_{\phi\delta} - M_{\delta\delta}M_{\phi\phi}} + \frac{M_{\phi\phi}k_4}{M_{\delta\phi}M_{\phi\delta} - M_{\delta\delta}M_{\phi\phi}} \end{array} \right], \quad (4.44)$$

$$A_{1z} = \begin{bmatrix} 0 & 1 & 0 & 0 \\ 9.0766 & -1.0830 & -89.2077 & -3.2788 \\ 0 & 0 & 0 & 1 \\ 26.1173 & 37.7376 & -183.1122 & -31.7685 \end{bmatrix}; \quad (4.45)$$

- Bicycle2

$$A_{2z} = \begin{bmatrix} 0 \\ \frac{K_{0\phi\phi}M_{\delta\delta}g - K_{0\delta\phi}M_{\phi\delta}g + K_{2\phi\phi}M_{\delta\delta}v^2 - K_{2\delta\phi}M_{\phi\delta}v^2}{M_{\delta\phi}M_{\phi\delta} - M_{\delta\delta}M_{\phi\phi}} - \frac{M_{\phi\delta}k_1}{M_{\delta\phi}M_{\phi\delta} - M_{\delta\delta}M_{\phi\phi}} \\ 0 \\ \frac{M_{\phi\phi}k_1}{M_{\delta\phi}M_{\phi\delta} - M_{\delta\delta}M_{\phi\phi}} - \frac{K_{0\phi\phi}M_{\delta\phi}g - K_{0\delta\phi}M_{\phi\phi}g + K_{2\phi\phi}M_{\delta\phi}v^2 - K_{2\delta\phi}M_{\phi\phi}v^2}{M_{\delta\phi}M_{\phi\delta} - M_{\delta\delta}M_{\phi\phi}} \\ \dots \\ 0 \\ 0 \\ \hline 1 \\ \frac{M_{\delta\delta}b_r}{M_{\delta\phi}M_{\phi\delta} - M_{\delta\delta}M_{\phi\phi}} - \frac{M_{\delta\delta}b_m}{M_{\delta\phi}M_{\phi\delta} - M_{\delta\delta}M_{\phi\phi}} - \frac{C_{\delta\phi}M_{\phi\delta}v - C_{\phi\phi}M_{\delta\delta}v}{M_{\delta\phi}M_{\phi\delta} - M_{\delta\delta}M_{\phi\phi}} - \frac{M_{\phi\delta}k_2}{M_{\delta\phi}M_{\phi\delta} - M_{\delta\delta}M_{\phi\phi}} \\ \dots \\ \frac{C_{\delta\phi}M_{\phi\phi}v - C_{\phi\phi}M_{\delta\phi}v}{M_{\delta\phi}M_{\phi\delta} - M_{\delta\delta}M_{\phi\phi}} + \frac{M_{\phi\phi}k_2}{M_{\delta\phi}M_{\phi\delta} - M_{\delta\delta}M_{\phi\phi}} \\ 0 \\ \frac{b_m}{I_I} \end{bmatrix}$$

$$\begin{array}{c}
0 \\
\frac{K_{0\phi\delta}M_{\delta\delta}g - K_{0\delta\delta}M_{\phi\delta}g + K_{2\phi\delta}M_{\delta\delta}v^2 - K_{2\delta\delta}M_{\phi\delta}v^2}{M_{\delta\phi}M_{\phi\delta} - M_{\delta\delta}M_{\phi\phi}} - \frac{M_{\phi\delta}k_3}{M_{\delta\phi}M_{\phi\delta} - M_{\delta\delta}M_{\phi\phi}} \\
0 \\
\frac{M_{\phi\phi}k_3}{M_{\delta\phi}M_{\phi\delta} - M_{\delta\delta}M_{\phi\phi}} - \frac{K_{0\phi\delta}M_{\delta\phi}g - K_{0\delta\delta}M_{\phi\phi}g + K_{2\phi\delta}M_{\delta\phi}v^2 - K_{2\delta\delta}M_{\phi\phi}v^2}{M_{\delta\phi}M_{\phi\delta} - M_{\delta\delta}M_{\phi\phi}} \\
0 \\
0 \\
0 \\
-\frac{C_{\delta\delta}M_{\phi\delta}v - C_{\phi\delta}M_{\delta\delta}v}{M_{\delta\phi}M_{\phi\delta} - M_{\delta\delta}M_{\phi\phi}} - \frac{M_{\phi\delta}k_4}{M_{\delta\phi}M_{\phi\delta} - M_{\delta\delta}M_{\phi\phi}} \\
1 \\
\frac{C_{\delta\delta}M_{\phi\phi}v - C_{\phi\delta}M_{\delta\phi}v}{M_{\delta\phi}M_{\phi\delta} - M_{\delta\delta}M_{\phi\phi}} + \frac{M_{\phi\phi}k_4}{M_{\delta\phi}M_{\phi\delta} - M_{\delta\delta}M_{\phi\phi}} \\
0 \\
0 \\
0 \\
0 \\
0 \\
-\frac{M_{\phi\delta}k_5}{M_{\delta\phi}M_{\phi\delta} - M_{\delta\delta}M_{\phi\phi}} \quad \frac{M_{\delta\delta}b_m}{M_{\delta\phi}M_{\phi\delta} - M_{\delta\delta}M_{\phi\phi}} - \frac{M_{\phi\delta}k_6}{M_{\delta\phi}M_{\phi\delta} - M_{\delta\delta}M_{\phi\phi}} \\
0 \\
\cdots \\
\frac{M_{\phi\phi}k_5}{M_{\delta\phi}M_{\phi\delta} - M_{\delta\delta}M_{\phi\phi}} \quad \frac{M_{\phi\phi}k_6}{M_{\delta\phi}M_{\phi\delta} - M_{\delta\delta}M_{\phi\phi}} \\
0 \quad 1 \\
0 \quad -\frac{b_I + b_m}{I_L}
\end{array} \Bigg] , \quad (4.46)$$

$$A_{2z} = \begin{bmatrix} 0 & 1.0 & 0 & 0 & 0 & 0 \\ -11.2708 & -6.7273 & -0.2547 & -0.0684 & -0.0005 & -0.3030 \\ 0 & 0 & 0 & 1 & 0 & 0 \\ 758.2650 & 239.7560 & -14.2467 & -12.3459 & 0.0173 & 10.7986 \\ 0 & 0 & 0 & 0 & 0 & 1 \\ 0 & 0.0004 & 0 & 0 & 0 & -0.0008 \end{bmatrix}; \quad (4.47)$$

- Bicycle3

$$\begin{aligned}
A_{3z} = & \left[\begin{array}{c}
0 \\
0 \\
-\frac{K_{0\phi\phi}M_{\delta\phi}g - K_{0\delta\phi}M_{\phi\phi}g + K_{2\phi\phi}M_{\delta\phi}v^2 - K_{2\delta\phi}M_{\phi\phi}v^2}{M_{\delta\phi}M_{\phi\delta} - M_{\delta\delta}M_{\phi\phi}} \dots \\
0 \\
-\frac{k_1}{I_I} \\
\hline
1 \\
\frac{M_{\delta\delta}b_r}{M_{\delta\phi}M_{\phi\delta} - M_{\delta\delta}M_{\phi\phi}} - \frac{M_{\delta\delta}b_m}{M_{\delta\phi}M_{\phi\delta} - M_{\delta\delta}M_{\phi\phi}} - \frac{C_{\delta\phi}M_{\phi\delta}v - C_{\phi\phi}M_{\delta\delta}v}{M_{\delta\phi}M_{\phi\delta} - M_{\delta\delta}M_{\phi\phi}} + \frac{M_{\delta\delta}k_2}{M_{\delta\phi}M_{\phi\delta} - M_{\delta\delta}M_{\phi\phi}} \dots \\
0 \\
\dots \\
\frac{C_{\delta\phi}M_{\phi\phi}v - C_{\phi\phi}M_{\delta\phi}v}{M_{\delta\phi}M_{\phi\delta} - M_{\delta\delta}M_{\phi\phi}} \\
0 \\
\frac{b_m}{I_I} - \frac{k_2}{I_I} \\
\hline
0 \\
\frac{K_{0\phi\delta}M_{\delta\delta}g - K_{0\delta\delta}M_{\phi\delta}g + K_{2\phi\delta}M_{\delta\delta}v^2 - K_{2\delta\delta}M_{\phi\delta}v^2}{M_{\delta\phi}M_{\phi\delta} - M_{\delta\delta}M_{\phi\phi}} + \frac{M_{\delta\delta}k_3}{M_{\delta\phi}M_{\phi\delta} - M_{\delta\delta}M_{\phi\phi}} \dots \\
0 \\
\dots \\
\frac{K_{0\phi\delta}M_{\delta\phi}g - K_{0\delta\delta}M_{\phi\phi}g + K_{2\phi\delta}M_{\delta\phi}v^2 - K_{2\delta\delta}M_{\phi\phi}v^2}{M_{\delta\phi}M_{\phi\delta} - M_{\delta\delta}M_{\phi\phi}} \\
0 \\
-\frac{k_3}{I_I} \\
\hline
0 \\
\frac{M_{\delta\delta}k_4}{M_{\delta\phi}M_{\phi\delta} - M_{\delta\delta}M_{\phi\phi}} - \frac{C_{\delta\delta}M_{\phi\delta}v - C_{\phi\delta}M_{\delta\delta}v}{M_{\delta\phi}M_{\phi\delta} - M_{\delta\delta}M_{\phi\phi}} \dots \\
1 \\
\dots \\
\frac{C_{\delta\delta}M_{\phi\phi}v - C_{\phi\delta}M_{\delta\phi}v}{M_{\delta\phi}M_{\phi\delta} - M_{\delta\delta}M_{\phi\phi}} \\
0 \\
-\frac{k_4}{I_I}
\end{array} \right]
\end{aligned}$$

$$\begin{bmatrix} 0 & 0 \\ \frac{M_{\delta\delta}k_5}{M_{\delta\phi}M_{\phi\delta}-M_{\delta\delta}M_{\phi\phi}} & \frac{M_{\delta\delta}b_m}{M_{\delta\phi}M_{\phi\delta}-M_{\delta\delta}M_{\phi\phi}} + \frac{M_{\delta\delta}k_6}{M_{\delta\phi}M_{\phi\delta}-M_{\delta\delta}M_{\phi\phi}} \\ \dots & \dots \\ 0 & 0 \\ 0 & 0 \\ 0 & 1 \\ -\frac{k_5}{I_I} & -\frac{b_I+b_m}{I_I} - \frac{k_6}{I_I} \end{bmatrix}, \quad (4.48)$$

$$\mathbf{A}_{3z} = \begin{bmatrix} 0 & 1 & 0 & 0 & 0 & 0 \\ -36.3275 & -14.7924 & -176.7630 & -23.2804 & -0.0137 & -0.0477 \\ 0 & 0 & 0 & 1 & 0 & 0 \\ 11.4693 & 3.6737 & 34.3316 & -3.0879 & 0 & 0 \\ 0 & 0 & 0 & 0 & 0 & 1 \\ -1342.5400 & -428.6110 & -5110.4700 & -669.7100 & -0.4000 & -1.3919 \end{bmatrix}; \quad (4.49)$$

• Bicycle4

$$\mathbf{A}_{4z} =$$

$$= \begin{bmatrix} 0 \\ \frac{K_{0\phi\phi}M_{\delta\delta}g-K_{0\delta\phi}M_{\phi\delta}g+K_{2\phi\phi}M_{\delta\delta}v^2-K_{2\delta\phi}M_{\phi\delta}v^2}{M_{\delta\phi}M_{\phi\delta}-M_{\delta\delta}M_{\phi\phi}} + \frac{M_{\delta\delta}k_{31}}{M_{\delta\phi}M_{\phi\delta}-M_{\delta\delta}M_{\phi\phi}} - \frac{M_{\phi\delta}k_{21}}{M_{\delta\phi}M_{\phi\delta}-M_{\delta\delta}M_{\phi\phi}} \\ 0 \\ \frac{M_{\phi\phi}k_{21}}{M_{\delta\phi}M_{\phi\delta}-M_{\delta\delta}M_{\phi\phi}} - \frac{K_{0\phi\phi}M_{\delta\phi}g-K_{0\delta\phi}M_{\phi\phi}g+K_{2\phi\phi}M_{\delta\phi}v^2-K_{2\delta\phi}M_{\phi\phi}v^2}{M_{\delta\phi}M_{\phi\delta}-M_{\delta\delta}M_{\phi\phi}} \\ 0 \\ -\frac{k_{31}}{I_I} \\ \dots \\ 1 \\ \frac{M_{\delta\delta}b_r}{M_{\delta\phi}M_{\phi\delta}-M_{\delta\delta}M_{\phi\phi}} - \frac{M_{\delta\delta}b_m}{M_{\delta\phi}M_{\phi\delta}-M_{\delta\delta}M_{\phi\phi}} - \frac{C_{\delta\phi}M_{\phi\delta}v-C_{\phi\phi}M_{\delta\delta}v}{M_{\delta\phi}M_{\phi\delta}-M_{\delta\delta}M_{\phi\phi}} + \frac{M_{\delta\delta}k_{32}}{M_{\delta\phi}M_{\phi\delta}-M_{\delta\delta}M_{\phi\phi}} - \frac{M_{\phi\delta}k_{22}}{M_{\delta\phi}M_{\phi\delta}-M_{\delta\delta}M_{\phi\phi}} \\ 0 \\ \dots \\ \frac{C_{\delta\phi}M_{\phi\phi}v-C_{\phi\phi}M_{\delta\phi}v}{M_{\delta\phi}M_{\phi\delta}-M_{\delta\delta}M_{\phi\phi}} + \frac{M_{\phi\phi}k_{22}}{M_{\delta\phi}M_{\phi\delta}-M_{\delta\delta}M_{\phi\phi}} \\ 0 \\ \frac{b_m}{I_I} - \frac{k_{32}}{I_I} \\ \dots \end{bmatrix}$$

$$\begin{array}{c}
0 \\
\frac{K_{0\phi\delta}M_{\delta\delta}g - K_{0\delta\delta}M_{\phi\delta}g + K_{2\phi\delta}M_{\delta\delta}v^2 - K_{2\delta\delta}M_{\phi\delta}v^2}{M_{\delta\phi}M_{\phi\delta} - M_{\delta\delta}M_{\phi\phi}} + \frac{M_{\delta\delta}k_{33}}{M_{\delta\phi}M_{\phi\delta} - M_{\delta\delta}M_{\phi\phi}} - \frac{M_{\phi\delta}k_{23}}{M_{\delta\phi}M_{\phi\delta} - M_{\delta\delta}M_{\phi\phi}} \\
0 \\
\cdots \\
\frac{M_{\phi\phi}k_{23}}{M_{\delta\phi}M_{\phi\delta} - M_{\delta\delta}M_{\phi\phi}} - \frac{K_{0\phi\delta}M_{\delta\phi}g - K_{0\delta\delta}M_{\phi\phi}g + K_{2\phi\delta}M_{\delta\phi}v^2 - K_{2\delta\delta}M_{\phi\phi}v^2}{M_{\delta\phi}M_{\phi\delta} - M_{\delta\delta}M_{\phi\phi}} \\
0 \\
-\frac{k_{33}}{I_I} \\
0 \\
\frac{M_{\delta\delta}k_{34}}{M_{\delta\phi}M_{\phi\delta} - M_{\delta\delta}M_{\phi\phi}} - \frac{C_{\delta\delta}M_{\phi\delta}v - C_{\phi\delta}M_{\delta\delta}v}{M_{\delta\phi}M_{\phi\delta} - M_{\delta\delta}M_{\phi\phi}} - \frac{M_{\phi\delta}k_{24}}{M_{\delta\phi}M_{\phi\delta} - M_{\delta\delta}M_{\phi\phi}} \\
1 \\
\cdots \\
\frac{C_{\delta\delta}M_{\phi\phi}v - C_{\phi\delta}M_{\delta\phi}v}{M_{\delta\phi}M_{\phi\delta} - M_{\delta\delta}M_{\phi\phi}} + \frac{M_{\phi\phi}k_{24}}{M_{\delta\phi}M_{\phi\delta} - M_{\delta\delta}M_{\phi\phi}} \\
0 \\
-\frac{k_{34}}{I_I} \\
\hline
0 & 0 \\
\frac{M_{\delta\delta}k_{35}}{M_{\delta\phi}M_{\phi\delta} - M_{\delta\delta}M_{\phi\phi}} - \frac{M_{\phi\delta}k_{25}}{M_{\delta\phi}M_{\phi\delta} - M_{\delta\delta}M_{\phi\phi}} & \frac{M_{\delta\delta}b_m}{M_{\delta\phi}M_{\phi\delta} - M_{\delta\delta}M_{\phi\phi}} + \frac{M_{\delta\delta}k_{36}}{M_{\delta\phi}M_{\phi\delta} - M_{\delta\delta}M_{\phi\phi}} - \frac{M_{\phi\delta}k_{26}}{M_{\delta\phi}M_{\phi\delta} - M_{\delta\delta}M_{\phi\phi}} \\
0 & 0 \\
\cdots & \\
\frac{M_{\phi\phi}k_{25}}{M_{\delta\phi}M_{\phi\delta} - M_{\delta\delta}M_{\phi\phi}} & \frac{M_{\phi\phi}k_{26}}{M_{\delta\phi}M_{\phi\delta} - M_{\delta\delta}M_{\phi\phi}} \\
0 & 1 \\
-\frac{k_{35}}{I_I} & -\frac{b_I + b_m}{I_I} - \frac{k_{36}}{I_I} \\
\end{array} \Bigg] , \quad (4.50)$$

$$\mathbf{A}_{4z} = \left[\begin{array}{cccccc}
0 & 1 & 0 & 0 & 0 & 0 \\
9.6836 & -0.1031 & -1.6177 & -0.3282 & 0 & 0 \\
0 & 0 & 0 & 1 & 0 & 0 \\
11.4693 & 3.6737 & 34.3316 & -3.0879 & 0 & 0 \\
0 & 0 & 0 & 0 & 0 & 1 \\
0 & 0.0004 & 0 & 0 & 0 & -0.0008
\end{array} \right]. \quad (4.51)$$

The most complex system is the Bicycle4. It has the highest number of degrees of freedom and the highest number of control signals from all analysed systems.

This Section presents very significant part of this dissertation. It precisely describes important variants of the bicycle model with and without the reaction wheel and gives the opportunity to compare it (further analysis in following Sections). Moreover, this Section includes the solution of the control law for considered systems which ensures the optimal control (which minimizes the cost function) and stabilizes it in unstable equilibrium point.

4.4 Classical approach to stability analysis

In this Section, the stability of bicycle systems is analysed. The classical approach is adopted to find if the system is stable or not. Methods presented below are based on: step responses and eigenvalues characteristics. Six systems are considered which have been listed in Table 4.1.

The Bicycle5 and Bicycle6 bicycle are uncontrolled. It turned out that in some conditions the bicycle is self-stable [6, 8, 72]. Each bicycle has some range of velocity where it keeps the vertical position even if no torque acts on the handlebar. In this dissertation it is very important to check the stability of the bicycle with and without the control loop and prove if the bicycle with the reaction wheel has the best stability margin. It is worth to mention that the Bicycle5 differs from the Bicycle6 by having the reaction wheel.

The first stability test is focused on the eigenvalues. The second equation from Table 3.1 is mostly important here. Therefore, it is the same method as used in this dissertation for stability analysis of the reaction wheel. Eigenvalues give a good information about stability of the object and also about frequency and amplitude of oscillations. The result can be found in Table 4.4.

Table 4.4: Eigenvectors of different bicycle systems with velocity $v = 10\text{m/s}$

System	Eigenvector λ
Bicycle1	<ul style="list-style-type: none"> – 0.2026 – $3.8797 + 10.8341i$ – $3.8797 - 10.8341i$ – 24.8894

Table 4.4 – continued

System	Eigenvector λ
Bicycle2	<ul style="list-style-type: none"> – 24.8899 – $3.8893 + 10.8370i$ – $3.8893 - 10.8370i$ – $0.2153 + 0.0296i$ – $0.2153 - 0.0296i$ 0
Bicycle3	<ul style="list-style-type: none"> – 47.0059 – 24.8561 – $3.8066 + 10.8194i$ – $3.8066 - 10.8194i$ – 1.0002 – 0.1610
Bicycle4	<ul style="list-style-type: none"> – 47.0040 – 25.1245 – $3.9588 + 10.7477i$ – $3.9588 - 10.7477i$ – 0.2025 – 1.0002

Table 4.4 – continued

System	Eigenvector λ
Bicycle5	0.1611
	– 3.7202 + 10.9068 <i>i</i>
	– 3.7202 – 10.9068 <i>i</i>
	– 24.6246
Bicycle6	0
	– 24.6251
	– 3.7303 + 10.9097 <i>i</i>
	– 3.7303 – 10.9097 <i>i</i>
	0.1609
	– 0.2232

Each of six bicycles (see Table 4.1) travels with velocity equal to $v = 10 \text{ m/s}$ during this test. This parameter combined with all physical parameters from 3.7 and B.1 allows to calculate quadratic optimal control law (3.34). This actually gives the full closed-loop system which finally returns matrix A_z (4.43). This is sufficient to calculate the eigenvalues of the considered systems Table 4.1. This method is able to evaluate object with Multiple Inputs and Multiple Outputs (MIMO) which is a great advantage.

As can be noticed, first four models (Bicycle1-Bicycle4) which has the feedback control loop are stable because every real part of the eigenvalue is negative. Uncontrolled bicycles (Bicycle5-Bicycle6) are unstable for this particular velocity.

When the module of eigenvalue increases, then the system goes further from stability border. Certainly in this case the biggest module is in the Bicycle4. Thus, this system has a larger distance from stability margin than classical bicycle stabilized only by the handlebar (Bicycle1). This is a very important conclusion from this dissertation viewpoint.

It is interesting that absolute values of real parts of eigenvalues of Bicycle6 have bigger values than in Bicycle5. If the bicycle is heavier amplitudes of oscillations become smaller and they decreases more quickly. The turned off reaction wheel increases the mass of the bicycle which finally creates better stability margin. The Bicycle6 has more degrees of freedom therefore it has more roots.

In this work, there is also the second method used to test the stability of the systems listed in Table 4.1. This method is based on the transfer function theory which finally gives the step response. Every relation between input signal and output signal provides one transfer function. In this case the biggest number of transfer functions comes from the Bicycle4. It has two input signals and six output signals, what finally gives twelve combinations (twelve transfer functions). All transfer functions for all considered systems are listed in Table 4.5. It is worth to mention, that neither input signal nor output signal does not always has any physical interpretation in this case. This analysis is focused on the evaluation if the system is stable or not and it also gives information about the regulation time (can be read from the step response).

Table 4.5: Transfer functions of different bicycle systems

System	Transfer function
Bicycle1	$G_1(s) = \frac{-0.1241s^2 - 18.12s - 408.4}{s^4 + 32.85s^3 + 332.2s^2 + 3362s + 667.8}$ $G_2(s) = \frac{-0.1241s^3 - 18.12s^2 - 408.4s}{s^4 + 32.85s^3 + 332.2s^2 + 3362s + 667.8}$ $G_3(s) = \frac{4.324s^2 - 2.462e-05s - 42.49}{s^4 + 32.85s^3 + 332.2s^2 + 3362s + 667.8}$ $G_4(s) = \frac{4.324s^3 - 2.462e-05s^2 - 42.49s}{s^4 + 32.85s^3 + 332.2s^2 + 3362s + 667.8}$
Bicycle2	$G_1(s) = \frac{-0.1241s^4 - 18.15s^3 - 412.5s^2 - 91.17s + 9.692e-16}{s^6 + 33.1s^5 + 340.3s^4 + 3442s^3 + 1436s^2 + 155.9s - 1.945e-15}$ $G_2(s) = \frac{-0.1241s^5 - 18.15s^4 - 412.5s^3 - 91.17s^2}{s^6 + 33.1s^5 + 340.3s^4 + 3442s^3 + 1436s^2 + 155.9s - 1.945e-15}$ $G_3(s) = \frac{4.324s^4 + 1.055s^3 - 42.47s^2 - 9.484s + 4.625e-24}{s^6 + 33.1s^5 + 340.3s^4 + 3442s^3 + 1436s^2 + 155.9s - 1.945e-15}$ $G_4(s) = \frac{4.324s^5 + 1.055s^4 - 42.47s^3 - 9.484s^2 + 3.113e-35s}{s^6 + 33.1s^5 + 340.3s^4 + 3442s^3 + 1436s^2 + 155.9s - 1.945e-15}$ $G_5(s) = \frac{-0.01385s^3 - 2.022s^2 - 45.59s - 8.799e-15}{s^6 + 33.1s^5 + 340.3s^4 + 3442s^3 + 1436s^2 + 155.9s - 1.945e-15}$ $G_6(s) = \frac{-0.01385s^4 - 2.022s^3 - 45.59s^2 + 1.344e-14s + 5.678e-33}{s^6 + 33.1s^5 + 340.3s^4 + 3442s^3 + 1436s^2 + 155.9s - 1.945e-15}$
Bicycle3	$G_1(s) = \frac{-4.39s^4 - 135.9s^3 - 745s^2 - 81.46s - 1.002e-11}{s^6 + 80.64s^5 + 1939s^4 + 2.051e04s^3 + 1.753e05s^2 + 1.814e05s + 2.475e04}$ $G_2(s) = \frac{-4.39s^5 - 135.9s^4 - 745s^3 - 81.46s^2 - 6.968e-12s}{s^6 + 80.64s^5 + 1939s^4 + 2.051e04s^3 + 1.753e05s^2 + 1.814e05s + 2.475e04}$ $G_3(s) = \frac{-161.4s^3 - 69.46s^2 - 5.742s + 2.947e-12}{s^6 + 80.64s^5 + 1939s^4 + 2.051e04s^3 + 1.753e05s^2 + 1.814e05s + 2.475e04}$ $G_4(s) = \frac{-161.4s^4 - 69.46s^3 - 5.742s^2 + 6.483e-13s}{s^6 + 80.64s^5 + 1939s^4 + 2.051e04s^3 + 1.753e05s^2 + 1.814e05s + 2.475e04}$ $G_5(s) = \frac{46.99s^4 + 1500s^3 + 1.462e04s^2 + 1.513e05s - 2.475e04}{s^6 + 80.64s^5 + 1939s^4 + 2.051e04s^3 + 1.753e05s^2 + 1.814e05s + 2.475e04}$

Table 4.5 – continued

System	Transfer function
	$G_6(s) = \frac{46.99s^5 + 1500s^4 + 1.462e04s^3 + 1.513e05s^2 - 2.475e04s}{s^6 + 80.64s^5 + 1939s^4 + 2.051e04s^3 + 1.753e05s^2 + 1.814e05s + 2.475e04}$
Bicycle4	$G_{11}(s) = \frac{-4.39s^4 - 140.1s^3 - 842s^2 - 620.1s - 281.3}{s^6 + 81.25s^5 + 1980s^4 + 2.109e04s^3 + 1.779e05s^2 + 1.901e05s + 3.138e04}$ $G_{12}(s) = \frac{-4.39s^5 - 140.1s^4 - 842s^3 - 620.1s^2 - 281.3s}{s^6 + 81.25s^5 + 1980s^4 + 2.109e04s^3 + 1.779e05s^2 + 1.901e05s + 3.138e04}$ $G_{13}(s) = \frac{-160.2s^3 - 130s^2 - 66.63s - 29.26}{s^6 + 81.25s^5 + 1980s^4 + 2.109e04s^3 + 1.779e05s^2 + 1.901e05s + 3.138e04}$ $G_{14}(s) = \frac{-160.2s^4 - 130s^3 - 66.63s^2 - 29.26s}{s^6 + 81.25s^5 + 1980s^4 + 2.109e04s^3 + 1.779e05s^2 + 1.901e05s + 3.138e04}$ $G_{15}(s) = \frac{46.99s^4 + 1544s^3 + 1.562e04s^2 + 1.58e05s + 3.138e04}{s^6 + 81.25s^5 + 1980s^4 + 2.109e04s^3 + 1.779e05s^2 + 1.901e05s + 3.138e04}$ $G_{16}(s) = \frac{46.99s^5 + 1544s^4 + 1.562e04s^3 + 1.58e05s^2 + 3.138e04s}{s^6 + 81.25s^5 + 1980s^4 + 2.109e04s^3 + 1.779e05s^2 + 1.901e05s + 3.138e04}$ $G_{21}(s) = \frac{-0.1241s^4 - 25.39s^3 - 1303s^2 - 2.047e04s - 1.919e04}{s^6 + 81.25s^5 + 1980s^4 + 2.109e04s^3 + 1.779e05s^2 + 1.901e05s + 3.138e04}$ $G_{22}(s) = \frac{-0.1241s^5 - 25.39s^4 - 1303s^3 - 2.047e04s^2 - 1.919e04s}{s^6 + 81.25s^5 + 1980s^4 + 2.109e04s^3 + 1.779e05s^2 + 1.901e05s + 3.138e04}$ $G_{23}(s) = \frac{4.324s^4 + 209.3s^3 + 161.5s^2 - 2038s - 1996}{s^6 + 81.25s^5 + 1980s^4 + 2.109e04s^3 + 1.779e05s^2 + 1.901e05s + 3.138e04}$ $G_{24}(s) = \frac{4.324s^5 + 209.3s^4 + 161.5s^3 - 2038s^2 - 1996s}{s^6 + 81.25s^5 + 1980s^4 + 2.109e04s^3 + 1.779e05s^2 + 1.901e05s + 3.138e04}$ $G_{25}(s) = \frac{13.5s^3 + 126.8s^2 - 1688s - 459.9}{s^6 + 81.25s^5 + 1980s^4 + 2.109e04s^3 + 1.779e05s^2 + 1.901e05s + 3.138e04}$ $G_{26}(s) = \frac{13.5s^4 + 126.8s^3 - 1688s^2 - 459.9s}{s^6 + 81.25s^5 + 1980s^4 + 2.109e04s^3 + 1.779e05s^2 + 1.901e05s + 3.138e04}$
Bicycle5	$G_1(s) = \frac{-0.1241s^2 - 18.12s - 408.4}{s^4 + 31.9s^3 + 310.8s^2 + 3219s - 526.7}$ $G_2(s) = \frac{-0.1241s^3 - 18.12s^2 - 408.4s}{s^4 + 31.9s^3 + 310.8s^2 + 3219s - 526.7}$ $G_3(s) = \frac{4.324s^2 - 2.462 \cdot 10^{-5}s - 42.49}{s^4 + 31.9s^3 + 310.8s^2 + 3219s - 526.7}$ $G_4(s) = \frac{4.324s^3 - 2.462 \cdot 10^{-5}s^2 - 42.49s}{s^4 + 31.9s^3 + 310.8s^2 + 3219s - 526.7}$
Bicycle4	$G_{11}(s) = \frac{-0.1212s^4 - 18.04s^3 - 432.1s^2 - 413.3s - 165.8}{s^6 + 33.83s^5 + 355.2s^4 + 3725s^3 + 4098s^2 + 1987s + 256.7}$ $G_{12}(s) = \frac{-0.1212s^5 - 18.04s^4 - 432.1s^3 - 413.3s^2 - 165.8s}{s^6 + 33.83s^5 + 355.2s^4 + 3725s^3 + 4098s^2 + 1987s + 256.7}$ $G_{13}(s) = \frac{4.32s^4 + 4.233s^3 - 41.5s^2 - 42.35s - 17.29}{s^6 + 33.83s^5 + 355.2s^4 + 3725s^3 + 4098s^2 + 1987s + 256.7}$ $G_{14}(s) = \frac{4.32s^5 + 4.233s^4 - 41.5s^3 - 42.35s^2 - 17.29s}{s^6 + 33.83s^5 + 355.2s^4 + 3725s^3 + 4098s^2 + 1987s + 256.7}$

Table 4.5 – continued

System	Transfer function
	$G_{15}(s) = \frac{0.0003036s^3 + 0.03088s^2 + 0.3031s + 0.2008}{s^6 + 33.83s^5 + 355.2s^4 + 3725s^3 + 4098s^2 + 1987s + 256.7}$
	$G_{16}(s) = \frac{0.0003036s^4 + 0.03088s^3 + 0.3031s^2 + 0.2008s - 3.673e-17}{s^6 + 33.83s^5 + 355.2s^4 + 3725s^3 + 4098s^2 + 1987s + 256.7}$
	$G_{21}(s) = \frac{0.01371s^4 + 0.4361s^3 + 2.446s^2 + 0.8134s + 0.1297}{s^6 + 33.83s^5 + 355.2s^4 + 3725s^3 + 4098s^2 + 1987s + 256.7}$
	$G_{22}(s) = \frac{0.01371s^5 + 0.4361s^4 + 2.446s^3 + 0.8134s^2 + 0.1297s}{s^6 + 33.83s^5 + 355.2s^4 + 3725s^3 + 4098s^2 + 1987s + 256.7}$
	$G_{23}(s) = \frac{0.5074s^3 + 0.3419s^2 + 0.08427s + 0.01353}{s^6 + 33.83s^5 + 355.2s^4 + 3725s^3 + 4098s^2 + 1987s + 256.7}$
	$G_{24}(s) = \frac{0.5074s^4 + 0.3419s^3 + 0.08427s^2 + 0.01353s}{s^6 + 33.83s^5 + 355.2s^4 + 3725s^3 + 4098s^2 + 1987s + 256.7}$
	$G_{25}(s) = \frac{0.4s^4 + 13.14s^3 + 129s^2 + 1358s + 256.7}{s^6 + 33.83s^5 + 355.2s^4 + 3725s^3 + 4098s^2 + 1987s + 256.7}$
	$G_{26}(s) = \frac{0.4s^5 + 13.14s^4 + 129s^3 + 1358s^2 + 256.7s}{s^6 + 33.83s^5 + 355.2s^4 + 3725s^3 + 4098s^2 + 1987s + 256.7}$

The transfer function is an universal tool, and in this dissertation, used to calculate step responses presented in Figure 4.3.

Similarly like in Subsection 3.4 which describes the reaction wheel system, step responses of the open-loop systems (Bicycle5 and Bicycle6) are based on state space linear model (3.21) and (3.22) and closed-loop systems (Bicycle1-Bicycle4) are based on (3.72) and (3.22). Inputs are defined by B and outputs are defined by C .

The step response gives yet another information which can be used to compare considered systems. First of all it informs if the system is stable or not. Naturally, objects Bicycle1-Bicycle4 are stable and bicycles without control, i.e. Bicycle5 and Bicycle6 are non-stable. If it is stable the transfer function needs to reach finite values. Figures: 4.3(e) and 4.3(f) clearly show that after 400 s curves reach enormously big values which can be considered as infinite values. The transfer function can be used to evaluate the time response. This is the period of time after which one relation between input and output becomes stable. This is definitely valuable and important information in this dissertation. It can be used to evaluate which system reaches stability in shortest time. It directly proves that the reaction wheel shortens the regulation time. The optimal LQR regulator (with the same weights Table 4.2 in all considered systems) can stabilize the Bicycle4 within 5 s time. In contrast typical bicycle controlled by the handlebar torque (Bicycle1) needs more than 10 s.

Regulation time of the Bicycle2 is shorter than in Bicycle3. This is a very useful conclusion, that shows which method is faster and that the handlebar control can eventually be replaced by the reaction wheel. The bicycle which travels with velocity $v = 10$ m/s controlled by LQR control law (3.34) needs nearby 20 s to dump all oscillations.

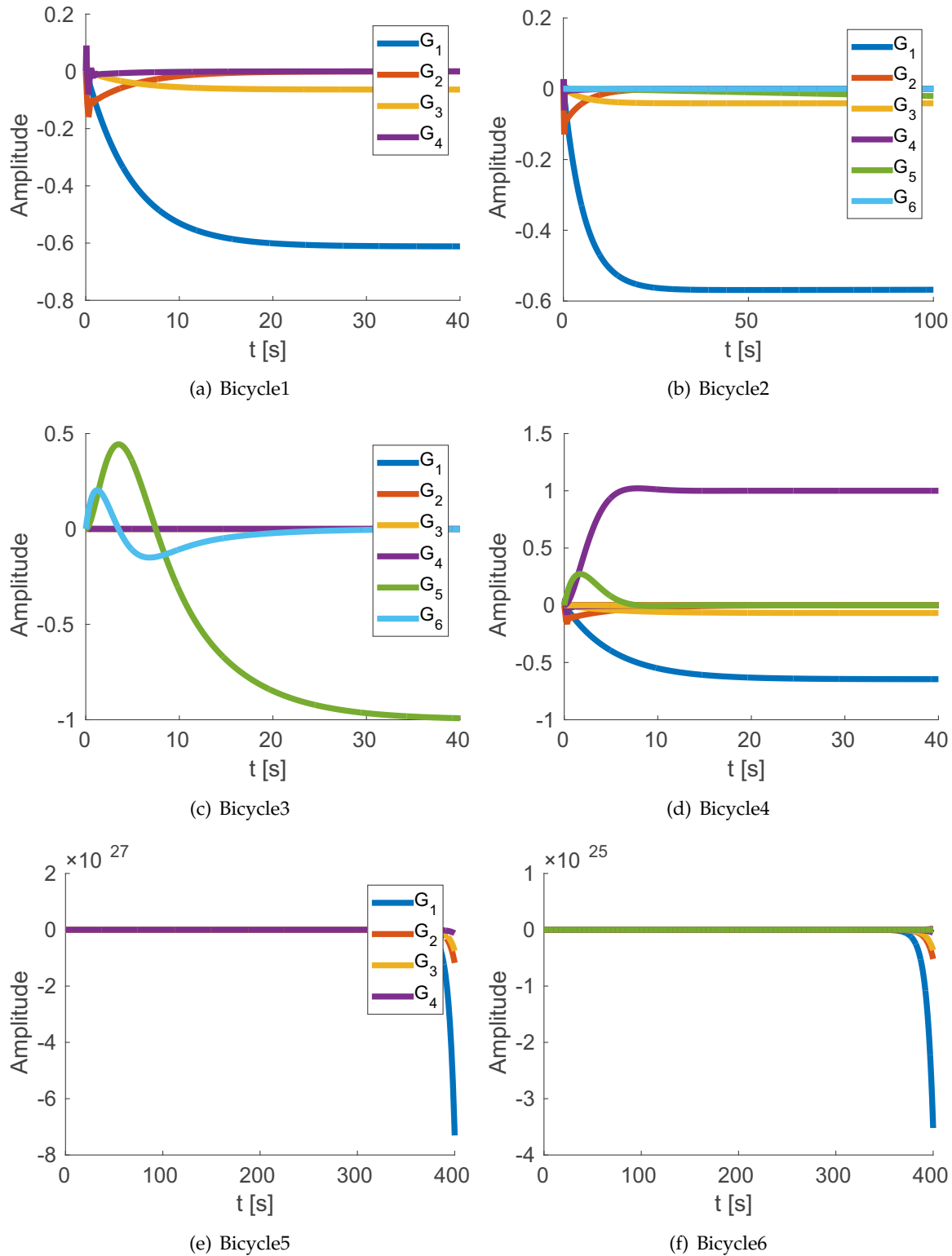


Figure 4.3: Step responses of different bicycle systems

Regulation times presented in step responses in Figure 4.3 are finally verified by a precise computer simulation described in Section 4.5. It turned out that these results are very similar to each other (step responses and computer simulation). This proves that this method is reliable and is useful for BIBO stability evaluation.

The last method presented in this Section is eigenvalues graph. Eigenvalues based on equation from Table 3.1 are calculated for specified range of parameter and, finally, transferred into the graph. This gives a very useful information about the stability of the object. A common parameter analysed in the literature [72, 75] is the velocity. A good question is: for what value of velocity the bicycle is the farthest from the stability margin? The same applies to the other parameters such as: mass or friction coefficient or many others. In this dissertation a few parameters are chosen which are especially important in real applications.

The eigenvalues graph is based on the A_z matrix of the state-space representation. Therefore, it includes the model of the closed-loop system. These method analyses the dynamics of the whole system which is a huge advantage. This method is also suitable for MIMO. The results are presented in Figures: 4.4-4.9.

Conclusions concerning stability analysis for the closed-loop system are complex. The main reason is that the control signals are unbounded. The real machine always has some limitations for outputs of the controller. It is necessary to find the right reference for this consideration. In this dissertation, a strong reference is the optimal LQR controller configured with the same weights (Tab. 4.2) every time. The optimum is only one for each system thus this is the reference – each considered system has the optimum control law. Figure 4.4 presents the roots of the Bicycle2 with velocity from range 0 to 10 m/s. As can be noticed, for low velocity (below 4 m/s) keeping balance is problematic. This is quite typical effect for the bicycle – it is difficult to travel by bicycle at low velocity. This is verified in Section 3.6 by computer simulation of the object. The most important fact is that this vehicle needs relatively high velocity to travel. On the other hand, Figure 4.5 presents the same bicycle but stabilized by the reaction wheel (Bicycle3). It is stable at every velocity tested. This is a strong difference between these two already mentioned systems. Therefore, the conclusion is that bicycle stabilized by the handlebar with relatively low velocity is definitely closer to stability margin than the one stabilized by the reaction wheel.

The stability analysis of the Bicycle4 presented in Figure 4.6 shows that combining the following two control signals: the handlebar torque and reaction wheel torque results in superior stability conclusions in the whole range of the velocity. Compared to the rest of systems each time the real part of eigenvalues is the lowest and always negative. This is equivalent to the strongest damping of oscillations of the considered vehicles. This is very important conclusion for this dissertation. This forms a part of the confirmation for the main thesis, that the reaction wheel helps to stabilize the bicycle.

There are also yet another three eigenvalues graphs: Figures 4.7-4.9. It describes the bicycle (Bicycle5) without any control signal. In this case, the analysis is more obvious, because there is no control and no control limits. The most important eigenvalues graph is presented in Figure 4.7. Similar graphs can be found in literature [71]. They give lot of information about the bicycle movement dynamics. In some range of velocity bicycle is self-stable – the

real part of roots is negative. It means that while traveling over certain velocity keeps the stability even if there are some lateral disturbances. The literature gives names for some of these eigenvalues lines. They are marked in presented Figure 4.7. These names are as follows: *capsize*, *weave* and *castering*.

Meaning of each of these expressions (modes) is explained in literature [92] (author has used this nomenclature first time ever). Generally, *capsize* represents the lateral fall without oscillations. The front wheel is uncontrolled and falls in the same direction as the bicycle. It is too weak to stop collapsing the bicycle. This process is often very slow and happens with high velocity of the bicycle. Usually *capsize* is used by drivers to initiate the turn. *Capsize* usually corresponds to stable bicycle for low velocity and unstable for high velocity.

The *weave* mode represents slow oscillations (0 – 4 Hz) of the rear frame around the steering axis. For most bicycles it is unstable for low velocity and becomes stable for high velocity – amplitude decreases and frequency rises.

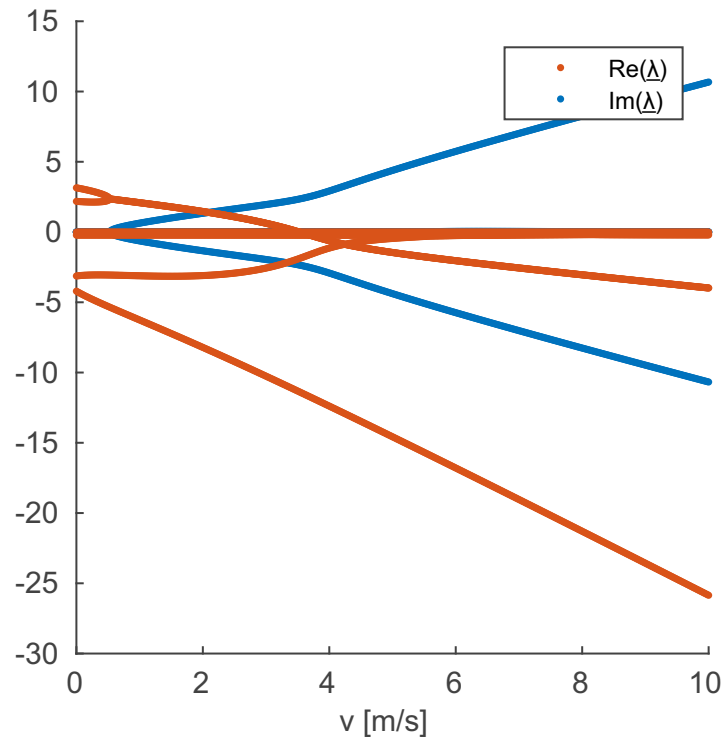
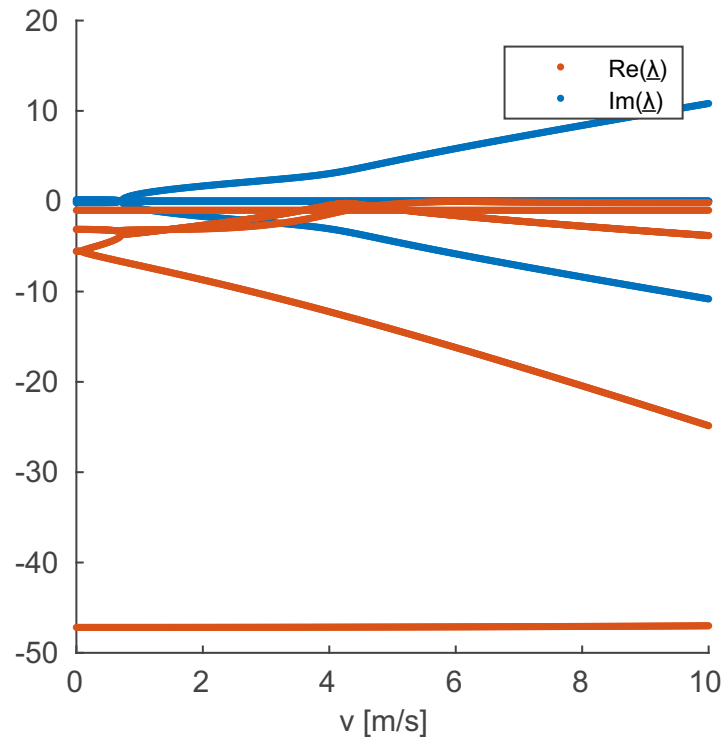
Next there is the *castering* mode. The front wheel is treated as a wheel of a trolley, which moves on the tractrix-like trajectory¹⁰. The root which corresponds with the line on the eigenvalue graph Figure 4.7 is always stable, because the real part is big and negative.

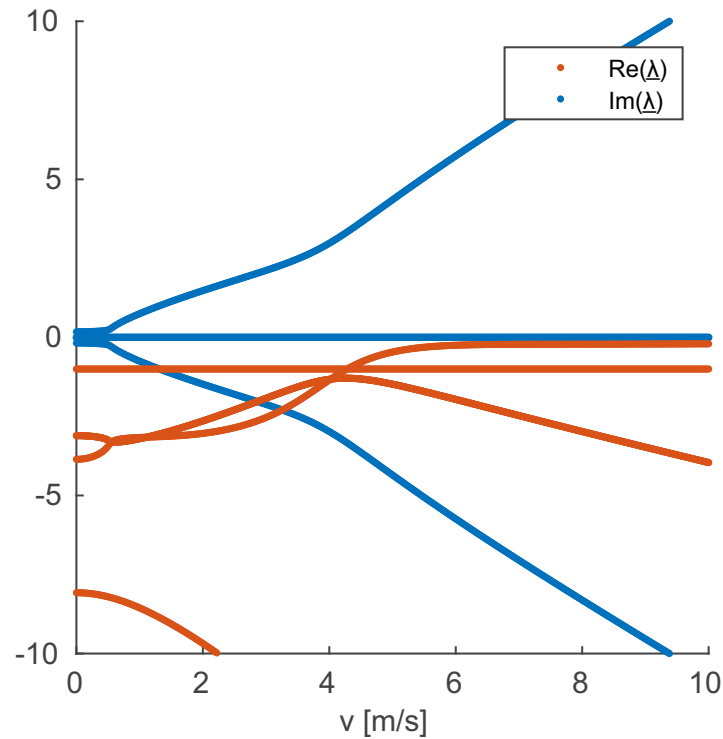
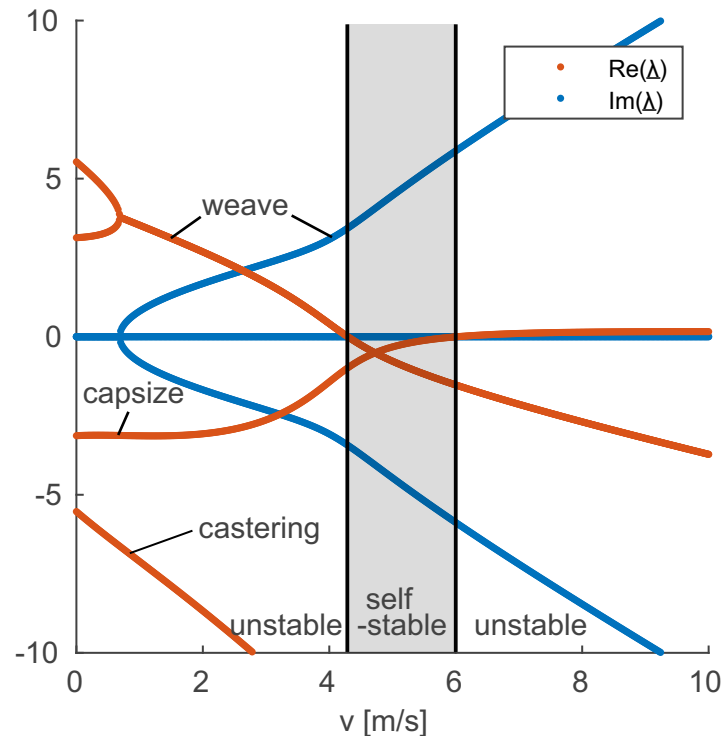
The last mode is the *wobble*. It is always discussed with the bicycle dynamics in literature. It represents fast oscillations of the steering wheel (4 – 10 Hz). It can also appear in the rear part of frame if it is too flexible. This phenomenon can be noticed in shopping trolleys or in wheels of landing planes. It is easy to avoid it by taking care of speed, position and force acting on the handlebar, however left without control can be destructive. The frequency of the oscillation can be modified by stiffening the frame or the handlebar, by decreasing the weight or changing the velocity. A great influence on this effect have tyres and frame deformations. However, in this work, this instability can be omitted because it is assumed that the frame and wheels are perfectly rigid. This also does not appear in the Figure 4.7. It can be taken into account when more detailed bicycle model is used like in [26, 89–91].

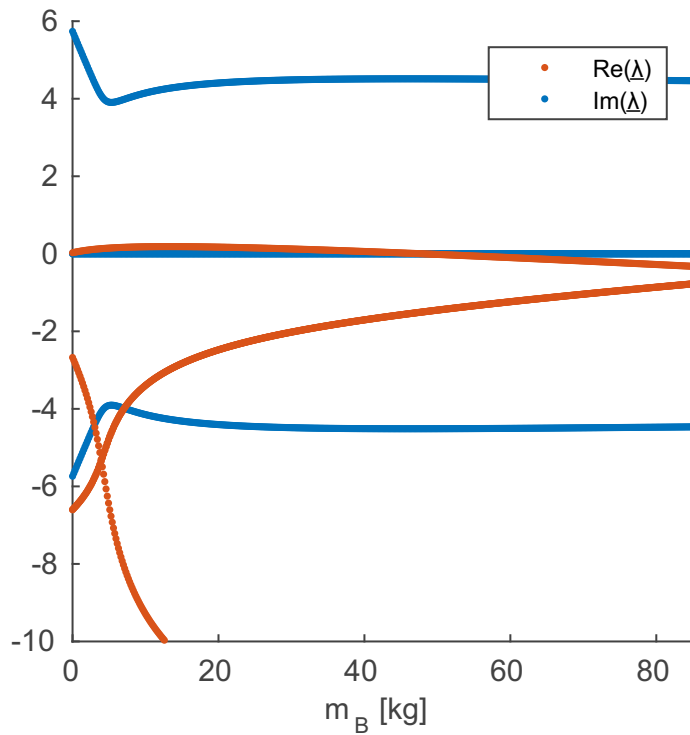
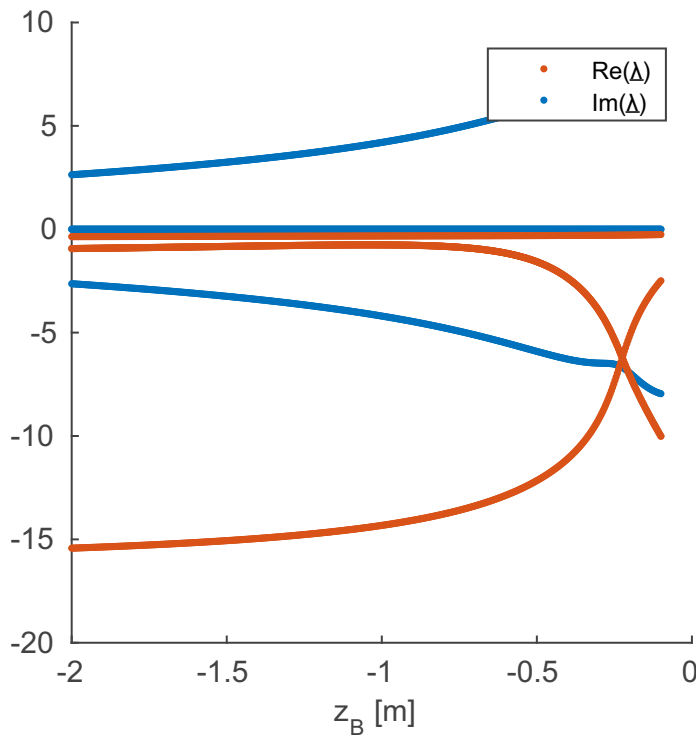
The last two eigenvalues graphs of the bicycle (Bicycle5) are presented in Figures 4.8 and 4.9. They present the stability measure depending on a specific range of the considered parameters: body weight m_B (Fig. 4.8) and distance from ground to the center of mass of the body z_B (Fig. 4.9). This time the velocity is fixed and is equal to $v = 5 \text{ m/s}$. As can be noticed, when the body weight rises, the average absolute real part values decreases. If this parameter is too low, the bicycle is unstable. Distance z_B has a different influence. The stability margin is the biggest for the highest considered value of this parameter. When it tends to zero, real parts of two roots decrease and the system tends to being unstable.

To summarize, in this Section the stability of the bicycle with and without the reaction wheel is presented. There are several theoretical proofs of improving stability of the bicycle by reaction wheel. The considerations are based on sophisticated bicycle model from the latest literature. This model is modified in this dissertation and mathematical techniques are used to analysed it. Conclusions about stability have been mainly drawn on the basis of eigenvalues, step responses and eigenvalues graphs.

¹⁰Object moves along the tractrix curve, when is pulled horizontally under the influence of friction, when starts from nonzero vertical position

Figure 4.4: Bicycle2 – eigenvalues graph for time-varying v Figure 4.5: Bicycle3 – eigenvalues graph for time-varying v

Figure 4.6: Bicycle4 – eigenvalues graph for time-varying v Figure 4.7: Bicycle5 – eigenvalues graph for time-varying v

Figure 4.8: Bicycle5 – eigenvalues graph for time-varying m_B Figure 4.9: Bicycle5 – eigenvalues graph for time-varying z_B

4.5 Computer simulation and evaluation

In this Section, series of computer simulations are presented. The simulated system is the bicycle with the reaction wheel. The main aim is to find any proofs that confirm that the reaction wheel can improve stability of the bicycle. Finally, results are promising: the visual interpretation of plots and performance indices undoubtedly support the main thesis of this dissertation.

It was decided to simulate four systems to support the main thesis of this dissertation as much as possible: Bicycle2, Bicycle3, Bicycle4 and Bicycle6. These systems are sufficient to show a good sides and bad sides of controlling the bicycle by the handlebar (classical approach) and by the reaction wheel. These four systems have the same physical parameters. The only difference is the control signal: uncontrolled, controlled by the handlebar, controlled by the reaction wheel and controlled by the handlebar and the reaction wheel simultaneously. A full list of computer simulations of bicycle systems can be found in Table 4.6.

Table 4.6: A full list of computer simulations of bicycle systems (see Table 4.1)

Number	Description
1	Bicycle6 – initial velocity: $v = 1 \text{ m/s}$
2	Bicycle6 – initial velocity: $v = 5 \text{ m/s}$
3	Bicycle6 – initial velocity: $v = 10 \text{ m/s}$
4	Bicycle2 – initial velocity: $v = 0.1 \text{ m/s}$
5	Bicycle2 – initial velocity: $v = 1 \text{ m/s}$
6	Bicycle2 – initial velocity: $v = 5 \text{ m/s}$
7	Bicycle2 – initial velocity: $v = 10 \text{ m/s}$
8	Bicycle3
9	Bicycle4 – initial velocity: $v = 0.1 \text{ m/s}$
10	Bicycle4 – initial velocity: $v = 1 \text{ m/s}$
11	Bicycle4 – initial velocity: $v = 5 \text{ m/s}$

Table 4.6 – continued

Number	Description
12	Bicycle4 – initial velocity: $v = 10 \text{ m/s}$

Back to Section 4.4 and systems from Table 4.1 – if the system Bicycle6 behaves similarly as the system Bicycle5, then presumably the system Bicycle2 behaves as the system Bicycle1. For systems Bicycle1 and Bicycle2 is a similar deduction as before: both systems are the bicycles controlled by the handlebar and one has a slightly bigger weight because of having the reaction wheel attached. Thus, conclusions from computer **Simulations 1** and **2** can be also referred to the bicycle without the reaction wheel. They describes when the bicycle is stable or not, how important is the control system in single-track vehicle, when it is self-stable and how selected parameters can change it.

The dedicated bicycle computer simulator was prepared for this research. It is able to find the full state trajectory of the object by doing the Euler integration [39] of dynamic equations and visualise result in the graphical interface. The 3D model was designed in Autodesk Inventor 2016 computer software and next transported into Matlab Simscape Multibody. The second has an enormous capabilities to simulate multibody dynamics. However, in this work this was used only to create visualisation of the analysed object. The final result can be found in Figure 4.10.

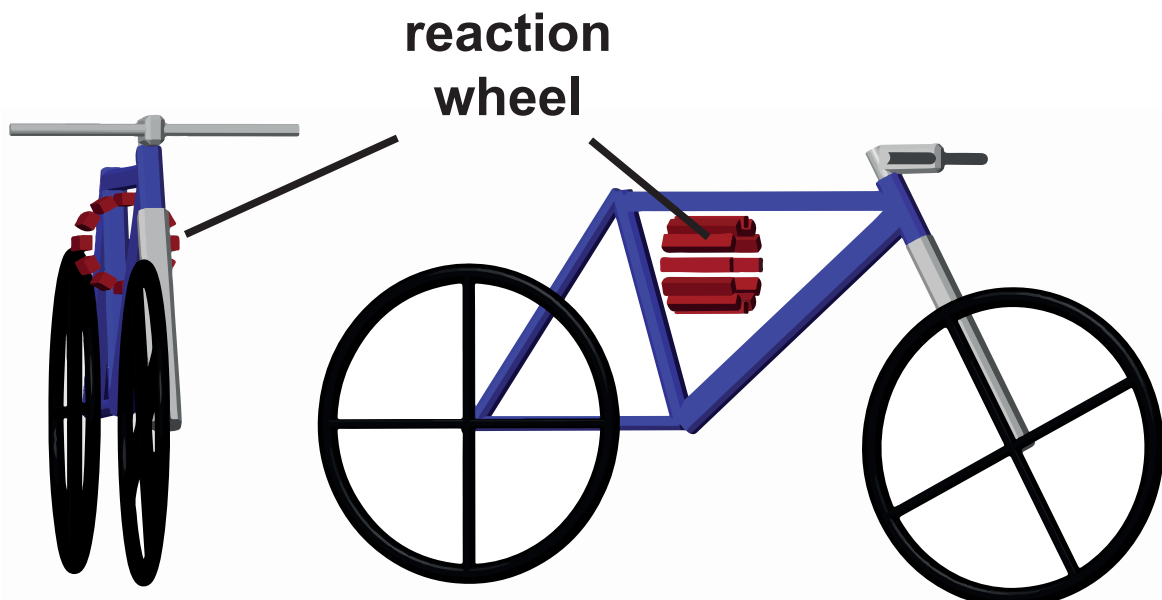


Figure 4.10: Computer simulator of the bicycle with the reaction wheel

The computer simulation uses the dynamic differential equations of the bicycle (4.17)-(4.18) and of the bicycle with the reaction wheel (4.34)-(4.35). Next they are integrated and plotted in graphs. Each simulation has been performed in the time domain. At first, the full attention is paid to the bicycle dynamics (**Simulations 1-3**). It is analysed how the bicycle behaves for different velocities when it is controlled or not. Afterwards the reaction wheel is examined. Additional performance indices are calculated and studied to evaluate precisely whether the reaction wheel improves control quality of the vehicle.

It is necessary to satisfy many conditions to stabilize the bicycle. In this case, the important parameter is the bicycle velocity v and the control strategy. Everyone who has ever tried to ride a bicycle knows it needs much experience. It is possible to stabilize a bicycle even if it is uncontrolled ($u_2 = 0$). This phenomenon is called self-stability and is proven here by the computer simulation.

Each computer simulation starts from the state $x_0 = [0.2618 \text{ rad}, 0 \text{ rad/s}, 0 \text{ rad}, 0 \text{ rad/s}, 0 \text{ rad}, 0 \text{ rad/s}]^T$. Then differential equations of motion are integrated by Euler method reaching several seconds long trajectory.

In first three **Simulations 1-3** the control system is turned off and there is no handlebar torque. Next in **Simulations 4-7** is the opposite – the system is closed by LQR feedback. Generally, there are examined three velocities of the uncontrolled bicycle: 1 m/s, 5 m/s and 10 m/s and four velocities of the controlled bicycle: 0.1 m/s, 1 m/s, 5 m/s and 10 m/s.

After short analysis it can be quickly noticed that in two cases the system is unstable: when the velocity is too low (1 m/s) and when the velocity is too high (10 m/s). This can be found in the **Simulation 1** and **3**. In both situations angle from the vertical x_1 dangerously rises finally reaching $\pi/2$ rad (full contact with the ground). However, when the velocity is high it happens a lot slower than when the velocity is low. Of course, this refers to exact parameters of the object. Additionally, it is worth to mention, that this confirms correctness of eigenvalues from Table 4.4 – small positive value of the real part of the one root of the system Bicycle5 (from Table 4.1).

Next, **Simulation 2** needs to be described. It shows the uncontrolled self-stable bicycle. It proved to be that when this vehicle travels with the velocity $v = 5 \text{ m/s}$ it is stable even if there is no torque acting on the handlebar. It confirms a great phenomenon which tells that every bicycle has certain range of velocity where it becomes self-stable [66, 72]. This is the state when the handlebar follows every lean of the bicycle which finally creates centrifugal force and then stabilizes the whole system.

Simulations 4-7 present stable systems. This time the bicycle is controlled by the LQR regulator which controls the handlebar torque. As can be noticed, the bicycle remains stable even if the velocity is low (1 m/s, **Simulation 4**) or is high (10 m/s, **Simulation 7**). As probably everyone knows that traveling by bicycle with relatively low velocity is difficult and sometimes impossible. This can be read from **Simulation 4**. It is the truth that this system is stable (the whole state goes to zero level) however the control torque is bigger (40 Nm) than in bicycle which travels with higher velocity.

It is worth to describe **Simulation 6**. It presents the bicycle which travels with the velocity from self-stable area like in **Simulation 2**. However, this time bicycle is controlled by

LQR regulator. The feedback control loop shortens the regulation time from approximately 9 to 6 s. Therefore, the regulation makes the system faster and more resistant to external forces acting on the bicycle.

Simulation 4 presents the bicycle which travels with very low velocity i.e. $v = 0.1 \text{ m/s}$. The object almost does not move forward. This chart proves, that keeping the stability in such conditions is extremely difficult. The control torque reaches almost 1000 Nm which is difficult to create by the real machine. The worst thing is that the angle of rotation of the handlebar is bigger than $\pi/2$ which is unacceptable – the bicycle falls down. In this case it is worth to use the additional control system, which can help in keeping stability of the considered system. In this dissertation the reaction wheel module is proposed. The stability analysis from Section 4.4 guarantees, that single-track vehicle with the reaction wheel is stable even if the velocity is zero or near to zero (Fig. 4.6). In the rest of this Section there are some additional proofs which supports this concept.

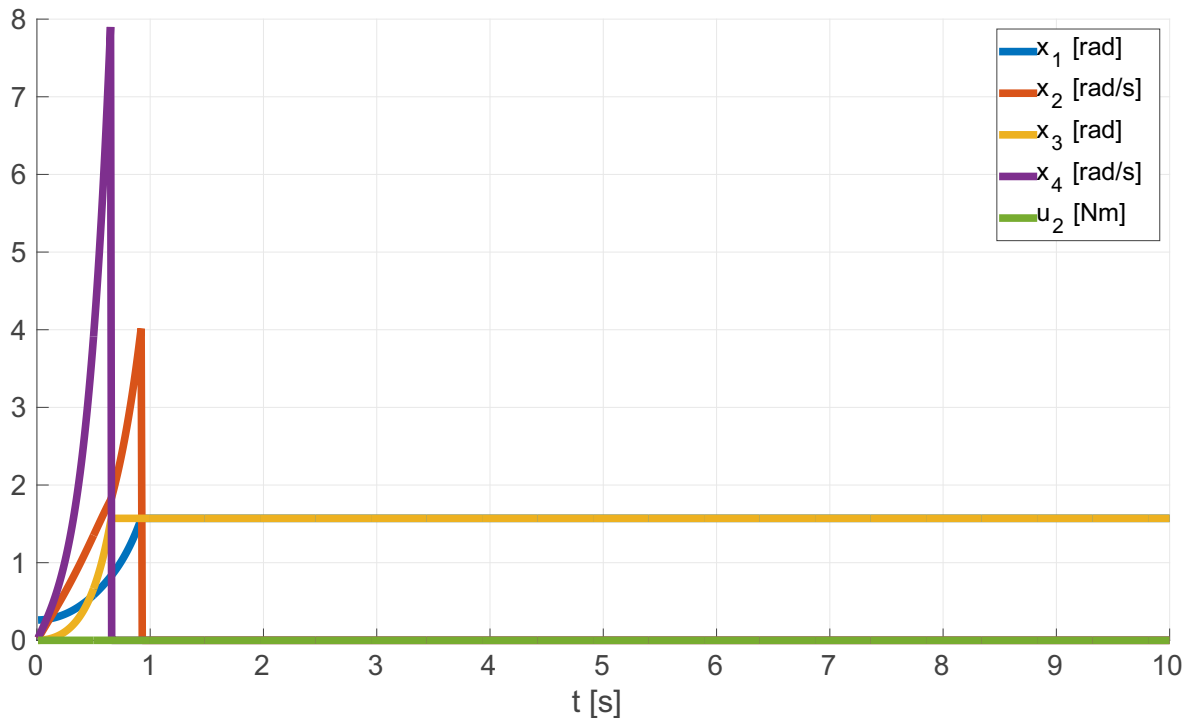
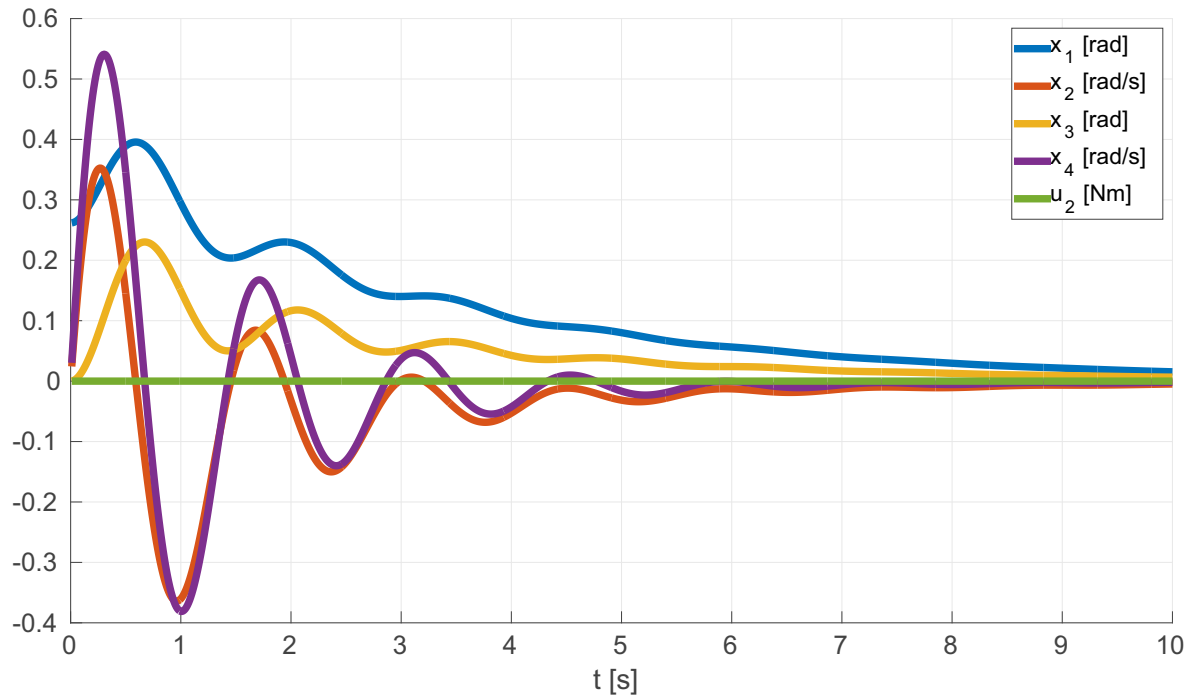
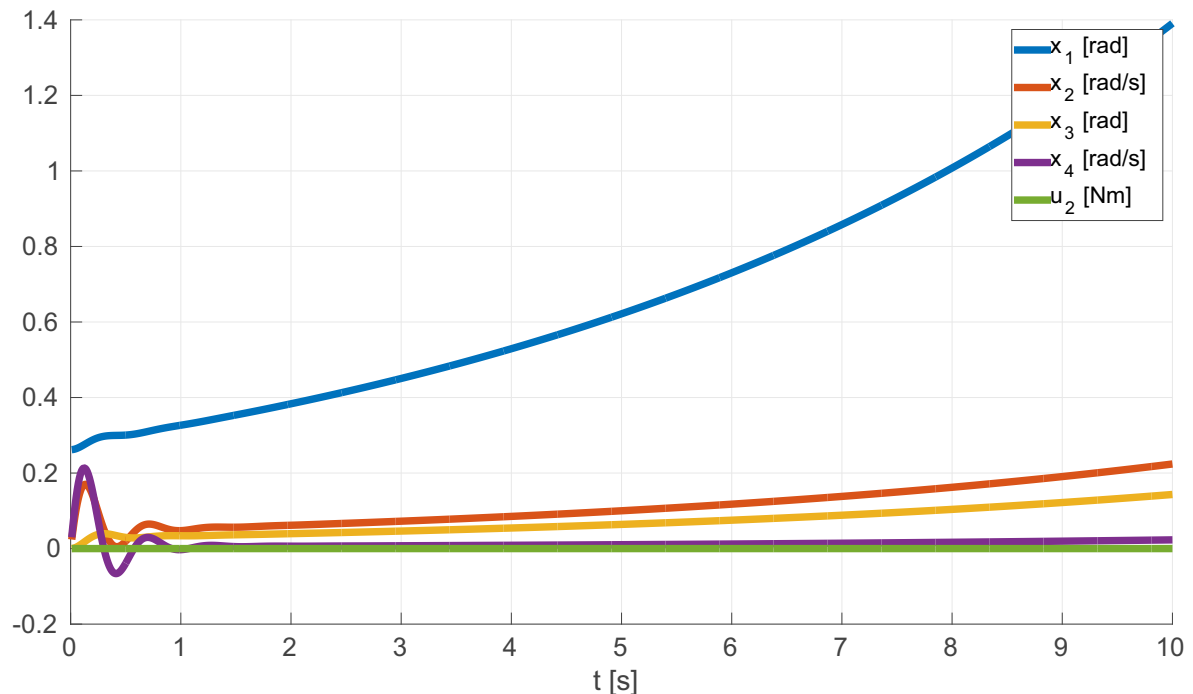
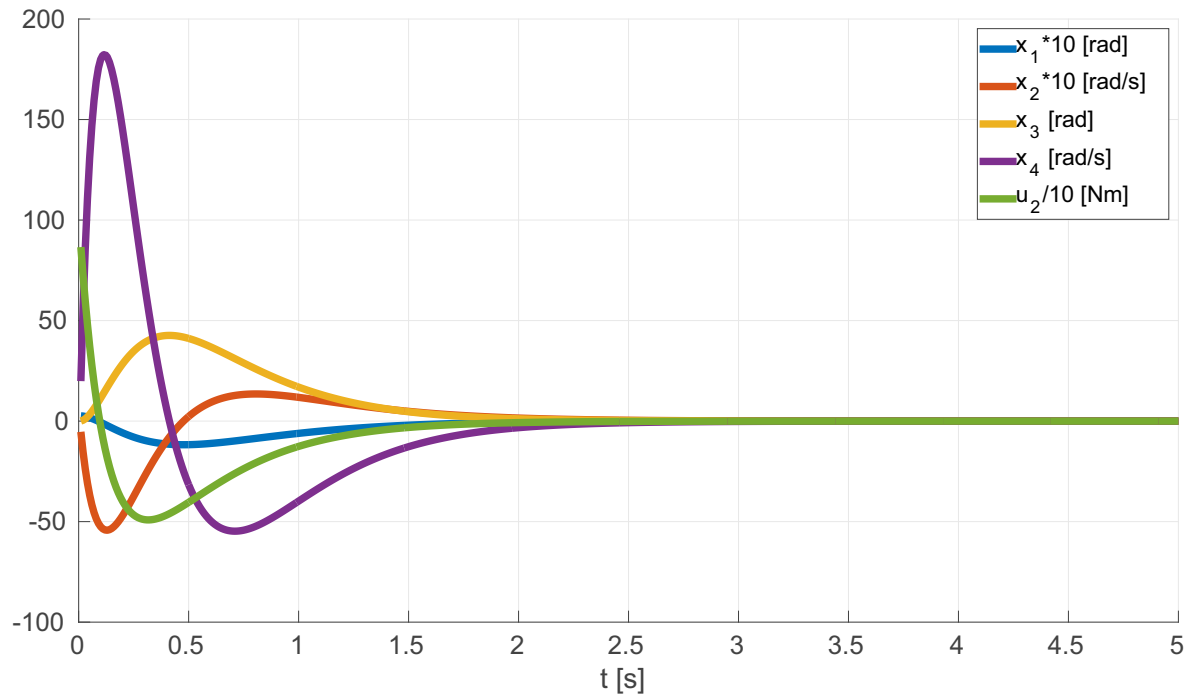
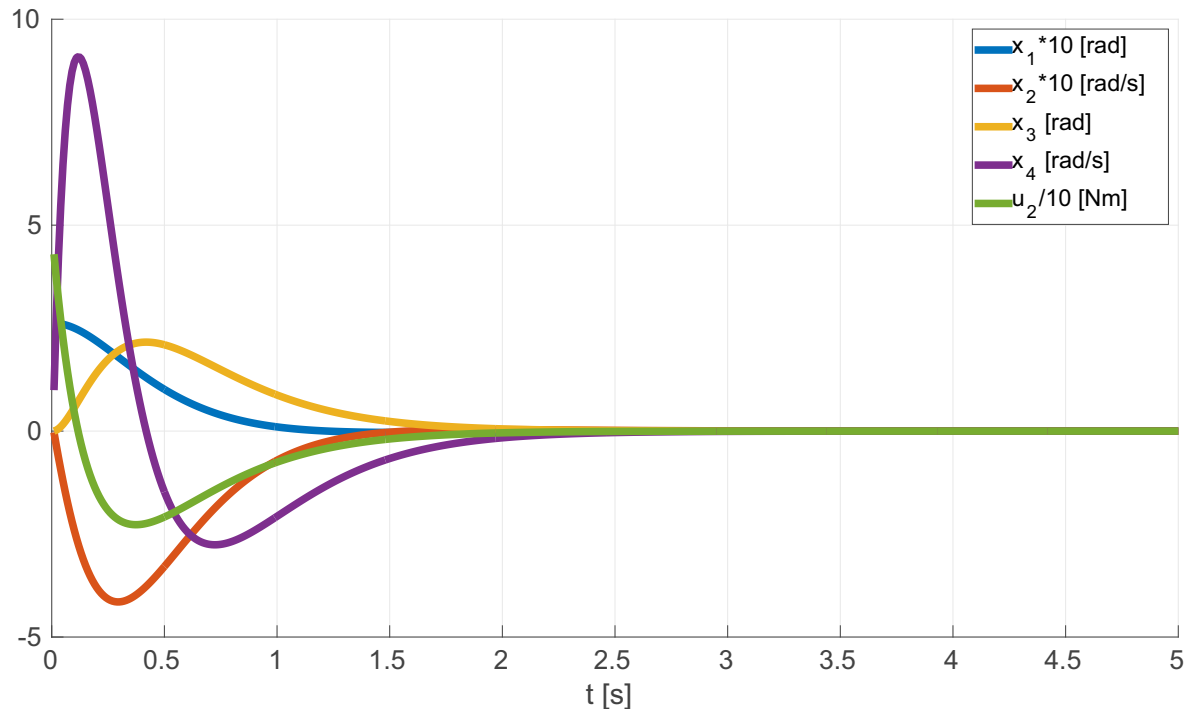
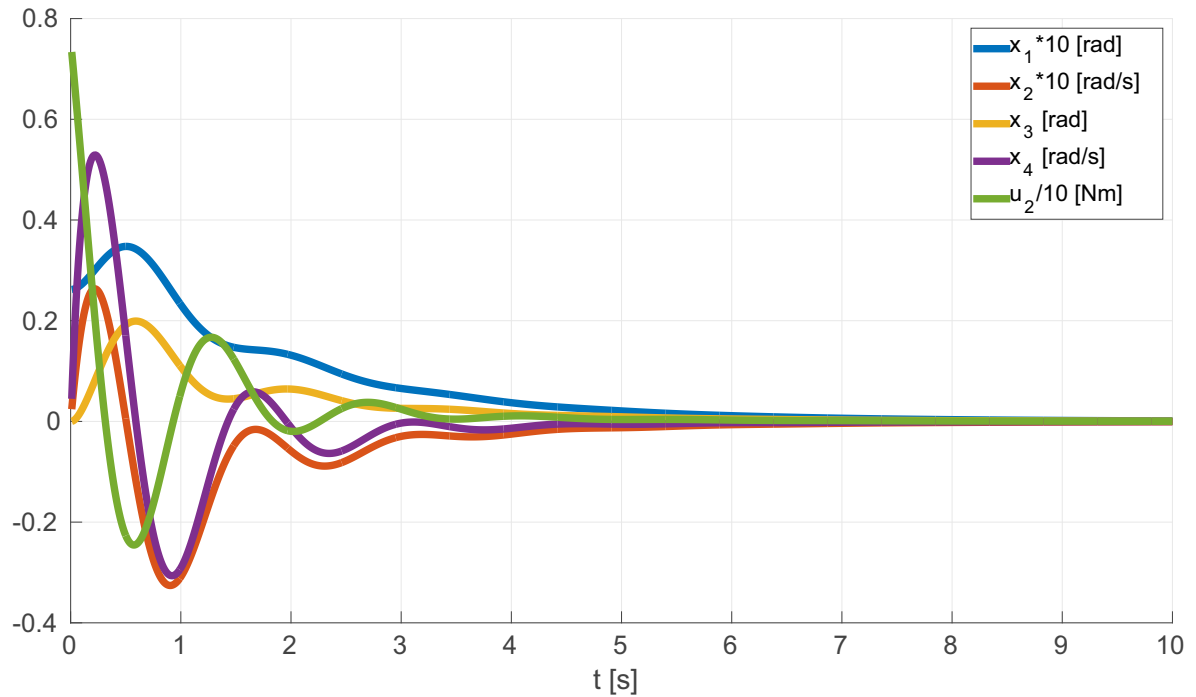
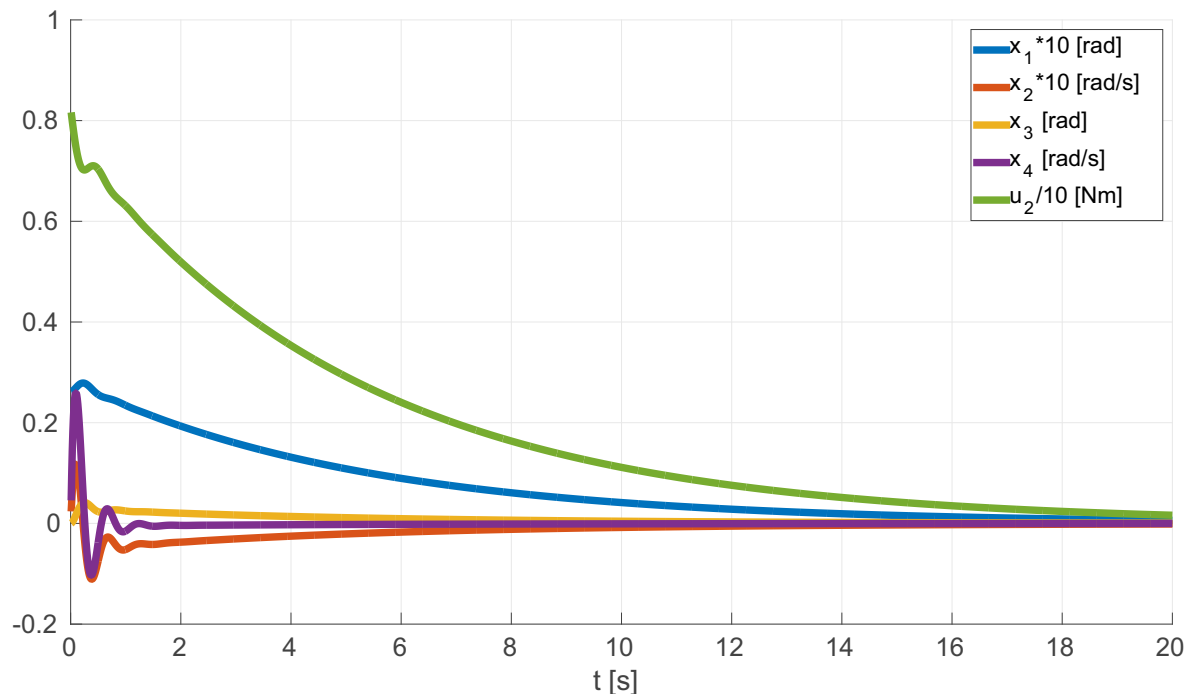


Figure 4.11: **Simulation 1** (specified in Table 4.1)

Figure 4.12: **Simulation 2** (specified in Table 4.1)Figure 4.13: **Simulation 3** (specified in Table 4.1)

Figure 4.14: **Simulation 4** (specified in Table 4.1)Figure 4.15: **Simulation 5** (specified in Table 4.1)

Figure 4.16: **Simulation 6** (specified in Table 4.1)Figure 4.17: **Simulation 7** (specified in Table 4.1)

Up to this point, the bicycle model has been described with the reaction wheel turned off. It is a good starting point to know basis of the physical nature of the bicycle dynamics (sometimes unexpected like self-stabilisation). It is necessary to compare the bicycle with the reaction wheel turned on and turned off.

Comparison can be done by graphical interpretation of charts or by calculating performance indices. The first generalized coordinate is the most important (angle of the bicycle from the vertical ϕ) and is described by first two state variables: x_1 and x_2 . Therefore, the performance indices are:

$$J_j = \sum_{n=0}^N x_j^2(n) \quad (j = 1, 2), \quad (4.52)$$

$$J = \sum_{j=1}^2 J_j, \quad (4.53)$$

where J_j is the performance index of x_j , J is the sum of all performance indices, n is the simulation step and N number of simulation steps. The lower value of the performance index is, the better regulation process becomes.

Another parameter to measure the performance of the control system is the energy it consumes. Generally, the full bicycle model with the reaction wheel (4.34)-(4.35) includes three control values. However, in this dissertation it is assumed that first control is zero, thus its energy is also zero

$$E_1 = 0. \quad (4.54)$$

Rest of energies are:

$$E_2 = \sum_{n=1}^N P_2(n) \Delta t, \quad (4.55)$$

$$E_3 = \sum_{n=1}^N P_3(n) \Delta t, \quad (4.56)$$

$$E_2 = \sum_{n=1}^N u_2(n) x_4(n) \Delta t, \quad (4.57)$$

$$E_3 = \sum_{n=1}^N u_3(n) x_6(n) \Delta t, \quad (4.58)$$

$$E = \sum_{j=1}^3 E_j, \quad (4.59)$$

where E_2 is the energy of the control u_2 (handlebar torque), E_3 is the energy of the control u_3 (reaction wheel torque), E is the sum of energies, P_2 and P_3 are powers of controls and Δt is the time increment.

Computer simulations of the bicycle with the reaction wheel turned on have been performed and results can be found in two Tables: 4.7 and 4.8 and five **Symulations: 8-12**.

Table 4.7: Performance indices for three different systems in accordance with Table 4.1

System	J_1	J_2	J
Bicycle2, $v = 0.1 \text{ m/s}$	8555	69386	77942
Bicycle2, $v = 1 \text{ m/s}$	214	781	995
Bicycle2, $v = 5 \text{ m/s}$	1331	743	2074
Bicycle2, $v = 10 \text{ m/s}$	2090	100	2190
Bicycle3, $v = \text{var m/s}$	151	1132	1283
Bicycle4, $v = 0.1 \text{ m/s}$	561	6201	6762
Bicycle4, $v = 1 \text{ m/s}$	214	784	998
Bicycle4, $v = 5 \text{ m/s}$	1331	743	2074
Bicycle4, $v = 10 \text{ m/s}$	2090	100	2190

Table 4.8: Energy of control signals for three different systems in accordance with Table 4.1

System	$E_2 [J]$	$E_3 [J]$	$E [J]$
Bicycle2, $v = 0.1 \text{ m/s}$	21439.00	—	—
Bicycle2, $v = 1 \text{ m/s}$	52.03	—	—
Bicycle2, $v = 5 \text{ m/s}$	0.07	—	—
Bicycle2, $v = 10 \text{ m/s}$	0.06	—	—
Bicycle3, $v = \text{var m/s}$	—	2701.00	—
Bicycle4, $v = 0.1 \text{ m/s}$	1223.10	2299.80	3522.90
Bicycle4, $v = 1 \text{ m/s}$	51.20	0.25	51.45
Bicycle4, $v = 5 \text{ m/s}$	0.07	0.00	0.07
Bicycle4, $v = 10 \text{ m/s}$	0.06	0.00	0.06

It gives a strong evidence that using the reaction wheel improves stability of the bicycle. It also confirms the stability analysis from Section 4.4. The considered modification of the single-track vehicle presented in this dissertation shortens the regulation time, decreases the performance indices and brings benefits in energy consumption (in some physical conditions).

At first, it is good to compare computer simulations of the Bicycle2 (**Simulations 4-7**) and the Bicycle3 (**Simulation 8**). The graphic interpretation of these charts says that usually Bicycle2 needs lower control torque than Bicycle3. Both are controlled by the optimal LQR controller with the same weights. However, there is one exception: when the velocity is close to zero ($v = 0.1 \text{ m/s}$), therefore the bicycle virtually does not move, the control torque is significantly bigger in Bicycle2 (more than 800 Nm) than in Bicycle3 (500 Nm). Bicycle3 is almost independent of the velocity, thus for all velocities from zero to $v = 10 \text{ m/s}$ it needs the same control trajectory. It proves that reaction wheel allows to keep the balance for the bicycle even if the velocity is around zero. It means that reaction wheel improves stability of the bicycle.

Now, it is worth to analyse computer simulations of the Bicycle4 (**Simulations 9-12**) and compare them with simulations of the Bicycle2 (**Simulations 4-7**). It turned out that using handlebar torque with the reaction wheel torque simultaneously does not bring any significant improvement for velocities equal or greater than $v = 1 \text{ m/s}$. Regulation times are almost the same and the maximum handlebar torques are also similar. Obviously, it is caused by the optimal LQR controller which gives similar control trajectories for Bicycle2 and Bicycle4. Using the reaction wheel for velocities bigger than $v = 1 \text{ m/s}$ must be unprofitable and must increase the quadratic cost function (3.35). Different situation happens when the bicycle travels with near-zero velocity. Then it is optimal to use the reaction wheel torque to stabilize the bicycle. For the considered velocity $v = 0.1 \text{ m/s}$ the initial handlebar torque is around 200 Nm and reaction wheel torque is 400 Nm. In other words, when the velocity is low the reaction wheel becomes significant.

When the bicycle is self-stable ($v = 5 \text{ m/s}$) and is uncontrolled (Bicycle6, **Simulation 2**) it needs 10 s to be stabilized. Controlling it by handlebar torque (mainly) and reaction wheel torque shortens this time to around 5 s. This is presented by Bicycle2 and Bicycle4 in **Simulations 6 and 11**.

The graphic interpretation of graphs gives rise to meaningful conclusions. However, to have a precise evaluation, it is necessary to use numeric approach. There are two Tables: 4.7 and 4.8 with performance indices and energies of control signals. First of all, Bicycle2 produces much bigger performance indices than Bicycle3 for velocities $v = 0.1 \text{ m/s}$ and $v = 10 \text{ m/s}$. When the bicycle travels at very low velocity it is much better to control it by the reaction wheel instead of the handlebar. When the bicycle travels with huge velocity ($v = 10 \text{ m/s}$) and is stabilized by handlebar torque, it needs very long time (almost 20 s) to reach the vertical position. The handlebar control is the best solution for this velocity, however on the other hand it strongly increases performance indices. Bicycle3 is stabilized with the same short time and it is independent of the velocity. Only for the velocity $v = 1 \text{ m/s}$ Bicycle2 has smaller total sum of performance indices J probably because it is stabilized

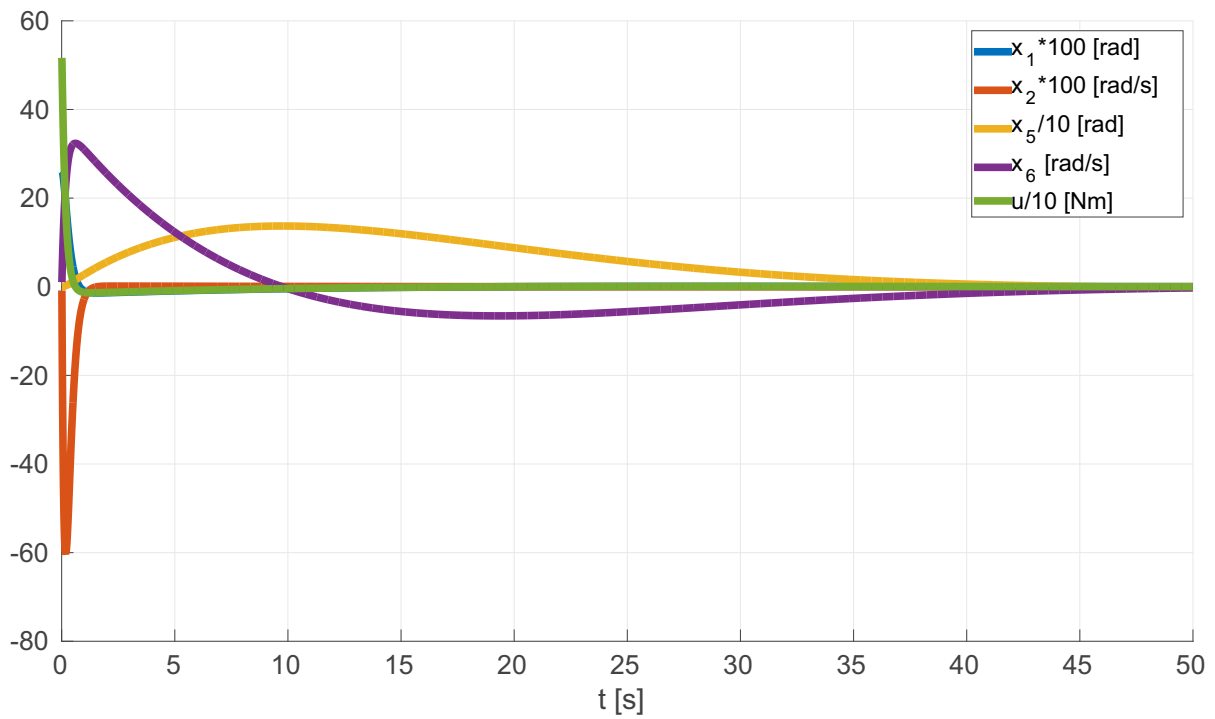
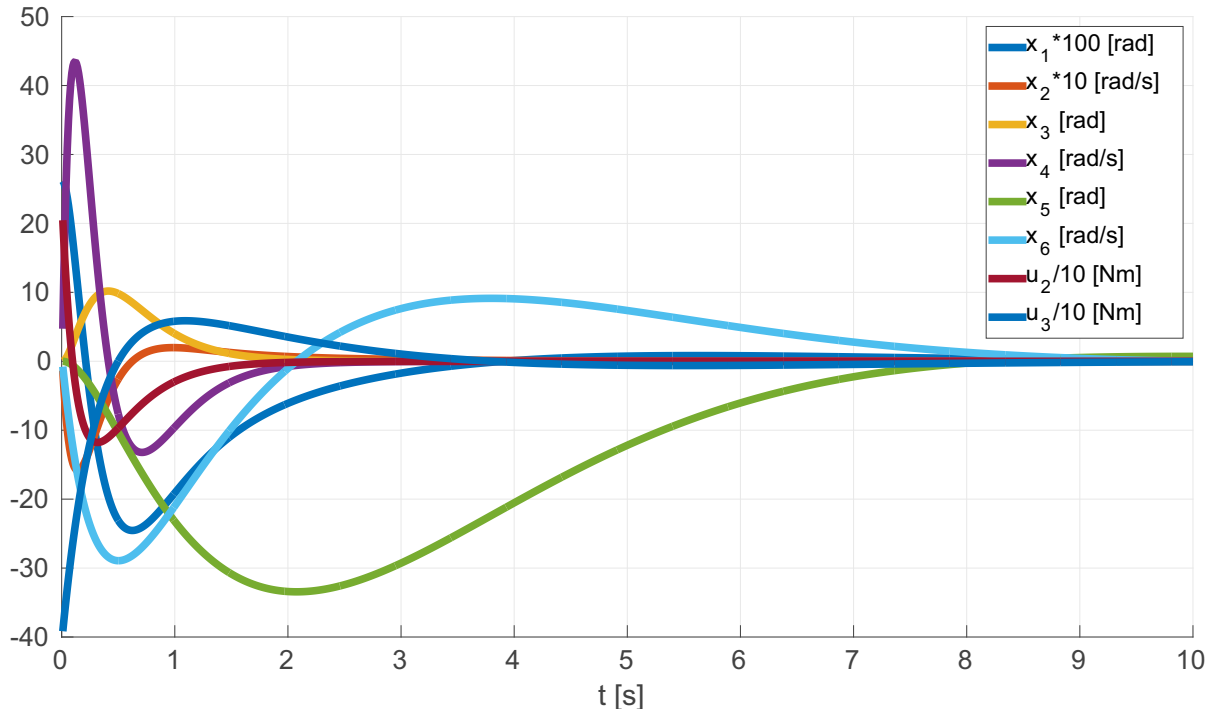
more smoothly (smaller maximum x_2 value) than Bicycle4. Generally, there is a rule that if velocity increases the bicycle controlled by the handlebar needs more time to be stabilized with the proposed control law.

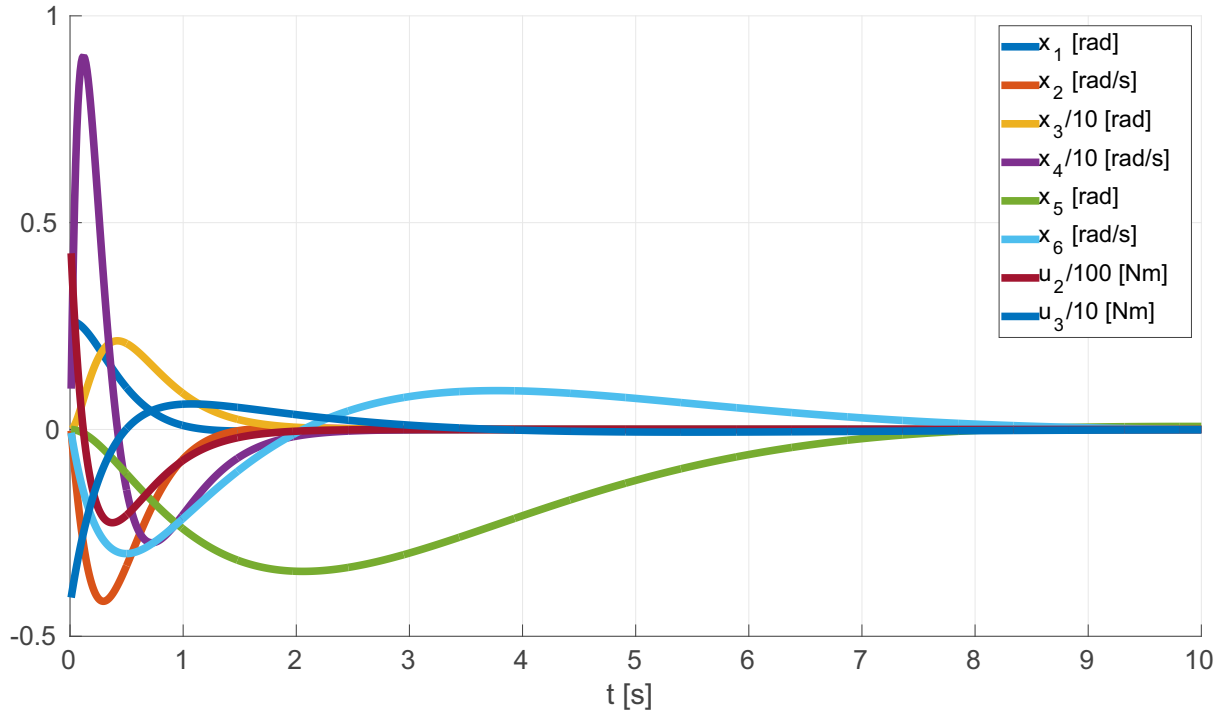
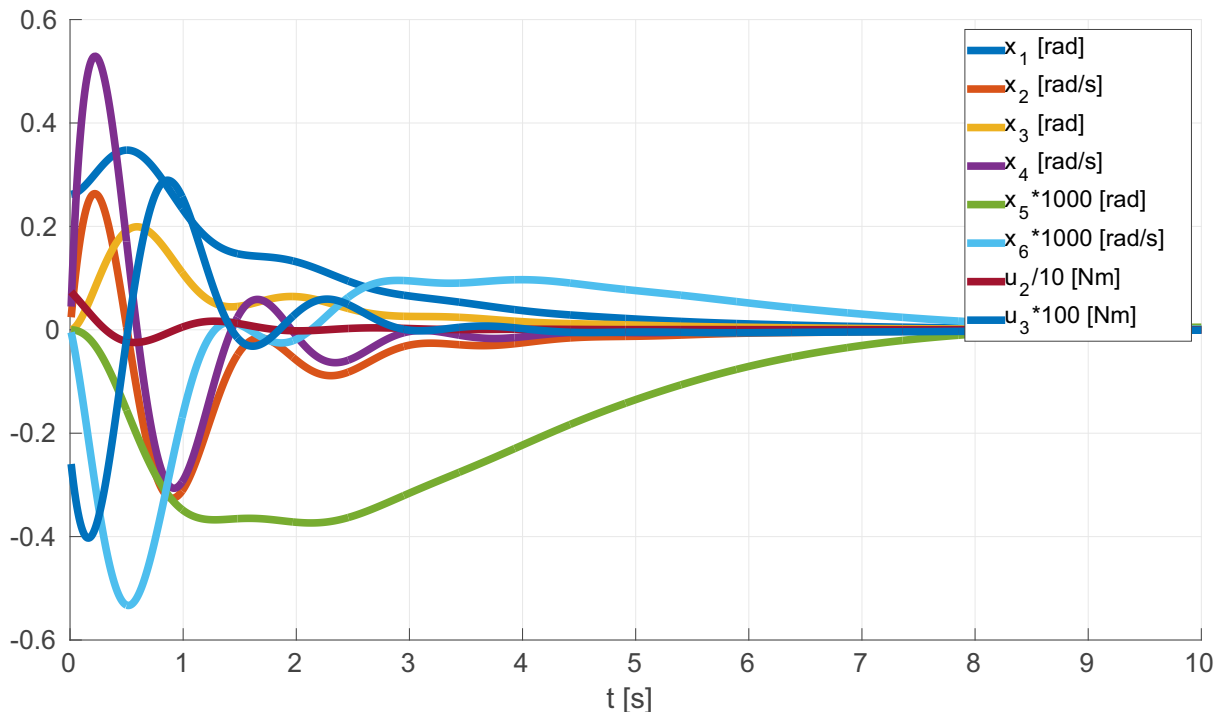
Bicycle2 and Bicycle4 have almost the same performance indices for velocities equal or greater than $v = 1 \text{ m/s}$. As it was mentioned before, solving the optimal LQR controller returns control law, which uses mainly the handlebar torque without the reaction wheel torque. It guarantees the smallest quadratic cost function (3.35). When the velocity is nearby zero, the performance indices are significantly lower for Bicycle4 than for Bicycle2. This gives yet another argument that reaction wheel improves stability for the bicycle.

Table 4.8 presents energies produced by control torques. Power can be calculated using torque and angular velocity. When power is integrated numerically it returns the energy. This result is taken into account here. Bicycle2 consumes more energy than Bicycle3 only for small velocity ($v = 0.1 \text{ m/s}$). When the velocity of Bicycle2 increases, the energy efficiency rises – it needs less energy to be stabilized by proposed control law.

Another benefit of the reaction wheel can be seen in Bicycle4. It also needs less energy to bring the vehicle to the vertical position while traveling slowly. It is specially noticeable for velocity around zero, however when $v = 1 \text{ m/s}$ the reaction wheel slightly decreases energy consumption from 52.03 J to 51.20 J. When the bicycle travels fast it is optimal to use more handlebar torque instead reaction wheel.

This Section has presented series of the computer simulations and its interpretation. It is focused on the bicycle vehicle stabilized by the handlebar and the reaction wheel. At the beginning, the uncontrolled bicycle is analysed. There is an evidence that for some velocity bicycle becomes self-stable. However, when it travels too slow or too fast it becomes unstable. Generally, the classical handlebar torque works perfectly for velocities bigger than ($v = 1 \text{ m/s}$). When the bicycle travels slower then reaction wheel becomes more effective. It is possible to use both systems simultaneously and calculate the LQR control law for current velocity. It guarantees perfect synergy of these two systems. The graphical and numerical analysis of series of computer simulations proves that the reaction wheel improves stability of the bicycle.

Figure 4.18: **Simulation 8** (specified in Table 4.1)Figure 4.19: **Simulation 9** (specified in Table 4.1)

Figure 4.20: **Simulation 10** (specified in Table 4.1)Figure 4.21: **Simulation 11** (specified in Table 4.1)

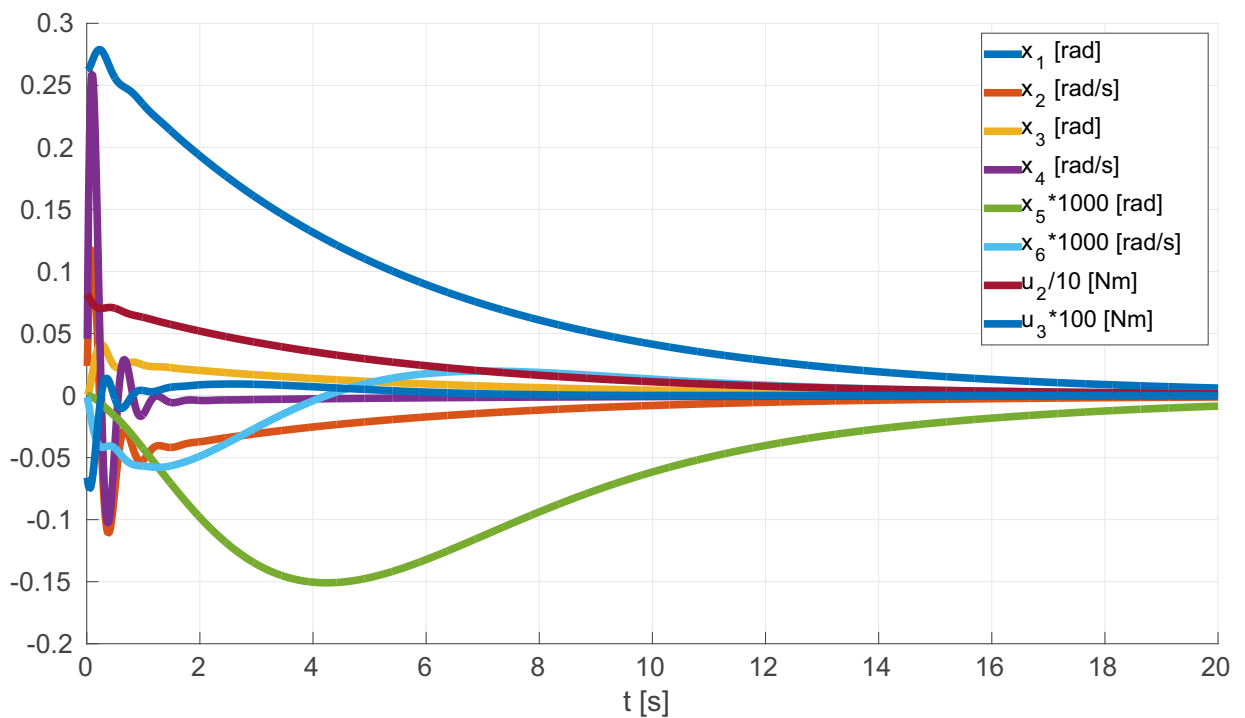


Figure 4.22: **Simulation 12** (specified in Table 4.1)

Chapter 5

Conclusions

5.1 Summary

The results presented in this dissertation prove that the reaction wheel helps in keeping stability of the bicycle. Detailed research confirms that this system is promising and is definitely worth to use in single-track vehicles. Currently, connecting the bicycle with the additional motor which accelerates rotating mass gives entirely new object difficult to find in the scientific literature. In this work, there are several control techniques which stabilizes this plant presented. It is considered when stabilizing is the most or the least difficult or when the bicycle is self-stable. It gives the concept how to increase the use of the bicycles.

The dissertation starts with current state-of-the-art analysis. In this work, the novelty is the control object, namely connection of the bicycle with the reaction wheel. Next, the optimal control law is designed to stabilize the system minimizing the cost function with specified weight matrices. Several references are mentioned in which the reaction wheel principle is described. It is indicated where this actuation method is commonly use these days. Next, literature concerning the bicycle dynamics was analysed. It has turned out that mathematical modeling of the bicycle is highly complex problem and still not solved. Detailed nonlinear mathematical model of the bicycle (or the motorcycle) is not yet created – currently there is no model which is able to reflect the most important states of the real vehicle especially those which threaten human life. A good understanding of available mathematical models of the bicycle allowed to choose a candidate which can sufficiently mimic the dynamics of the bicycle and shows these states where keeping stability is problematic. This can significantly contribute to the development of the bicycle. It was decided to extend mathematical model of the bicycle which was published in 2007 in [72], called the canonical bicycle by authors of that publication.

It is very important to deeply understand the reaction wheel. To reach this aim, the reaction wheel pendulum is precisely analysed with a detailed mathematical model of this object given. The study allowed to draw very important conclusions in the context of dissertation. Accurate description of the energy transformation over time from one form to another brought a great hope for a good support to the use the reaction wheel as an universal unit which can stabilize inverted pendulum-like structure. In this case, maintaining a balance in the unstable equilibrium point costs zero energy (if there is no external disturbance acting on the object). This is a huge advantage of this system as an actuator.

The inverted wheel pendulum is the underactuated system with many control limits. Therefore, it is a huge challenge for the automatic control system design. A large and important part of the thesis is an analytical solution of several variants of the control law. For this

purpose the linear-quadratic control is chosen. Moreover, the LQR controller is modified to another forms as: tracking system and feedback system with additional integration block. Next there are a series of tests of the proposed stabilizing algorithms included. After that there is a profound stability analysis of the closed-loop system (with the controller). There is the impact of the parameters change checked (as: radius of mass of the rotating disc, mounting height) on the stability. This allows to optimise the right proportions of physical structure of the object. At this stage the results are very promising what reveals a great need of testing it on the real object. A good practice is to examine the trajectory of state in the computer simulation. Actually this also gives undoubted result that reaction wheel perfectly stabilizes two degree of freedom inverted pendulum. The experiment on the real machine confirms that proposed control law is the right solution for this case. Working with electronic devices requires overcoming several problems, however, for this machine it gave rise to drawing new conclusions and discovering some facts. An innovative way of state estimation using the gyro sensor with little involvement of the accelerometer is proposed. There is the unique method of autonomic determining of the equilibrium point of the inverted pendulum like object using the synergy of the gyro sensor and linear-quadratic control.

The bicycle model is thoroughly analysed. The research shows that keeping balance using only the handlebar torque sometimes is difficult if even not impossible. It is noticed that this kind of control is unreliable for small velocity. When the velocity is less than $v = 1 \text{ m/s}$ then problems arise. Theoretically, the optimal control law LQR still guarantees the stability, however the control signal reaches very high levels which might be difficult achieve in the real application. This also applies to state variables which exceed the limits. It is noted that the energy consumed by the system in this situation is relatively large. All the conclusions inspire to find some ways to improve the typical bicycle. It turns out that sometimes the bicycle is easy to fall down and dangerous to use. This was the main inspiration to do research presented in this dissertation in general. This type of extension of the functionality of the bicycle can bring many benefits and many new features such as allowing cycling to people with mobility problems or creating the fully autonomous and robotic bicycle controlled by the humanoid. These findings fully justify the great need to link these two issues, namely, the bicycle and the reaction wheel.

Initially, the bicycle with the reaction wheel is presented by dynamic differential equations. The modified canonical bicycle model is combined with the reaction wheel pendulum creating the new object difficult to find in current literature. Thanks to the latter, it was possible to perform a wide range of tests and analysis and to create the concept of the appropriate control law. The dissertation presents the LQR control law. For the whole closed-loop system, a several elements are important in this case: eigenvalues graphs, step responses and series of computer simulations. All of them give a set of arguments which confirm the main thesis of this dissertation. It proves that the bicycle which travels with low velocity (below 1 m/s) can be stabilized more effectively by the reaction wheel instead of the classical handlebar torque: the regulation time and energy needed for control process become better. In these conditions stabilization by reaction wheel costs less energy and total cost function returns lower values. All real parts of eigenvalues of the system are significantly below zero.

Results show that classical approach to stabilisation of the bicycle based on the handlebar torque has indisputable advantages. With the increase in the velocity of the bicycle effectiveness of this control is rapidly growing. For relatively high velocities, stabilization of the bicycle requires very little energy. For this case, it is difficult to imagine a system that could replace or even support such stabilization. Perhaps this is the main reason why bicycles generally not changed their form since many years except minor adjustments in the shape and the materials used to build the structure. Perhaps this is the reason why it is so difficult to change anything in this perfect invention. This dissertation tries to break this pattern to show well-known single-track vehicle from completely new site.

5.2 Conclusions and contribution

The aim of this work is to solve the main problem stated in the subject and in the main thesis and support it by series of arguments. Generally, it is focused on mathematical modeling of the bicycle and on the description of the dynamic motion of the reaction wheel. Author hopes that many ideas and thoughts are universal and could be useful for all those who are interested in this scientific area. The most significant conclusions included in the dissertation are:

1. The LQR control algorithm is able to stabilize the reaction wheel pendulum with two degrees of freedom (Fig. 3.10-3.23).
2. It is possible to stabilize the inverted pendulum with the reaction wheel using only one gyroscopic sensor. When the reaction wheel system is stabilized by the LQR controller using only gyroscope it allows to estimate the actual position of equilibrium point and current deflection angle from the vertical of the system (Fig. 3.15-3.16).
3. When the LQI regulator is used to stabilize the inverted pendulum with the reaction wheel it is possible to track the changing in time actual equilibrium point of the system. The model of the object can change in time and the algorithm constantly corrects the energetically optimal position of the system (Fig. 3.17-3.18).
4. It is possible to design the linear-quadratic control law for the reaction wheel pendulum. It allows to move the object in the state space without loosing the stability. The control process is still optimal for changing in time reference signal (Fig. 3.13).
5. The inverted pendulum stabilized by the reaction wheel is energetically effective. The system does not need any additional energy to do stabilisation task when is located in unstable equilibrium point (upright position) without any external disturbances (Fig. 3.20).
6. The stability analysis based on eigenvalues plots and step responses allows to optimise physical parameters of the object. It is a great approach to correct the stability of the inverted pendulum system stabilized by the reaction wheel (Fig. 3.6-3.7).

7. When the velocity of the bicycle rises, the stabilisation based on the handlebar torque becomes more effective. In this context, effective means difficult to be replaced by other stabilisation methods (Fig. 4.15-4.17).
8. When the velocity of the bicycle tends to zero, it becomes more difficult to stabilize the system using the handlebar torque. The energy needed to do the control process dangerously rises to the level which is difficult to reach in the real application. Moreover, the angle of the handlebar is out of range (for typical bicycle construction) (Tab. 4.8, Fig. 4.14).
9. When the bicycle travels with low velocity, the reaction wheel torque is more useful than handlebar torque to stabilize the bicycle. It costs less energy and takes less time. Stabilising the bicycle by the handlebar means taking advantage of the centrifugal force which appears only when the velocity is greater than zero (Tab. 4.8, Fig. 4.19).
10. The mathematical model of the bicycle with the reaction wheel proposed in this work allows to make analysis of the stability using eigenvalues plots and step responses. Additionally, it is a great tool to conduct the computer simulations using Euler integration method to find the changing in time trajectory of the state to predict the motion of the object (Subsection 4.2.2, Sections: 4.4, 4.5).
11. The LQR controller is able to stabilize the bicycle with the reaction wheel using two systems at the same time: the handlebar and the reaction wheel. The minimisation of the cost function guarantees a perfect synergy of these systems using them with correct intensity depending on the velocity of the bicycle (Tab. 4.8, Fig. 4.18-4.22).

In this dissertation it is possible to find several innovative concepts of using the reaction wheel to stabilize the bicycle. In the current literature, it is difficult to find a detailed description of this issue. On the one hand, this research uses available knowledge about mathematical modeling of the single-track vehicles but on the other hand the bicycle is expanded by additional degree of freedom and finally described by new complete dynamic differential equations of motion. Below a collection of the most important aspects which represent the contribution of the dissertation is presented:

- I Derivation of the detailed mathematical model of the reaction wheel pendulum.
- II Complete research about the inverted pendulum stabilized by the reaction wheel which includes: stability analysis, computer simulation and experimental tests.
- III Creating the algorithm of localization of the unstable equilibrium point of the reaction wheel pendulum using gyro sensor with its imperfections (the gyro drift).
- IV Preparing of the mathematical model of the bicycle with the reaction wheel. For this purpose the canonical bicycle model has been used, based on the aforementioned literature, and, modified into the state space form and finally extended it with the additional degree of freedom which is the rotating mass system based on original mathematical model (made by the author).

V For the bicycle with the reaction wheel, conducting stability analysis using eigenvalue plots and step responses for series of different physical parameters and performing computer simulations of motion.

Taking into account all conclusions presented above, it can be stated that the main thesis of the dissertation has been proven. The reaction wheel in combination with a selected control algorithms is able to improve the stability of the bicycle.

5.3 Future work

This work presents many advantages of using the reaction wheel. There are many possible ways of development of this issue.

Most of all it would be valuable to create the real model of the bicycle with the reaction wheel and try if presented control algorithms correctly correspond to the simulation results. The machine should include multiple sensors and microcontrollers. Probably it should have three main electric motors to accelerate: the bicycle, the handlebar and the rotating mass. It would be the best if motors could be strong enough to lift a human body. However, if it were too difficult to create such a powerful machine probably, it would be better to start with an unmanned autonomic bicycle robot, what should allow to verify many theoretical considerations.

Another way might be extending the mathematical model of the dynamics of the bicycle into a non-linear form to reflect the reality to the greater extent. Current global trends about simulations of two-wheeled vehicles are mainly based on the differential equations which take into account factors as: elasticity of tires, the movement of the front and rear suspension and losing contact with the ground. Using such a sophisticated description certainly would increase the chance to use the system in real applications that people use for everyday transport.

Naturally, there is always something to improve in control algorithm. In this study, the LQR algorithm is used, which is well-suited for non-linear objects in close surroundings of linearization points. The bicycle has the dynamic nature what means that it moves in vast area of the state space, therefore there is a huge chance, to appear occasionally at a very distant point, which is far from operating region. Methods such as backstepping or sliding mode control are designed for non-linear systems and perhaps could give better results in this case.

After verifying simulations by experiments on the real object probably new questions would appear about extended use of the reaction wheel in the bicycle. Possibly supporting slow-moving standing in place bicycle could be a secondary goal of this system. There is a chance that increasing the level of safety of a human driver would be more important than anything else. The reaction wheel could be activated immediately after the detection of dangerous situation that threatens human life. Some combination of: velocity, angle from the vertical of the machine, angle of the handlebar, relation of center of mass of the bicycle and driver, could help find emergency situations. It would be a challenge to develop proper algorithms for control and right assessment of the situation.

Probably in the future technology will be aimed mostly at helping elderly and handicapped people. Presented in this work solution could be a kind of assistant to help cycling. If it were properly configured and designed as a commercial solution, it could give a new chance to ride a bicycle by people with significant mobility difficulties.

There is a chance that in the near future the autonomous robotic single-track vehicles supported by the reaction wheel will appear. Such bicycles would be completely different from these we see nowadays. They could be far more dynamic and difficult to resist by any human body. It might, however, cost a lot of effort to rescale physical parameters of the bicycle to this purpose.

Appendix A

Physical parameters of the bicycle

$$m_T = m_R + m_B + m_H + m_F, \quad (\text{A.1})$$

$$x_T = \frac{x_B m_B + x_H m_H + w m_F}{m_T}, \quad (\text{A.2})$$

$$z_T = \frac{-r_R m_R + z_B m_B + z_H m_H - r_F m_F}{m_T}, \quad (\text{A.3})$$

$$I_{Txx} = I_{Rxx} + I_{Bxx} + I_{Hxx} + I_{Fxx} + m_R r_R^2 + m_B z_B^2 + m_H z_H^2 + m_F r_F^2, \quad (\text{A.4})$$

$$I_{Txz} = I_{Bxz} + I_{Hxz} - m_B x_B z_B - m_H x_H z_H + m_F w r_F, \quad (\text{A.5})$$

$$I_{Rzz} = I_{Rxx}, \quad (\text{A.6})$$

$$I_{Fzz} = I_{Fxx}, \quad (\text{A.7})$$

$$I_{Tzz} = I_{Rzz} + I_{Bzz} + I_{Hzz} + I_{Fzz} + m_B x_B^2 + m_H x_H^2 + m_F w^2, \quad (\text{A.8})$$

$$m_A = m_H + m_F, \quad (\text{A.9})$$

$$x_A = \frac{x_H m_H + w m_F}{m_A}, \quad (\text{A.10})$$

$$z_A = \frac{z_H m_H - r_F m_F}{m_A}, \quad (\text{A.11})$$

$$I_{Axx} = I_{Hxx} + I_{Fxx} + m_H(z_H - z_A)^2 + m_F(r_F + z_A)^2, \quad (\text{A.12})$$

$$I_{Axz} = I_{Hxz} - m_H(x_H - x_A)(z_H - z_A) + m_F(w - x_A)(r_F + z_A), \quad (\text{A.13})$$

$$I_{Azz} = I_{Hzz} + I_{Fzz} + m_H(x_H - x_A)^2 + m_F(w - x_A)^2, \quad (\text{A.14})$$

$$u_A = (x_A - w - c)\cos(\lambda) - z_A\sin(\lambda), \quad (\text{A.15})$$

$$I_{A\lambda\lambda} = m_A u_A^2 + I_{Axx}(\sin(\lambda))^2 + 2I_{Axz}\sin(\lambda)\cos(\lambda) + I_{Azz}(\cos(\lambda))^2, \quad (\text{A.16})$$

$$I_{A\lambda x} = -m_A u_A z_A + I_{Axx}\sin(\lambda) + I_{Axz}\cos(\lambda), \quad (\text{A.17})$$

$$I_{A\lambda z} = m_A u_A x_A + I_{Axz}\sin(\lambda) + I_{Azz}\cos(\lambda), \quad (\text{A.18})$$

$$\mu = \frac{c}{w\cos(\lambda)}, \quad (\text{A.19})$$

$$S_R = \frac{I_{Ryy}}{r_R}, \quad (\text{A.20})$$

$$S_F = \frac{I_{Fyy}}{r_F}, \quad (\text{A.21})$$

$$S_T = S_R + S_F, \quad (\text{A.22})$$

$$S_A = m_A u_A + \mu m_T x_T, \quad (\text{A.23})$$

$$M_{\phi\phi} = I_{Txx}, \quad (\text{A.24})$$

$$M_{\phi\delta} = I_{A\lambda x} + \mu I_{Txz}, \quad (\text{A.25})$$

$$M_{\delta\phi} = M_{\phi\delta}, \quad (\text{A.26})$$

$$M_{\delta\delta} = I_{A\lambda\lambda} + 2\mu I_{A\lambda z} + \mu^2 I_{Tzz}, \quad (\text{A.27})$$

$$K_{0\phi\phi} = m_T z_T, \quad (\text{A.28})$$

$$K_{0\phi\delta} = -S_A, \quad (\text{A.29})$$

$$K_{0\delta\phi} = K_{0\phi\delta}, \quad (\text{A.30})$$

$$K_{0\delta\delta} = -S_A \sin(\lambda), \quad (\text{A.31})$$

$$K_{2\phi\phi} = 0, \quad (\text{A.32})$$

$$K_{2\phi\delta} = \frac{(S_T - m_T z_T)}{w \cos(\lambda)}, \quad (\text{A.33})$$

$$K_{2\delta\phi} = 0, \quad (\text{A.34})$$

$$K_{2\delta\delta} = \frac{S_A + S_F \sin(\lambda)}{w \cos(\lambda)}, \quad (\text{A.35})$$

$$C_{\phi\phi} = 0, \quad (\text{A.36})$$

$$C_{\phi\delta} = \mu S_T + S_F \cos(\lambda) + \frac{I_{Txz}}{w \cos(\lambda)} - \mu m_T z_T, \quad (\text{A.37})$$

$$C_{\delta\phi} = -(\mu S_T + S_F \cos(\lambda)), \quad (\text{A.38})$$

$$C_{\delta\delta} = \frac{I_{A\lambda z}}{w \cos(\lambda)} + \mu \frac{S_A + I_{Tzz}}{w \cos(\lambda)}. \quad (\text{A.39})$$

Table A.1: Physical parameters of the bicycle

Name	Value	Unit
g	9.81	m/s^2
w	1.02	m
c	0.08	m
λ	$\pi/10$	rad
r_R	0.3	m
m_R	2	kg
I_{Rxx}	0.0603	kg m^2
I_{Ryy}	0.12	kg m^2
x_B	0.3	m

Table A.1 – continued

Name	Value	Unit
z_B	-0.9	m
m_B	85	kg
I_{Bxx}	9.2	kg m ²
I_{Bxz}	2.4	kg m ²
I_{Byy}	11	kg m ²
I_{Bxz}	2.4	kg m ²
I_{Bzz}	2.8	kg m ²
x_H	0.9	m
z_H	-0.7	m
m_H	4	kg
I_{Hxx}	0.05892	kg m ²
I_{Hxz}	-0.00756	kg m ²
I_{Hyy}	0.06	kg m ²
I_{Hxz}	-0.00756	kg m ²
I_{Hzz}	0.00708	kg m ²
r_F	0.35	m
m_F	3	kg
I_{Fxx}	0.1405	kg m ²
I_{Fyy}	0.28	kg m ²

Appendix B

Physical parameters of the reaction wheel mounted on the bicycle

Table B.1: Physical parameters of the reaction wheel mounted on the bicycle

Name	Value	Unit
m_I	20	kg
r_I	0.5	m
I_I	2.5000	kg m ²
b_r	0.001	N m s
b_m	0.001	N m s
b_I	0.001	N m s

Bibliography

- [1] H. Abou-Kandil, G. Freiling, V. Ionescu and G. Jank. Matrix Riccati equations in control and systems theory, *Birkhäuser Basel*, 2003.
- [2] V. Acosta, C. L. Cowan and B.J Graham. Podstawy fizyki współczesnej. *Wydawnictwo Naukowe PWN*, Warszawa, 1981.
- [3] O. Al-Buraiki and M. B. Thabit. Model predictive control design approach for autonomous bicycle kinematics stabilization, *Control and Automation (MED), 2014 22nd Mediterranean Conference of Palermo*, 2014, pp. 380-383.
- [4] O. Al-Buraiki and E. S. Ferik. Adaptive control of autonomous bicycle kinematics, Control, Automation and Systems (ICCAS), *13th International Conference on Gwangju*, 2013, pp. 783-787.
- [5] K. Amborski. Teoria sterowania. *Państwowe Wydawnictwo Naukowe*, Warszawa, 1987.
- [6] R. Ando and A. Li. An analysis on users' evaluation for self-balancing two-wheeled personal mobility vehicles, *2012 15th International IEEE Conference on Intelligent Transportation Systems*, pp. 1525-1530, Anchorage, AK, 2012.
- [7] K. J. Åström, D. Block and M. Spong. The reaction wheel pendulum, *Synthesis Lectures on Controls and Mechatronics*, Vol. 0, *Morgan and Claypool Publishers*, 2007.
- [8] K. J. Åström, R. E. Klein and A. Lennartsson. Bicycle dynamics and control: adapted bicycles for education and research, *IEEE Control Systems*, Vol. 25, No. 4, pp. 26-47, Aug. 2005.
- [9] K. J. Åström, R. E. Klein and A. Lennartsson. Bicycles, motorcycles and models, *IEEE Trans. Magn.*, 10, 34-61, 2006.
- [10] K. J. Åström and T. Hagglund. Advanced PID Control, *ISA Instrumentation, Systems and Automation Society*, 2006.
- [11] J. Baichtal. Make: Bicycle Projects: Upgrade, accessorize, and customize with electronics, mechanics, and metalwork, *Maker Media, Inc*, 1st edition, September 7, 2015.

- [12] P. Baldi, M. Blanke, P. Castaldi, N. Mimmo and S. Simani, Adaptive FTC based on control allocation and fault accommodation for satellite reaction wheels, *3rd Conference on Control and Fault-Tolerant Systems (SysTol)*, pp. 672-677, Barcelona, 2016.
- [13] R. Ballantine. Richard's 21st century bicycle book. *Pan Books*, 4th edition, October 6, 2000.
- [14] B. Bapiraju, K. N. Srinivas, P. Prem K. and L. Behera. On balancing control strategies for a reaction wheel pendulum, *Proceedings of the IEEE INDICON 2004. First India Annual Conference*, pp. 199-204, 2004.
- [15] A. V. Beznos. Control of autonomous motion of two-wheel bicycle with gyroscopic stabilisation, *Proceedings. IEEE International Conference on Robotics and Automation*, pp. 2670-2675 Vol. 3, Leuven, 1998.
- [16] K. Cameron. Honda shows self-balancing but non-gyro bike. Concept debuts at Consumer Electronics Show in Las Vegas, *Cycle World*, January 6, 2017.
- [17] S. Carpenter. Lit Motors hopes its C-1 becomes new personal transportation option, *Tribune Newspapers*, June 2012.
- [18] O. Castillo, L. Xu and S. Ao. Trends in intelligent systems and computer engineering, *Springer Science+Business Media*, 2008.
- [19] P. Castillo, R. Lozano and A. E. Dzul. Modelling and control of mini-flying machines, *Springer-Verlag London Limited*, 2005.
- [20] Bicycle: the definitive visual history, *DK*, 2016.
- [21] D. A. Bini, B. Iannazzo and B. Meini. Numerical solution of algebraic Riccati equations, *SIAM-Society for Industrial and Applied Mathematics*, 2012.
- [22] H. B. Brown and Y. Xu, A single-wheel, gyroscopically stabilized robot, *Proceedings of IEEE International Conference on Robotics and Automation*, Vol. 4, pp. 3658-3663, Minneapolis, MN, 1996.
- [23] E. Carvallo. Théorie du mouvement du monocycle et de la bicyclette, *Gauthier-Villars*, Paris, France, 1897.
- [24] V. Cerone, D. Andreo, M. Larsson and D. Regruto. Stabilization of a riderless bicycle [Applications of Control], *IEEE Control Systems*, Vol. 30, No. 5, pp. 23-32, Oct. 2010.
- [25] N. Clayton. A Short History of the Bicycle, *Amberley*, 2016.
- [26] V. Cossalter. Motorcycle Dynamics (Second Edition), *Lulu.com*, 2006.
- [27] P. J. Davis and P. Rabinowitz. Methods of numerical integration, *Dover Books on Mathematics*, 2nd edition, October 25, 2007.

- [28] A. Dietrich. Whole-body impedance control of wheeled humanoid robots Springer Tracts in Advanced Robotics 116, *Springer International Publishing*, 2016.
- [29] W. Dixon, D. M. Dawson, E. Zergeroglu and A. Behal. Nonlinear control of wheeled mobile robots, Lecture notes in control and information sciences, *Springer-Verlag London*, 2001.
- [30] E. Döhring, Die Stabilität von Einspurfahrzeugen, *Forschung auf dem Gebiet des Ingenieurwesens*, Volume 21, Issue 2, pp 50–62, Germany, March, 1955.
- [31] Y. Ebihara, T. Hagiwara and M. Araki. Sequential tuning methods of LQ/LQI controllers for multivariable systems and their application to hot strip mills, *Proceedings of the 38th IEEE Conference on Decision and Control*, Vol. 1, pp. 767-772, Phoenix, AZ, 1999.
- [32] F. Fahimi. Autonomous robots: modeling, path planning, and control, *Springer International Publishing*, 1st edition, December 4, 2008.
- [33] J. Forester. Bicycle transportation, Second Edition: A Handbook for Cycling Transportation Engineers, *The MIT Press*, 1994.
- [34] M. Gajamohan, M. Merz, I. Thommen and R. D'Andrea. The Cubli: A Cube that can Jump Up and Balance, *Proc. IEEE/RSJ International Conference of Intelligent Robots and Systems*, pp. 3722-3727, Algarve, Portugal, October 2012.
- [35] M. Gajamohan, M. Muehlebach, T. Widmer and R. D'Andrea. The cubli: a reaction wheel-based 3D inverted pendulum, *Proc. European Control Conference*, pp. 268-274, Zurich, Switzerland, July 2013.
- [36] Q. Gao. Universal fuzzy controllers for non-affine nonlinear systems, *Springer*, Singapore, 2017.
- [37] N. H. Getz and J. E. Marsden. Control for an autonomous bicycle, *Proceedings of 1995 IEEE International Conference on Robotics and Automation*, pp. 1397-1402 Vol. 2, Nagoya, 1995.
- [38] J. Gościński and A. Owczarkowski, Zaawansowane sterowanie wahadłem odwróconym z napędem inercyjnym, 2011.
- [39] D. F. Griffiths and D. J. Higham. Numerical Methods for Ordinary Differential Equations: Initial Value Problems, Chapter: Euler's Method, *Springer London*, pp. 19-31 2010.
- [40] Guide for the development of bicycle facilities, *American Association of State Highway and Transportation Officials*, June 1, 2012.
- [41] Habib. Bioinspiration and robotics – walking and climbing robots, *Itech*, 2007.
- [42] T. Hadland, H. E. Lessing, N. Clayton and G. W. Sanderson. Bicycle design: an illustrated history, *The MIT Press*, 2014.

- [43] L. N. Hand and J. D. Finch. Analytical mechanics, *Cambridge University Press*. United States of America, 1998.
- [44] J. Heine. The Golden Age of Handbuilt Bicycles, *Vintage Bicycle Press* February 17, 2015.
- [45] D. Hayduk. Bicycle metallurgy for the cyclist, *Vitesse Pr*, January, 1990.
- [46] Z. Hendzel and W. Żylski. Mechanika ogólna - statyka, *Oficyna Wydawnicza Politechniki Rzeszowskiej*. Rzeszów, September, 2000.
- [47] D. V. Herlihy. Bicycle: The History, *Yale University Press*, 2004.
- [48] J. P. Hespanha. Lecture notes on LQR/LQG controller design, February 27, 2005.
- [49] Y. Huang, Q. Liao, S. Wei and L. Guo. Dynamic modeling of a bicycle robot with front-wheel drive based on Kane's method, *Information and Automation (ICIA) IEEE International Conference*, pp. 758-764, Harbin, 2010.
- [50] C. L. Hwang, H. M. Wu and C. L. Shih. Fuzzy Sliding-Mode Underactuated Control for Autonomous Dynamic Balance of an Electrical Bicycle, *IEEE Transactions on Control Systems Technology*, Vol. 17, No. 3, May 2009, pp. 658-670.
- [51] K. Iuchi, H. Niki and T. Murakami, Attitude control of bicycle motion by steering angle and variable COG control, *31st Annual Conference of IEEE Industrial Electronics Society (IECON)*, pp. 6, 2005.
- [52] T. Kaczorek. Teoria sterowania i systemów, *Wydawnictwo Naukowe PWN*, 3rd edition, Warszawa, 1999.
- [53] Kane, R. Thomas and A. D. Levinson. Dynamics, Theory and Applications, *McGraw-Hill*, New York, 1985.
- [54] B.J. Kawak. Development of a low-cost, low micro-vibration CMG for small agile satellite applications, *Acta Astronautica*, Volume 131, pages 113–122, February 2017.
- [55] L. Keo, K. Yoshino, M. Kawaguchi and M. Yamakita. Experimental results for stabilizing of a bicycle with a flywheel balancer, *IEEE International Conference on Robotics and Automation*, pp. 6150-6155, Shanghai, 2011.
- [56] M. J. Kolin and D. M. De La R. The custom bicycle: buying, setting up, and riding the quality bicycle, *Rodale Press*, 1st edition, November 22, 1979.
- [57] H. K. Khalil. Nonlinear systems, *Prentice Hall*, 3rd edition, New Jersey, 2002.
- [58] F. Klein and A. Sommerfeld, Über Die Theorie Des Kreisels, *Druck Und Verlag Von B.G. Teubner*, Vol. IV, Leipzig, Germany, 1910.
- [59] M. Kristić, I. Kanellakopoulos and P. Kokotović. Nonlinear and adaptive control, *John Wiley & Sons, Inc.*, New York, 1995.

- [60] W. Krysicki and L. Włodarski. Analiza matematyczna w zadaniach, *Wydawnictwo naukowe PWN*, część 1, Warszawa, 1999.
- [61] W. Krysicki and L. Włodarski. Analiza matematyczna w zadaniach, *Wydawnictwo naukowe PWN*, część 2, Warszawa, 1999.
- [62] H. Kwakernaak and R. Sivan. Linear optimal control systems, *John Wiley & Sons, Inc.* New York, NY, USA 1972.
- [63] V. J. Lappas, W. H. Steyn and C. I. Underwood. Control moment gyro (CMG) gimbal angle compensation using magnetic control during external disturbances, *Electronics Letters*, Vol. 37, No. 9, pp. 603-604, 26 Apr 2001.
- [64] V. J. Lappas, W. H. Steyn and C. I. Underwood. Torque amplification of control moment gyros, *Electronics Letters*, Vol. 38, No. 15, pp. 837-839, 18 Jul 2002.
- [65] F. A. Leve. Evaluation of steering algorithm optimality for single-gimbal control moment gyroscopes, *IEEE Transactions on Control Systems Technology*, Vol. 22, No. 3, pp. 1130-1134, May 2014.
- [66] D. J. N. Limebeer and R.S. Sharp. Bicycles, motorcycles, and models, *IEEE Control Systems*, Vol. 26, No. 5, Oct. 2006, pp. 34-61.
- [67] C. Liu. Foundations of MEMS, *Pearson*, 2nd edition, March 14, 2011.
- [68] J. M. Maciejowski. Multivariable feedback design, *Addison Wesley Publishing Company, Inc.*, Cornwall, Great Britain, 1989.
- [69] J. M. Maciejowski. Predictive control with constraints, *Prentice Hall*, 1st edition, September 6, 2000.
- [70] F. Markley, F. Landis, G. R. Reynolds, F. X. Liu and L. K. Lebsack. Maximum torque and momentum envelopes for reaction wheel arrays, *Journal of Guidance, Control and Dynamics*, Vol. 33, No. 5, september-october 2010.
- [71] J. P. Meijaard, J.M. Papadopoulos, A. Ruina and A.L. Schwab. Benchmark results on the linearized equations of motion of an uncontrolled bicycle, *Journal of Mechanical Science and Technology*, Volume 19, Supplement 1, pp 292–304, January 2005.
- [72] J. P. Meijaard, J. M. Papadopoulos, A. Ruina and A. L. Schwab. Linearized dynamics equations for the balance and steer of a bicycle: a benchmark and review, *Proceedings of the Royal Society A: Mathematical, Physical and Engineering Sciences*, Vol. 463, issue 2084, 11 June 2007, pp. 1955-1982.
- [73] W. T. Miller III, R. S. Sutton and P. J. Werbos. Neural networks for control, *A Bradford Book*, March 2, 1995.
- [74] W. C. Morchin and H. Oman. Electric bicycles. A guide to design, *A John Wiley & Sons Inc.*, 2006.

- [75] J. K. Moore. Human Control of a Bicycle, UC Davis Doctoral Dissertation, 2012.
- [76] J. Moore and M. Hubbard. Parametric study of bicycle stability (P207), *The Engineering of Sport*, 7 - Vol. 2, pp. 312-318, Springer-Berlag France, Paris, 2008.
- [77] M. Muehlebach and R. D'Andrea. Nonlinear analysis and control of a reaction-wheel-based 3-D inverted pendulum, *IEEE Transactions on Control Systems Technology*, 2016.
- [78] M. Muehlebach, G. Mohanarajah and R. D'Andrea. Nonlinear analysis and control of a reaction wheel-based 3D inverted pendulum, *Proc. Conference on Decision and Control*, Florence, Italy, 2013.
- [79] J. Norwood. Fizyka współczesna. Wydawnictwo Naukowe PWN, Warszawa, 1982.
- [80] A. Owczarkowski and D. Horla. A comparison of control strategies for 4DoF model of unmanned bicycle robot stabilised by inertial wheel, *Progress in Automation, Robotics and Measuring Techniques, Advances in Intelligent Systems and Computing*, Szewczyk Roman et al. (Eds.), Vol. 351, pp. 211-221, 2015.
- [81] A. Owczarkowski, P. Bachman, J. Gościński, P. Owczarek and R. Regulski. Sterowanie nieliniowe backstepping wahadła odwróconego z napędem inercyjnym, *Prace Instytutu Elektrotechniki*, nr 264/2014, Warszawa, April, 2014.
- [82] A. Owczarkowski and D. Horla. Robust LQR and LQI control with actuator failure of 2DOF unmanned bicycle robot stabilized by inertial wheel, *International Journal of Applied Mathematics and Computer Science*, Vol. 26(2), 2016.
- [83] A. Owczarkowski, J. Gościński, P. Owczarek and D. Rybarczyk. Badanie i porównanie algorytmów LQR i backstepping do sterowania wahadła odwróconego z napędem inercyjnym, *Pomiary Automatyka Kontrola*, nr 10, Vol. 59, s. 1016-1019, Warszawa, October, 2013.
- [84] J.M. Papadopoulos. Bicycle steering dynamics and self-stability: a summary report on work in progress. Technical report, Cornell Bicycle Research Project, Cornell University, Ithaca, NY. 1987.
- [85] T. Paterek. Manual for bicycle framebuilders, 3rd edition, 2004.
- [86] Peterson and L. Dale. Bicycle dynamics: modelling and experimental validation, Doctoral Dissertation, University of California, Davis, 2013.
- [87] A. M. Plamitzer. Maszyny elektryczne, Wydawnictwo Naukowo-Techniczne, Warszawa, 1986.
- [88] R. Resnik and D. Halliday. Fizyka. Wydawnictwo Naukowe PWN, Vol. 1, Warszawa, 1999.
- [89] R.S. Sharp, S. Evangelou and D.J.N. Limebeer. Advances in the modelling of motorcycle dynamics, *Multibody Syst. Dyn.*, Vol. 12, No. 3, pp. 251-283, 2004.

- [90] R. S. Sharp. Stability, control and steering responses of motorcycles, *Vehicle System Dynamics*, 35, 4-5, 2001.
- [91] R. S. Sharp. The lateral dynamics of motorcycles and bicycles, *Article in Vehicle System Dynamics*, 14(4-6):265-283, June, 1985.
- [92] R. S. Sharp. The stability and control of motorcycles, *Journal of Mechanical Engineering Science*, 13(5), 316-329, 1971.
- [93] S. Singh. Theory of machines, *Pearson India*, December, 2011.
- [94] J. J. E. Slotine and W. Li. Applied nonlinear control, *Prentice Hall*, Engiewood Cliffs, New Jersey, 1991.
- [95] H. Sutherland. Sutherland's handbook for bicycle mechanics, *Sutherland Pubns*, May 16, 1995.
- [96] Y. Tanaka and T. Murakami, Self sustaining bicycle robot with steering controller, Advanced Motion Control (AMC), *The 8th IEEE International Workshop*, pp. 193-197, 2004.
- [97] J. R. Taylor. Classical mechanics. *University Science Books*, Sausalito, California, 2005.
- [98] E. S. Tehrani, K. Khorasani and S. Tafazoli. Dynamic neural network-based estimator for fault diagnosis in reaction wheel actuator of satellite attitude control system, *Proceedings on 2005 IEEE International Joint Conference on Neural Networks*, 2005, pp. 2347-2352 Vol. 4, Montreal, Que., 2005.
- [99] D. J. Todd, Walking Machines: an Introduction to legged robots, *Anchor Press Ltd., Kogan Page publishing*, 1985.
- [100] F. J. W. Whipple. The stability of the motion of a bicycle, *Quarterly Journal of Pure and Applied Mathematics*, Vol. 30, pp. 312-348, 1899.
- [101] D. G. Wilson and J. Papadopoulos. Bicycling science, *MIT press*, 2004.
- [102] D. G. Wilson. Bicycling science, *The MIT Press*, 3rd edition, Cambridge, Massachusetts, 2004.
- [103] A. K. Wróblewski, J.A. Zakrzewski Wstęp do fizyki, Vol. 1 and 2, *Wydawnictwo Naukowe PWN*, Warszawa, 1991.
- [104] W. Wróblewski. Sterowanie procesami ciągłymi i dyskretnymi – lecture material, Poland, Poznań, 2017.
- [105] L. A. Vivanco. Reconsidering the Bicycle: An anthropological perspective on a New (Old) Thing, *Routledge*, 1st edition, February 16, 2013.
- [106] M. Xie, S. Dubowsky, J. Fontaine, M. O. Tokhi and G. S. Virk. Advances in climbing and walking robots, *World Scientific Publishing Company*, 2007.

- [107] Y. Xu and Y. Ou. Control of single wheel robots, Springer Tracts in Advanced Robotics 20 Periodical, *Springer-Verlag Berlin Heidelberg*, 2005.
- [108] J. Yi, D. Song, A. Levandowski and S. Jayasuriya. Trajectory tracking and balance stabilization control of autonomous motorcycles, *Proceedings IEEE International Conference on Robotics and Automation (ICRA)*, pp. 2583-2589, Orlando, FL, 2006.
- [109] J. Ziętkiewicz, D. Horla and A. Owczarkowski. Robust actuator fault-tolerant LQR control of unmanned bicycle robot. A feedback linearization approach, *Advances in Intelligent Systems and Computing*, Springer, Vol. 440 p. 411-421, 2016.
- [110] J. Ziętkiewicz, A. Owczarkowski and D. Horla. Performance of feedback linearization based control of bicycle robot in consideration of model inaccuracy, *Advances in Intelligent Systems and Computing*, Springer, Vol. 440 p. 399-410, 2016.